Airborne and Ground-Based Lidar Systems for Forest Measurement: Background and Principles

David L.B. Jupp and Jenny L. Lovell

CSIRO Marine and Atmospheric Research Papers.
Number 017

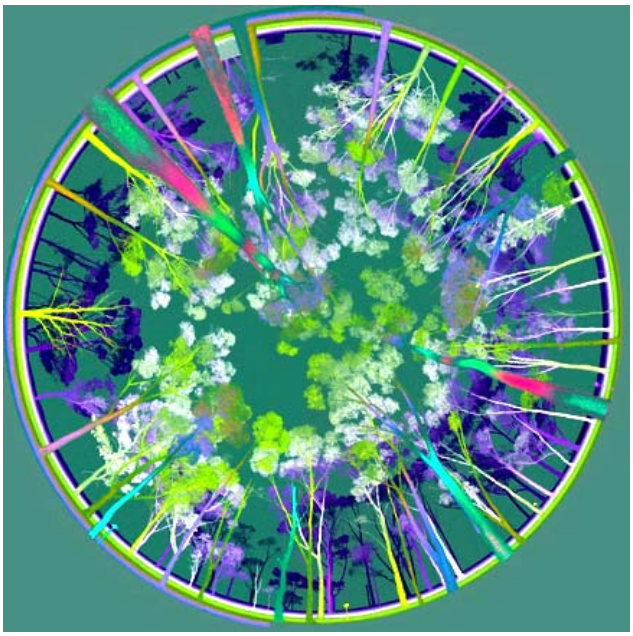

Enquiries should be addressed to:

Dr. David Jupp

CSIRO Marine and Atmospheric Research
GPO Box 3023
Canberra ACT 2061
Phone. +61 2 6246 5985
Fax. +61 2 6246 5988
Email. David.Jupp@csiro.au

Jupp, David L. B.
Airborne and ground-based lidar systems for forest measurement : background and principles.

Bibliography.
Includes index.
ISBN 9781921232688.

1. Optical radar. 2. Forests and forestry - Measurement - Remote sensing. I. Lovell, Jennifer L. II. CSIRO. Marine and Atmospheric Research. III. Title.

621.3678

Copyright and Disclaimer

Important Disclaimer

FOREWORD

This report has been developed from a design document written between July 2000 and March 2002. The original document entitled “Product background and description for airborne (VSIS) and ground-based (ECHIDNA®) canopy lidar systems” provided historical and theoretical background and principles for the CSIRO workplan during the development of the CSIRO Canopy Lidar Initiative (CLI). The CLI has developed methods for airborne canopy Lidar analysis, developed a new ground based instrument to validate methods discussed here for the intended commercial “ECHIDNA®” and undertaken studies aimed at exploiting the synergy between ground based and airborne Lidar for forest measurement and mapping. Ongoing patenting has protected the innovative aspects developed in the CLI and the task of validation has been recently pursued with support from the Forest and Wood Products Research & Development Corporation (FWPRDC) in Australia. This document has been provided as a general scientific review of the field and to provide background information to support the final reporting for the FWPRDC project. The CLI has led to many outcomes and papers since March 2002. However, apart from some references to more recent work the material in this report has been left at the stage it reached at that time and has not been fundamentally updated. It therefore represents a baseline as of March 2002. The field of Lidar applications in forests has, however, developed very rapidly in recent years and the CLI has also moved on significantly from this baseline. The more recent developments can be found in the growing literature and reports and represent probably the most exciting and productive development in remote sensing of forests and woodlands in recent years.

Cover Picture: Hemispherical canopy image produced by CSIRO ground-based prototype canopy scanning Lidar – the ECHIDNA® Validation Instrument (EVI). Gap frequency by angle and range can be determined.

Table of Contents

List of Tables

List of Figures

List of Abbreviations & Acronyms

Acronym/Abbreviation/ Special Item	Expansion
ALADIN	Atmospheric LAser Doppler INstrument
ALISSA	l'Atmosphere par LIdar Sur SAliout
AOL	Airborne Oceanographic Lidar
API	Air Photograph Interpretation
ATBD	Algorithm Technical Basis Document
ATLID	ATmospheric LIDar
BA	Basal Area
BOREAS	Boreal Ecosystem Atmosphere Study
BRDF	Bi-Directional Reflectance Distribution Function
BSD (see FHD)	Bird Species Diversity index
CAD	Crown Area Density
CAR	CSIRO Atmospheric Research
CC	Crown Cover
CFFP	CSIRO Forestry and Forest Products
CLI	CSIRO Lidar Initiative
CSIRO	Commonwealth Scientific and Industrial Research Organisation
CW	Continuous Wave (laser)
DBH	Diameter at Breast Height (1.3m, over bark)
DEM (also see DTM)	Digital Elevation Model
DEMON	A CSIRO Direct solar beam LAI measuring device
DTM (also see DEM)	Digital Terrain Model
ECHIDNA®	Name of CSIRO ground based Lidar system
ESA	European Space Agency
ESSP	Earth System Science Pathfinder
ETBD	Engineering Technical Basic Document
FAI	Foliage Area Index
FHD (see BSD)	Foliage Height Diversity index
FOLIG	Foliage Profile computer program
FP	Foliage Profile
FWPRDC	Forests and Wood Products Research and Development Corporation
GLAS	Geoscience Laser Altimeter System
GPS	Global Positioning System
INS	Inertial Navigation System
IPCC	Intergovernmental Panel on Climate Change
IRM	Integrated Resource Model
LADS	Laser Airborne Depth Sounder
LAI	Leaf Area Index
LIDAR	LIght Detection And Ranging
LVIS	Lidar Vegetation Imaging System
MAESTRO	An array based physiological canopy model
MAI	Mean Annual Increment

MDB	Murray Darling Basin
MOLA	Mars Orbiter Laser Altimeter
NASA	National Aeronautics and Space Administration
NLWRA	National Land and Water Resources Audit
NSW	New South Wales (Australian State)
NVIS	National Vegetation Information system
OECD	Organisation for Economic Cooperation and Development
PAR	Photosynthetically Available Radiation
PFC	Projected Foliage Cover
QMCH	Quadratic Mean Canopy Height
RF	Radio Frequency
RMS	Root Mean Square
RMSE	Root Mean Square Error
SHOALS	Scanning Hydrographic Operational Airborne LIDAR Survey
SLA	Shuttle Laser Altimeter
SLICER	Scanning Lidar Imager of Canopies by Echo Recovery
SNR	Signal to Noise Ratio
TRAC	Tracing Radiation and Architecture of Canopies
VCL	Vegetation Canopy Lidar
VSIS	Vegetation Structure Imaging System

Complex Structure in native forest – It must be measured but how?

1 INTRODUCTION

1.1 Forest Measurement – Introduction & Background

Measurement of vegetation is a primary activity in the provision of information for agriculture, forestry, ecology, hydrology and many related areas. Required outputs include structure and function as well as volume or area of components (e.g. wood volume, leaf area, light or water interception area etc). Therefore, the measurements involve plant spacing and amount (volume or area) as well as arrangements and sizes of components. Terms like height, density, cover, basal area and gap in forests relate to the distributions of distances between different elements of the canopy and all are involved in some way in the general idea of vegetation "structure".

Measurement of vegetation structure is difficult as well as time consuming and costly as forests are spatially highly variable and native forests (in particular) can include very complex associations of species, age classes and growth forms in a complete structural description. When the objective is to assess biomass, the situation is made harder as many of the available indirect measurements provide measures of component surface area (such as leaf area) or projected surface area rather than volume and mass. Trees grow to occupy quite large volumes within leaf-filled crowns having very high area to volume ratios while conversely trunks provide much higher volume and mass compared with their visible area and much greater apparent structural openness. The components with greatest contributions to total area and those with the greatest contributions to total biomass are therefore often in quite different parts of a canopy and have different structural descriptions.

Forestry is a very large, world-wide industry, producing sawlogs and pulp (woodchipping) and other wood products and includes in its scope for resource harvesting large areas of natural forests as well as plantations and smaller areas with ancillary uses such as salinity amelioration, erosion control, fuel and windbreaks. In addition to production forestry, environmental activities with requirements for vegetation measurement in management, reporting, compliance and certification include:

- Environmental reporting
- Environmental management
- Monitoring for sustainable land use
- Bio-diversity and fauna/bird survey
- Hydrological assessment and modelling
- Rehabilitation (minesites, defence areas and degraded lands)
- Power line surveys in forested areas
- Corridor planning
- Fire protection
- Assessment of landscape trafficability
- Greenhouse inventory and monitoring

The Montreal and Kyoto Protocols on Greenhouse may yet put considerable pressure on countries to account for changes in their forest covers as they relate to carbon storage and emissions. The Kyoto Protocol certainly opens up the possibility for countries and companies to "trade" carbon through the use of forests as "sinks", in addition to ensuring that net carbon emission from forest and land use activities is not contributing to the country's target. Such certification requires vegetation measurement methods that are consistent, repeatable and applicable to a range of land cover classes.

Commercial forestry areas are broadly divided into Native Forests and Plantation categories. Native forests occupy a large area of the landmass of the world and have previously been "mined" for timber and pulpwood. However, foresters generally aim at sustainability and have followed practices for sustainable use for many years and moved to create plantations as an alternative. Measurement of stem size and structure is a key to assessing current and potential yield as well as the sustainability of harvesting activities in Native Forests. The "vertical" nature of the stems leads to measurement methods that work at the forest floor in horizontal directions (to obtain basal area and deviational for example) and the development of surrogate data collection techniques using data that can be obtained quickly or possibly sensed remotely – such as crown cover, crown size, basal area and tree height.

Plantation forests for timber and pulp are rapidly increasing all over the world and possibly at a greater rate in Australia than other countries. Plantation forests have well defined management activities that use traditional forestry measurements and well-established correlations to estimate yield at harvest. This emphasis has led to differences of approach between traditional forestry measurements and ecological measurements. However, the rapid increase in areas planted and the introduction of new species has led to a situation where greater attention is being placed on precision measurement. The use of growth models to predict yield has called for more information relevant to functional aspects such as leaf area and canopy structure that affect productivity and therefore the annual increment in biomass stored as wood. Structural information on "condition" (such as poorly performing areas, competition and understorey) has also brought plantation foresters to place more emphasis on ecological measurements.

In the face of this, there is high interest among people who measure forests – whether for environmental purpose or for forestry – in new technology that may provide enhanced accuracy or achieve the information with reductions in time and/or cost. This document has been put together as a background document for the CSIRO canopy Lidar Initiative (CLI). The aim of the CLI is to promote and exploit the opportunities of Lidar technology in forest measurement and vegetation structural assessment. However, it is important to review both the opportunities of the technology as well as the environment in which it will operate. In this document this is done through listing and discussing the current techniques of measurement for vegetation structure as well as outlining opportunities for Lidar technology. Forests are complex and often inaccessible. Investigating how Lidar may be able to help overcome some of the problems their measurement poses is our aim.

1.2 Canopy Lidar applications

A Lidar (or Light/Laser Radar or Light/Laser Detection And Ranging) is an instrument in which a beam of Laser energy in the visible light or similar spectral region (such as the near infrared region) is transmitted in a specified direction and the time (or phase) and intensity of any return signals from the pulse used to measure distance to and amount of scatterers in the direction of the beam. Lasers have, in recent times, become highly developed and affordable instruments with many applications. The primary type of Laser method we will consider is the pulsed Lidar in which a finite width, but peaked, pulse of laser energy (or "shot") is sent out and the time of return of signals measured to obtain range to a scattering event. It is also possible to utilise CW (Continuous Wave) Lidars, in which a continuous wave is sent and the phase of the return radiation is used to measure delay and obtain range in the same way – but this will not be pursued here.

Lidars already have a very wide application for remote sensing including atmospheric sounding, atmospheric species measurement, water depth and properties of water bodies including algae and even sub-surface temperature (Measures, 1992; Ansmann *et al*., 1997). Lidar systems for mapping water depth were developed in the 1970's in Australia (LADS), Canada (SHOALS) and the USA (AOL). In atmospheric remote sensing, Lidars have a well-established place for determining cloud and aerosol properties or wind vectors (using doppler effects) from ground based systems (Measures, 1992; McCormick, 1995; Nakajima *et al.*, 1996; Ansmann *et al*., 1997) and there are a range of airborne and spaceborne instruments which will be deployed in the future making use of the ranging property of Lidars – sometimes called "coherent laser radars". There are, in fact, five planned space Lidar missions for cloud and aerosol measurement (ALADIN, ALISSA, ATLID, GLAS, LIDAR) as well as one vegetation canopy Lidar (VCL). VCL is being developed as part of NASA's Earth System Science Pathfinder (ESSP) program (Dubayah *et al*., 1997). There are a number of space experiments (including the shuttle experiment SLA and the MOLA mission to Mars) which have used Lidars for terrain mapping – or Laser altimetry and the GLAS and Laser Altimeter (ESA) instruments are planned primarily as terrain mapping instruments.

The worldwide market and business activity associated with the use of Lidars (often called terrain Lidars or Laser altimeters) to measure topography and generate digital terrain images is very large and well developed. These instruments use a high spatial density of small footprint laser pulses, or "shots", to enable each shot to penetrate gaps in canopies without attenuation to create a sufficient number and power of returns from the ground to sense terrain height under many levels of cover. Terrain Lidars have also been used to map vegetation canopy height (c.f. Nelson *et al*., 1984; Bufton, 1989; Nilsson, 1996; Naesset, 1997a,b; Magnussen *et al*., 1999). While it is feasible for a very high density of small footprint returns to be spatially aggregated to derive information about vegetation, the processing issues involved, the high spatial variance, the effects of reflectance "speckle" and the lack of calibration in most current systems has made this difficult. Just as significant, the costs of covering large areas with such a system would be very high so that terrain Lidars do not provide a practical approach to regional vegetation mapping.

Fortunately, there are now airborne Lidar systems such as the Scanning Lidar Imager of Canopies by Echo Recovery (SLICER) system (Harding, 2000; Harding *et al*., 2000) that, together with a planned spaceborne (VCL or Vegetation Canopy Lidar) system[1], go further to meet the needs of vegetation canopy mapping. These systems measure the return power of the laser pulse by digitising the whole of the return and use a relatively large footprint (such as 10-25 metres) so that signals from all reachable elements of the canopy profile are recorded in a single return trace. The time of the return of the peak of the pulse is a measure of the target range and the strength of the return an indicator of the target scattering cross section and reflectivity. By combining the digitising of the return with a larger, but variable, beam footprint and a scanning laser it is possible to cover the kinds of area needed for regional vegetation survey and retrieve canopy information that has not been obtainable by any other form of remote sensing. A set of traces from a SLICER mission over Boreal forests is shown in Figure 1.1:

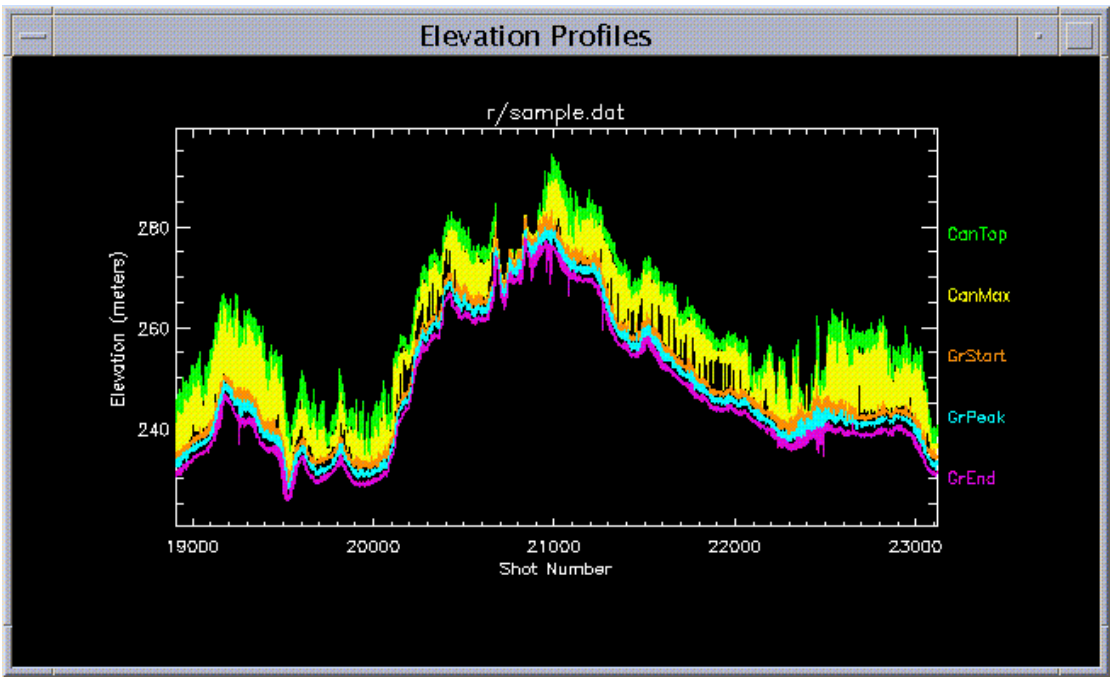

Figure 1.1. Typical SLICER transect over Boreal forest. (Data courtesy of NASA, BOREAS Project, colour key at right)

In this transect, the intensity of the Lidar returns are recorded as a function of time since the "shot". Using GPS and INS the time is translated into distance from the position of the aircraft, which can be translated to height above sea level in metres. Colouring the returns close to the aircraft as canopy top (green), the mid-range as yellow and the broad ground return as three colours with its peak (assumed position of the ground) in blue creates a clear schematic of the terrain surface and its tree cover.

Despite a long history of promising trials, impressive correlations and developments in Lidar sensing of forests (see Aldred and Bonner, 1985 and its discussion of Lidar developments in Canada from the mid-1960's and the paper by Maclean and Krabill, 1986 for the historical perspective), such operational vegetation Lidars have only relatively recently started to provide serious applications for mapping vegetation

[1] Unfortunately, VCL was not launched as planned but plans for a space borne canopy Lidar are still in progress in the US and Europe.

canopies. The opportunities are not yet fully exploited. Analysis remains exploratory and the technology is still improving and will greatly benefit from further improvements. A significant change has, however, been brought about by improvements in laser technology and falling prices. The main operational example of such a system at this time (for which data are available) is the NASA SLICER (Blair *et al.*, 1994; Means *et al*., 1999; Harding *et al.*, 1994, 2000, Harding *et al*., 2000).

There is also a lot of activity investigating data from a newer NASA instrument called LVIS (Blair *et al.*, 1999), which was developed as a proving technology for the VCL mission. VCL was designed to provide global coverage of surface Lidar data similar to SLICER with transects of data and footprints of 25 metres but unfortunately (due to various factors) VCL was not launched and the world must wait a little longer for a space-borne canopy Lidar. The airborne LVIS operates at altitudes of up to 10 km above the ground and can produce swaths of up to 1 km wide with footprints of 25m.

1.3 Scope of this document - the CLI Lidar "ATBD"

This CSIRO Canopy Lidar Initiative (CLI, see http://www.eoc.csiro.au under Canopy Lidar) has been working to realise the opportunity of canopy Lidar and see it used in Australian native and commercial forests and see its opportunities at work in forests throughout the world. This Canopy Lidar "Algorithm Technical Basis Document" (or "ATBD" – to use an abbreviation that has become well-known in NASA documentation) describes algorithms and methods that can and will be applied to derive forest cover and structural information from current and developing Australian airborne and ground based Lidar systems.

In this ATBD, a "Lidar" is treated as a tool that generates signals ("shots") and provides:

- Information on the range to a distributed group of scattering elements in a specific direction;
- The intensity of the return signals (which relates to scatterer reflectivity and amount at different ranges); and
- The way the intensity/time information in the returns changes with Lidar beam size and shape as well as its direction and position.

The spatial relationships and calibrated signals form a spatial data set that may be analysed for information on size, shape, porosity or gappiness, density and spacing of elements (such as leaves, stems, trunks, tree crowns, shrub crowns and grasses) in forests. Because of the statistical nature of our treatment, there is added discussion in an Appendix on statistical spatial models and geometric probability (see Appendix 4).

The variation of the return signals with Lidar beam direction is a significant information source. Horizontal beams interact strongly with trunks and vertical foliage components and vertically downward beams have a significant interaction with the horizontal components and background topography. As discussed above, the market and business activity associated with the use of terrain Lidars to generate digital terrain (DTM) information is well developed worldwide and also in Australia. Major limitations of the technology in DTM mapping are reached in areas with

significant tree cover where the over storey diffuses the return signals resulting in high variance and ambiguous ground reflections. Among the current airborne Lidar systems that are used to measure topography are those that time the first and last significant return of an outgoing pulse. This reduces the uncertainty for terrain mapping and also starts to provide more information for measuring above ground information. The Lidar beams are commonly very narrow to achieve greatest penetration through existing holes in the canopy or other aboveground obstructions and return a signal from the ground of sufficient power to be detected above a background threshold of "softer" canopy components. Intensity is rarely measured (other than its being above the threshold) as the existence of an above-threshold scattering event and its range are the key aspects of the data.

We will return to these data and their interpretation for vegetation information in later sections. However, it is useful here to consider the basic strategy being employed in terrain Lidars. If there are a number of scattering elements above the ground then the probability that a narrow beam will miss them and hit the ground depends on the "gap probability function" for the surface cover. Normally, this gap probability has very high spatial variance. Hence, if the surface is covered by a very dense set of narrow beam Lidar pulses, a few will generally penetrate the gaps and return individually strong signals to detect the position of the ground. Hopefully, enough will return to infer the position of the underlying surface. Since the beam cannot have zero width, parts of any Lidar beam may be scattered above the surface by different elements and provide a background from which the terrain signal needs to be extracted. Most terrain Lidars therefore measure first and last significant return to improve the classification of the ground returns.

The approach of using very high shot density and capitalising on high spatial variance to get a small but individually intense set of returns from a background characterises terrain Lidars. If the beam is broadened then the relative intensity of the ground signal reduces in relation to returns from the cover and the spatial variance and its causes (the upper canopy and vegetation structure) become more controlled and useable in the signal. The exploitation of this control defines a major difference between topographic and canopy Lidars. It is canopy Lidar that is the subject of this ATBD because we believe the exploitation of a variable beam width can be harnessed as a powerful tool to measure factors such as height, depth, projected area and biomass in vegetation canopies. Another major factor involved here is the expense of terrain Lidar data collection and processing when information about the canopies (rather than the terrain) is the base objective. But this will be addressed elsewhere.

The US SLICER (Means *et al*., 1999; Harding, 2000; Harding *et al*., 2000) and LVIS (Blair *et al*., 1999) are current airborne examples of canopy Lidars and the VCL instrument is a coming spaceborne Canopy Lidar. More information on VCL can be found at http://essp.gsfc.nasa.gov/vcl/ and the article by Dubayah and Drake (2000) very clearly outlines the issues separating the applications of topographic and vegetation Lidars as well as the objectives of the VCL mission. An important statement in Dubayah and Drake (2000) concerns an increasing realisation that there are many situations where canopy Lidars provide better topographic information than terrain Lidars. This tends to occur in dense (e.g. tropical) forests where there is significant relief. The high shot density of the terrain Lidar breaks into a large number of returns that are difficult to ascribe to vegetation or topography. Larger footprint,

digitised waveform Lidars can separate the signals provided they have high SNR. The principles underlying the trade-off between shot variance, pulse reflection and Lidar sensing of forest canopies is illustrated in Figure 1.2:

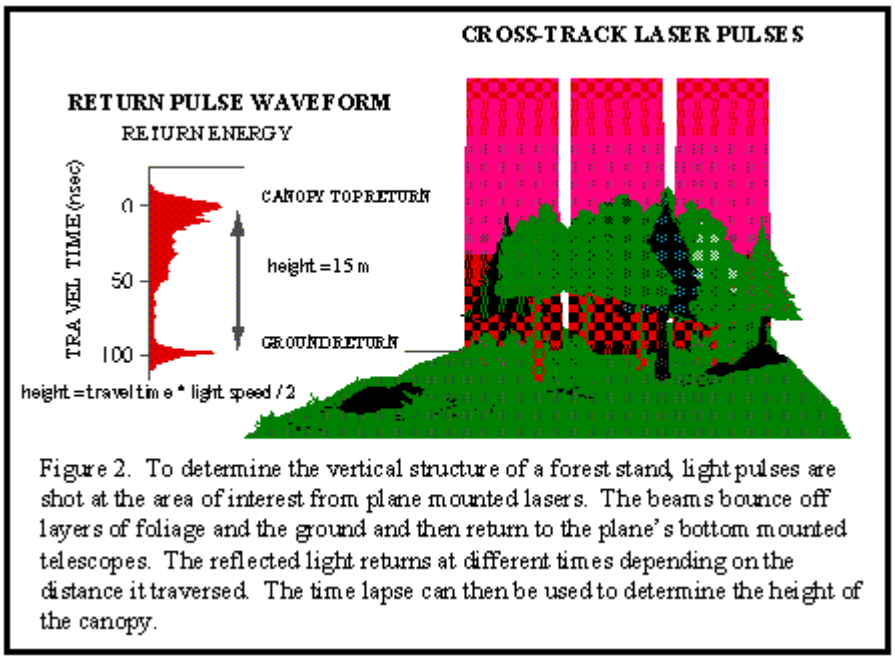

Figure 2. To determine the vertical structure of a forest stand, light pulses are shot at the area of interest from plane mounted lasers. The beams bounce off layers of foliage and the ground and then return to the plane's bottom mounted telescopes. The reflected light returns at different times depending on the distance it traversed. The time lapse can then be used to determine the height of the canopy.

Figure 1.2. Principle of Canopy Lidar operation

There are some basic uncertainties in the intensity of returns of Lidar data that underlie significant differences between the engineering specification and build of Lidar systems that only sense range and those seeking to measure advanced canopy structural information. In the former, range is obtained by time to peak of the pulse and intensity and pulse width is not so important. For all Lidars, this range to target is independent of the calibration of the intensity and is a highly significant data product by itself. However, if the opportunities that arise from recording intensity of the returns are to be realised, the instrument must be able to be calibrated so that the data can be resolved into units such as "return intensity" or "apparent reflectance". Apparent reflectance is the reflectance of a standard target that would return the same intensity from the same range. (Apparent reflectance will be discussed in more detail later).

Even when the data are calibrated, such calibrated intensity data can have a high level of uncertainty in regions containing distributed scatterers (such as leaves or the needles of conifers) in that a few scatterers having high reflectivity or with scattering surfaces aligned to the beam direction will give a similar overall intensity of return to many scatterers with low reflectivity or with effective area oblique to the direction of the beam. Similarly, "clumped" (see Appendix 4) canopies in which some elements occlude (hide) others may not be easily distinguished from lower density and less clumped canopies. These effects may be summarised as three "blind spots" that mainly affect airborne canopy Lidar systems that make use of the intensity of the returns. They are:

- The trade-off between scatterer density and reflectivity;

- The effects of foliage angle distribution;
- The effects of clumping and occlusion of foliage.

Analysis of the data must take these "blind spots" into account and find ways to resolve them. The way in which this can be done will also be discussed in later sections. In essence, we propose that relationships derived from an in-canopy ground-based Lidar can "calibrate" airborne and/or spaceborne Lidars to extend highly detailed structural information over wide areas.

The way in which instruments and supporting systems may be designed and constructed to achieve these data is the subject of the separate "Engineering Technical Basis Document" (or ETBD). Our plan here is to describe the interface region in between the engineering issues and the information ends and how the data may be exploited and analysed to provide significant structural information about forests and woodlands that is important for many uses and applications. These products form the market for the outputs of the technology. Significantly, we will develop tools that overcome the blindness of airborne and spaceborne Lidars due to their limited scanning and methods that derive data from Lidars that previously have not been considered to be reachable in practical forest measurement.

Briefly, the characteristics of the Lidar systems we are assuming provide data for the analysis are that they:

1. Obtain signals with high Signal to Noise Ratio (SNR) from vegetation at depth in canopies;
2. Measure intensity of return trace to nanosecond sampling;
3. Provide accurate range to target by pulse deconvolution;
4. Sound with variable beam width and shape;
5. Scan in multiple directions;
6. Capture and store data at radio-frequency (RF) rate.

However, beyond such specifications the Lidars themselves are only tools and means to the ends of forest measurements. It is the wealth of information that we can derive and their relevance to forest monitoring and assessment that will be the key objective here. At a most general level and independently of the measurement tool, the types of measurement we are considering are those reachable from information on:

- Projected cross sectional area of canopy elements (e.g. leaves, stems and trunks) at a given distance in a given direction;
- Size, shape and density of canopy elements in a volume;
- Canopy element distribution in trees and shrubs of varying heights and layers;
- The size of gaps and inter-element spacings at varying scales.

Of key value in determining these aspects of canopies is the use of varying size and shape of the Lidar beam. This, combined with the more commonly available range and waveform data makes the products described here richer than those currently available from existing Lidar or any other forest measurement systems.

Therefore, keeping in mind the issue of uncertainty between reflectance and amount (size and density) of scatterers we will proceed under the assumption that instruments

exist to carry out the six basic types of measurement listed above. By taking this approach, we have found that a vast range of previously under-utilised methodology and morphological operations can be re-vitalised to interpret the data and also many other areas not so far utilised for canopy structural measurement can be opened up for application and further research. These are topics of this ATBD.

To underline these primary objectives and to keep the principle that the Lidar is a tool in the activity rather than an end, the ATBD will be structured to outline:

1. Basic and essential forest structural measurement that the market needs and demands;

2. Existing methods – especially those that can be "re-vitalised" by accessible and advanced canopy Lidar data;

3. New and advanced methods enabled by the advancing technology.

By the end of the document we will have both a map for the software and processing directions as well as the interface specifications with which the needs of the market and its products can translate into system specifications.

2 MEASURING VEGETATION COVER AND STRUCTURE

2.1 Measurement of forests and component biomass

2.1.1 Forests – the Objective of the Measurement

Based on the definitions from the National Forest Inventory (NFI – see http://www.brs.gov.au:80/nfi/) a "forest" is:

"An area, incorporating all living and non-living components, that is dominated by trees having usually a single stem and a mature or potentially mature stand height exceeding 2 metres and with an existing or potential crown cover of overstorey strata about equal to or greater than 20 percent."

In later sections we will discuss the definition of crown cover and note that the above threshold can correspond in many cases to a projected foliage cover of about 10 percent. This definition therefore generally includes most of the open forests and woodlands of the remote parts of Australia.

The current focus of government agencies undertaking Greenhouse Inventory is also on such plant canopies of woody shrubs and trees (woody vegetation) that have a local crown cover above 20%, general height of their upper stratum greater than 2 metres and occurring in patches of no less than 50 hectares. This is the definition used by the OECD/IPCC in their Guidelines for National Greenhouse Gas Inventories (IPCC/OECD, 1995) and implemented in the Remote Sensing of Agricultural Land Cover Change 1990-1995 Project (Kitchin and Barson, 1998).

2.1.2 Phytometry of Plants, Plots and Stands

The measurements we will consider for these forests and woodlands can sometimes be made on individual plants but are more often taken on a group of plants to provide a statistical summary of forest properties. A local forest area where measurements are made will be called a "plot". A plot is assumed to be part of a larger area of similar type, composition and age class called a "stand". A stand can often also be identified as a unit of management for a forest.

Measurement of individual plants and assemblages of plants in stands is basic in agriculture, forestry, ecology and hydrology as well as in many related areas. The measurement of plants is sometimes called "Phytometry" (Ross, 1981) and direct phytometric measurements involve distinguishing the elements to be measured and providing data for their type as well as size, shape, area (e.g. surface area), volume and biomass. Measurement of plant assemblages involves their spacing as well as component arrangements and size so that terms like "cover" and "gap" (or porosity) in the canopies formed by the foliage of the trees in a stand mirror the distributions of distances between elements of the canopy. In this approach, the assemblages are described using spatial statistics and spatial models. A discussion of the terminology

used in spatial models in fields that are relevant to this document is provided in Appendix 4. The term "vegetation structure" is the ecological equivalent for this level of description and is dealt with in Section 2.2.

In many cases, phytometric measurements provide a means to study the light climate and availability in plant canopies and stands. Conversely, the measurement of the radiation field associated with plants has also been used for phytometric measurements due to their close interaction. More generally, indirect measurements can also make use of the strong correlations that exist between the sizes, shapes and distribution of canopy elements to develop "allometric" methods. These methods measure aspects of (e.g.) forests or trees using other (usually more accessible) measurements. Examples are the inference of foliage biomass from Diameter at Breast Height (DBH) or timber volume from basal area.

Very generally speaking, the growth of a forest in a period depends on the available light, water and nutrients and the age, condition and species makeup of the plant community at the time. The allocation of the increment of growth between different plant components (e.g. foliage, stems, trunks and roots) is usually highly correlated in a specific site and for a given mix of age classes and types of tree so that "size" as measured by any one of tree height, DBH, crown size, foliage amount etc all tend to change in a correlated way. This leads to the postulate that there are well-defined relationships between elements of a single "age class". Establishing these relationships in a particular community by direct measurements and estimating others by indirect measurements has been an important task for forest mensuration. However, for various reasons, including statistical sampling and the variability of vegetation properties, such relationships can be poor between stands in the same area and may not persist between sites across regions.

The search for allometric relationships is pursued because direct measurement of component biomass in forest canopies is difficult and time consuming. Forests are spatially highly variable and native forests (in particular) are very complex associations of species, age classes and plant growth-forms. When the objective is to assess biomass the situation is made harder as many indirect measurements (such as remote sensing) provide measures of component surface area (such as leaf area) or projected surface area rather than volume and mass. Trees grow to command quite large volumes in their crowns, which are filled with leaves having very high area to volume ratios. The components with greatest contribution to total area and those with the greatest contribution to total biomass are often in different parts of the canopy. For example, leaves have high surface area and low biomass compared with large stems and trunks. The large stems and trunks have a low area to volume relationship but usually form the most significant component of the overall biomass. On the other hand, if the objective is to assess water use by forests then leaf area density is a key measurement – but the task of measuring it accurately is no easier due to its spatially variable and often "clumped" distribution even within crowns.

This situation has led in many ways to the distinctions of approach between traditional forestry measurements and ecological measurements. The leaf area in a stand determines how it is able to capture light and use it in photosynthesis and also measures the respiring surface. Light and photosynthesis have traditionally been of greater interest to ecologists than foresters. In early stages of growth, trees develop

high amounts of leaf providing leaf area for photosynthesis and respiration. Stem wood is stored in trunks (for example) as a result of the annual increment in biomass production by the forest leading to older trees having a greater biomass in solid trunks. The "vertical" nature of these stems has led to forestry measurements that either work at the forest floor in horizontal directions (to obtain basal area and DBH for example) or else use surrogate data developed from plot measurements which are then used with the more convenient data that can be obtained quickly or sensed remotely – such as crown cover, crown size and tree height.

2.1.3 The activities that need to be addressed

To summarise the previous sections, the activities and industries associated with vegetation and vegetation cover mapping, monitoring and measurement may be broadly categorised as:

1. Environmental, Habitat and Conservation

   "Environmental" activities relevant to forest biomass and structural measurements include:

   Environmental reporting
   Environmental management
   Monitoring for sustainable land use
   Biodiversity & fauna/bird survey
   Water use and Water Table management
   Rehabilitation (minesites, defence areas & degraded lands)
   Powerline surveys for vegetation encroachment
   Corridor planning
   Assessment of landscape trafficability
   Greenhouse inventory and monitoring

   All of these require effective mapping, inventory, monitoring and assessment. We will discuss the general outline of the key variables that this measurement will need using as an example the National Vegetation Inventory System (NVIS) described below. The NVIS system has been established and is undergoing further development in the future by the National Land & Water Resources Audit (NLWRA) in Australia. It involves cover, structure, growth form and species at a range of levels of detail and also scale that will variously be needed to undertake vegetation measurement to support activities like those listed above.

2. Forestry

   Commercial forestry is a very large, worldwide industry producing sawlogs and pulp (woodchipping) and involves operations in many large areas of natural forests as well as extensive areas of plantation as well as smaller and more dispersed planted areas with ancillary uses such as salinity amelioration, erosion control, fuel production and windbreaks. These areas of operation will

be broadly divided into Native Forest and Plantation categories.

2.1.1 Native Forests

Native forests occupy a large area of the landmass of the world and are steadily being "mined" for timber and pulpwood. However, most foresters aim at sustainability and have followed practices of forest management for sustainable use for many years. Measurement is key to assessing current and potential yield as well as the sustainability of harvesting activities. Native forest measurement will provide a major challenge for new measurement technologies.

2.1.2 Plantations

Plantation forests for timber and pulp are rapidly increasing all over the world and also in Australia. Plantation forests are managed and have had well defined measurement activities in past years which essentially use traditional Forestry measurements and well established correlations to estimate yield at harvest. However, the rapid increase in areas planted and the introduction of new species has led to a situation where greater attention is being placed on measurement. The use of growth models to predict yield has called for more information relevant to environmental aspects (such as leaf area) and increased awareness of canopy structure. Structural information on "condition" (such as poorly performing areas, competition and understorey) has brought plantation foresters to place more emphasis on ecological, soil and physiological measurements.

3. Carbon

As previously mentioned, the Montreal and Kyoto Protocols have put considerable pressure on countries to account for changes in their forest covers as they relate to carbon storage and emissions. The Kyoto Protocol opens up the possibility for companies and countries to "trade" carbon through the use of forests as sinks in addition to ensuring that net carbon emission from forest and land use activities was not contributing to the countries target. Just how these effects can be accurately measured at the scale of a whole country is still not established.

In all of these areas of activity there are essential activities of forest measurement for inventory and monitoring. However, as the needs are different it is not surprising that different approaches have developed. Some of these are described in the following sections. In every case, the structure of the forest canopy is a primary attribute that is also very hard to measure directly in all but small and intensive plots and indirect methods (especially remote sensing) that can map structure are widely sought.

The Canopy Lidar Project has been exploring technology that has the capacity to combine remote sensing (such as from an airborne platform) with relatively direct measurement of forests and forest stands. It seeks to serve the needs for both ecological information (such as condition, water use and photosynthetic potential) as well as forestry information (such as biomass and timber volume) in a way that

currently used remote techniques are either unable or find difficult. The airborne Lidar systems described in this ATBD have been assessed to be the most likely technology that can assess vegetation structure remotely and the ground-based Lidar system as the most likely compatible technology for ground located plots. To describe the products the technology will produce and their relevance to forest measurement requires both an assessment of the ways in which vegetation cover and structure can be measured conventionally as well as through the information available from canopy Lidars.

2.2 Vegetation Structure

2.2.1 Environmental Mapping of Vegetation Structure

Vegetation Structure refers to the horizontal and vertical distribution of the components of biomass within a plant community (Walker and Hopkins, 1990). The vertical aspect of structure is usually expressed by stratification of the vegetation into layers that are related to age class and growth form variations in the vegetation. The vertical trace measuring the aggregate distribution of biomass at the level of plant components is the "Foliage Profile". The horizontal aspect of structure refers to the arrangement (spacing) and density (or cover) of plant material within a given layer and the size distributions of the "clearings" or "gaps" in the various layers. Spatial statistical models (see Appendix 4) and geometric probability provide very useful tools for the description and measurement of vegetation structure.

Although the emphasis in most of these definitions is on the foliage and other objects such as crowns and stems, the "gap" phase (or the spaces between foliage objects and clusters) through which light and rain can penetrate is as important in the way it determines the effects of canopy structure and also provides the means for (non-destructive) measurement of structure.

Vegetation structure has been recognised as a key variable in Australian native vegetation mapping. The base for the widely used structural descriptions by Carnahan *et al*. (1990), in the field guide of Walker and Hopkins (1990) and by Ritman (1995) can be traced from Wood (1930) through Williams (1950), Specht (1970, 1974), Beard (1976) and Carnahan (1976) to the more recent mapping activities. These classifications mostly recognise a triplet nomenclature for vegetation comprising upper, mid and lower layers (or strata) with varying functional characteristics (such as growth form, crown size, openness and cover) in the layers.

Walker and Hopkins (1990) stated that the minimum quantitative data set required to classify Australian vegetation according to structural formation includes, for each stratum, statistical summaries of:

- growth form (e.g. tree, shrub or grass),
- height (h),
- crown size (width, D and thickness T),
- crown cover (see below) and
- crown type (or openness).

These ideas have led to a number of canopy classifications in terms of structure. Recently, these have been brought together as part of the National Vegetation Inventory System (NVIS), which defines six levels of vegetation information shown in Table 1 taken from a working paper of the National Land and Water Resources Audit (NLWRA) (NLWRA, 2000a).

Table 1. The NVIS Information Hierarchy

Hierarchical Level	**Description**	**NVIS structural/floristic components required**
I	Class*	Dominant growth form for the ecologically dominant stratum.
II	Structural Formation*	Dominant growth form, cover and height for the ecologically dominant stratum.
III	Broad Floristic Formation**	Dominant growth form, cover, height and broad floristic code usually dominant land cover genus for the upper most or dominant stratum.
IV	Sub-Formation**	Dominant growth form, cover, height and broad floristic code usually dominant Genus and Family for the three traditional strata. (i.e. Upper, Mid and Ground).
V	Association**	Dominant growth form, height, cover and species (3 species) for the three traditional strata. (i.e. Upper, Mid and Ground).
VI	Sub-Association***	Dominant growth form, height, cover and species (5 species) for all layers/strata.

*Walker & Hopkins (1990)
**NVIS (defined for the NVIS Information Hierarchy)
***Beadle & Costin (1952)

This system, and the extensive range of data structures and definitions associated with it, is intended to integrate and unify currently used structural systems such as Specht (1995, 1974), Carnahan (1976, 1990), Beadle (1981), Walker & Hopkins (1990) and variants of the Carnahan and Specht systems that have been variously in use until recently.

The NVIS system ranges from a very broad description to very fine levels of detail. This range is needed to cover the interests and uses of national forests data, which include applications for environmental management and forestry. Among the differences claimed between the NVIS classification and previous ones is that it includes a finer definition of the strata (such as the addition of an "emergent" stratum) and a high level of species and structural description at the Association levels of the hierarchy. The definitions of growth form are also extended and detailed and the finest levels (IV-VI) include the scales of mapping relevant to forestry at the plot level. Many of these do, however, exist in some of the previous systems in various forms and the most important role of the NVIS classification is to provide a unifying description whereas before there had been a number of different descriptions.

The most serious question about this extensive scheme, however, is how it can be implemented at the scales of mapping needed for Australia-wide inventory and monitoring? It would seem that only remote sensing will be able to map effectively at

most of these scales over the whole of the country. However, current remote sensing technology is not successfully mapping at much below Levels I-III and then only as classes and not as measurements. There is clearly a need for improved remote sensing technology and compatible and linking ground level technology for Levels IV-VI if much of Australia is to be mapped in the way described by the NVIS at all of its Levels.

2.2.2 Applications to Forestry, Biodiversity & Carbon

In Forestry measurement, structure is usually interpreted as a result of age and only the Tree growth form in a dominant layer will normally be associated with a site of fair and merchantable quality. Structural measurements are usually focussed on the stem and trunks of the trees and the potential timber that they can yield. Measurements such as DBH, basal area, Crown length ratio and timber volume have evolved to describe this situation and will be addressed in more detail below. However, with the growing use of models to determine forest yield and interest in light climate and its implications for timber growth (Battaglia and Sands, 1998), there is now an increasing interest in canopies, light interception, leaf area and foliage profiles among forestry groups – and especially among managers of plantation forests.

For environmental applications and growth modelling, structure obviously determines canopy factors such as light climate and rainfall interception as well as ecological factors such as adaptation and competition between species in developing forests. In old growth forests, succession has been hypothesised to proceed largely via the generation of gaps by disturbance and consequent exploitation of the gaps by species with varying tolerance to light or shade (Shugart, 1984; Whitmore, 1989). The significance of structure for habitat and animal or bird populations is well known. For example, MacArthur and MacArthur (1961) described an early use of the vertical foliage distribution as a tool for inferring biodiversity (Bird Species Diversity). They showed how species number did not simply increase with height but was associated with the diversity of the foliage profile. Similarly, Peterson (1982) related bird species and densities to canopy structure through growth form and height. The existence of such relationships is not surprising – but the strength of some of them is.

In addition, an important driver for the work described here is the assessment of woody biomass in Greenhouse Inventory and monitoring changes in (above ground) woody biomass for such inventory and in environmental monitoring for both exploitation and rehabilitation. For example, in a recent effort to assess the release of carbon by forest clearing between 1990 and 1995, Barson *et al*. (2000) used Landsat imagery to determine the areas of change in woody vegetation cover to a high level of accuracy. To convert these to net carbon release, they first allocated the forest side of the change to a structural class – in this case a Carnahan class – which in most cases was defined from a very broad level map (Carnahan, 1990). They then completed the inference by associating biomass and carbon with each very broad structural class as in Table 2 (from Barson *et al*., 2000):

Table 2. National Greenhouse Gas Inventory biomass values and carbon content for major forest types

Forest type	Carnahan classes	Mature biomass (tonnes/ha)	Carbon (tonnes/ha)
Tropical /temperate forests	L4, M4, T3	227	113.5
Open forest	L3, M3	89	44.5
Woodland/ scrub	L2, M2	49	24.5

Clearly, an accurate determination of the structural class and local values of (minimally) cover and height of the areas of change is one major step in improving this methodology. Another will be the more accurate relationship between structural class and biomass – but this will need effective structural measurement technologies to be combined with traditional dry matter estimates and measurements at a variety of sites in Australia and may well require the relationship to be applied at a much more detailed level of a classification such as the NVIS one described above. Clearly, the influence of structure on these estimates and the key role of structural changes in determining carbon accounts and landscape rehabilitation makes it timely to review structural measurements and exploit newer technologies – such as airborne and spaceborne Lidars.

2.3 Vegetation Cover

The measurement of vegetation cover and related quantities is a key activity in forest and vegetation assessment. For the purposes of this document it is therefore useful to separate and discuss the various ideas of:

- Crown area density
- Crown cover
- Foliage area index
- Foliage cover

2.3.1 Crown area density (CAD)

Imagine that you mark out a sample plot and select all the trees with trunks in the plot. This is not always as easy as it sounds in the field and requires some principles of what is counted and what is not – especially with shrubs and other growth forms. Assuming these decisions can be made, if there are *n* such trees in the plot then the sample vertical crown area density is simply:

$$cad = \frac{1}{A_p}\sum_{j=1}^{n} a_j$$

where A_p is the area of the plot and a_j is the area of the vertical projection of the j'th crown with its trunk in the plot. (The use of lower case *cad* here denotes that it is a plot or sample estimate rather than an average or stand estimate). If enough plot samples are taken in a stand and the whole area is assumed to have a consistent underlying stand age, density of trees and access to resources the stand average Crown Area Density (upper case CAD) can be written:

$$CAD = \lambda \bar{A}$$

where λ is the underlying density of trees (number per hectare for instance) and $\bar{A}$ is the mean vertically projected crown area. This can be seen as the limit of increasing plot size (and number of trees it includes) of the estimate, which can be written:

$$\begin{aligned} cad &= \frac{n}{A_p}\left[\frac{1}{n}\sum_{j=1}^{n} a_j\right] \\ &= \lambda_n \bar{a}_n \end{aligned}$$

The CAD has been given various names by foresters and ecologists. Its sample estimate (*cad*) is a simple thing to measure in fixed size plots being the estimated tree density multiplied by the plot mean crown area. Some people have called it "treeness" and others "crown cover". However, it is not, as it stands, a measure of cover since the way the trees "cover" the ground depends on the way the trees (in fact, the tree trunks) are distributed on the ground.

If CAD is greater than 1.0 then the crowns will overlap. Because of this, CAD has been used as an index of competition although it is not very sensitive by itself. It is also worth pointing out that if the measured mean area parameter for the tree were cross sectional area of the trunks [measured using DBH] this quantity would be Basal Area.

2.3.2 Crown Cover (CC)

Crown Cover (CC) is related to, but not the same as, the CAD except when crowns do *not* overlap. It measures the percent of the area where a vertical ray will hit a crown (or 100 minus the percent of the area where a vertical ray will not hit a crown). For both a single sample patch and the mean for the whole stand, this value will depend on the way the trees are distributed and the overlap between the projected crowns – especially in vertically layered situations. However, it is a quantity that can be measured remotely by (for example) aerial photography in terms of the fractional area not covered by crowns.

If the trees are spatially randomly (or Poisson) distributed in an area then there is a simple relationship between Crown Cover and the Crown Area Density for the whole stand of the form:

$$\begin{aligned} CC &= 1 - e^{-CAD} \\ &= 1 - e^{-\lambda \bar{A}} \end{aligned}$$

This holds for the stand, however, and not for a patch unless the patch is allowed to become so large that its statistics are similar to those of the stand. The actual projected crown cover of the patch is highly variable and its relationship with the sample *cad* measured from (say) a fixed plot is complex. Cover is a characteristic of a forest that should be regarded as a statistical (or stand) measure rather than a plot measure. In

this statistical approach the objectives of measurement are therefore to estimate probabilities of gaps and possibly to use the variation of the samples from this probability to characterise the stand as well.

Since gaps are places where there is no cover, it is easy to see that we could just as well (and in the following prefer to) use the mean property of vertical gap probability in the form:

$$P_{gap,B} = e^{-CAD}$$
$$= e^{-\lambda \bar{A}}$$
$$CC = 1 - P_{gap,B}$$

where $P_{gap,B}$ is the Gap Probability or the probability of a gap in the stand for the passage of a vertical ray and the subscript "B" indicates that the gaps are "Between" the tree crowns.

Cover and Gap are complementary and since their inter-relationship will be extensively used in the following pages the relationships have been illustrated in Figure 2.1:

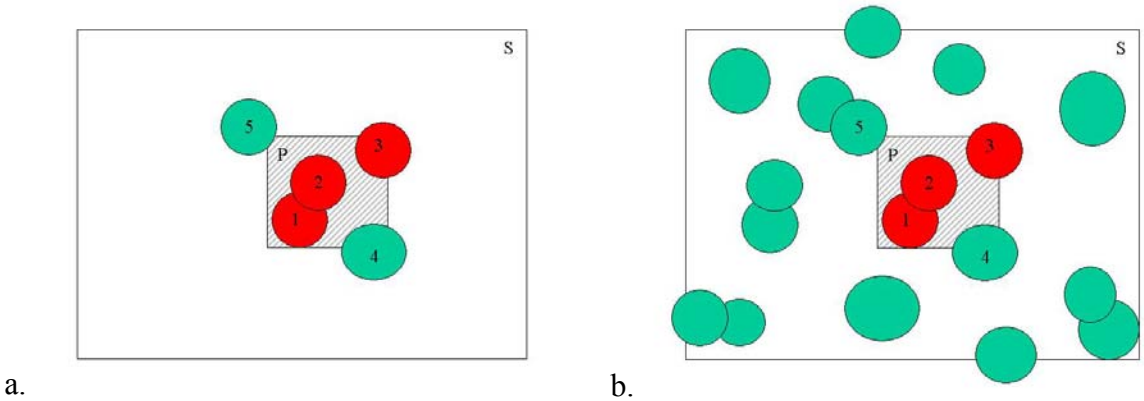

a. b.

Figure 2.1. (a) Measuring *cad* and crown cover in a Patch (or pixel or plot) P; (b) Measuring CAD and CC in a Stand or region S

In Figure 2.1 (a) a sample plot (or pixel or plot) is indicated and the three trees (marked 1, 2 and 3) with stems in the plot are coloured red. The trees marked 4 and 5 are not in – although they cover part of the plot. The relationship between the actual crown cover in the plot (the hatched area) and the computed sample *cad* is quite variable at this level as is the relationship between the number of trees (three) divided by the area of the plot and the stand density. For example, trees outside the plot can contribute to the sample CC in a plot. However, for the whole stand (Figure 2.1(b)) CAD (the sum of the areas of the crowns divided by the total area or the density multiplied by the mean crown area) and CC (the proportion of S covered by tree crown) will have converged and be predictable by the statistical relationship:

$$CC = 1 - e^{-CAD}$$

When the angle of view changes from the vertical, CAD and CC will also change in ways that depend on the size and shape of the crowns. Vertical views are "blind" to crown length or thickness (T) and only sense the crown diameter or width (D). Crown shape and crown length ratio (T/h, where h is the height of the tree) are therefore important additional measures needed to characterise crown cover. Among such additional measures, an important one is the Foliage Profile (Walker and Hopkins, 1990) that separates the vertical and horizontal factors in a plant canopy. This is introduced and derived in Section 2.6.

2.3.3 Foliage Area Index

If the primary interest is the foliage (as it would be for light interception and photosynthesis) then there is an equivalent notion to CAD of Foliage Area Index (FAI or sometimes LAI), which is the total of one-sided area of leaf, or foliage above a unit area of either a patch or stand.

In the case where we can define the FAI restricted to a single crown as FAI_W (where the subscript "W" indicates "within" crowns) it follows that the total FAI can be written as:

$$\begin{aligned} FAI &= \lambda\left[FAI_W \ \bar{A} \right] \\ &= CAD \times FAI_W \end{aligned}$$

This quantity is similar to "foliage cover" as defined by Walker and Hopkins (1990) but is more consistent as a measure of leaf amount than as a cover.

The FAI for a crown is the total one-sided leaf or foliage area in a crown divided by the projected crown area.

2.3.4 Foliage Cover

Another foliage measure, playing a similar role for foliage to that played by CC for crowns, is called Projected Foliage Cover (PFC). Specht (1974), Carnahan (1976) and Walker and Hopkins (1982; 1990) have used PFC in their classifications of Australian vegetation. PFC is the percent of the area where a vertical ray will hit at least one leaf or other foliage element. This type of "Cover" is more closely related to the amount of light that penetrates to the ground than CC – at least when the sun is near vertical in the sky.

If the trees are distributed with a Poisson distribution it can be shown that:

$$PFC = 1 - e^{-CAD*CF}$$

where CF is called the "Crown Factor". CF is introduced since a vertical ray may "hit" a crown but still pass through to the ground, as the crown is not completely filled by leaves. Crowns (especially those of Australian trees) are often quite open and should be regarded as clusters of foliage units rather than opaque or solid objects. In

field data the "Crown Factor" (CF) is the fraction of the vertical view covered by foliage within the crown for a vertical view from beneath the crown and therefore includes the cover of branches and small stems within the crown. CF is zero for an empty crown and 1.0 for an opaque crown.

We can also write:

$$CF = 1 - P_{gap,W}$$

where $P_{gap,W}$ is the average probability of finding a vertically accessible gap within (i.e. through) a crown. The estimate of PFC based on this is not strictly a "foliage" cover since branches and twigs are included, however, from a practical point of view it will still be referred to as PFC and a "pure" estimate of PFC is difficult if possible to measure in the field.

Walker and Hopkins (1990) defined "foliage cover" as their crown cover (i.e. CAD) multiplied by the crown factor. This definition, which mixes an amount of crown (CAD) with a projective cover (CF), is most useful in sparse canopies where foliage within the crowns clumps into relatively few modules and/or there is little or no overlap between crowns. If the leaves in crowns are sparse so that crowns are open (CF is small) and/or crown density is low (CAD is small) it can be seen that:

$$\begin{aligned} PFC &= 1 - e^{-CAD*CF} \\ &\approx CAD \times CF \end{aligned}$$

This expression, expressed as a percent, is the Walker and Hopkins (1990) "foliage cover" and is a useful measure over much of the Australian landscape. However, because we will work in both theory and practice with cases of densely filled crowns and/or high stem densities, we will not use the mixed quantity in this document. We have selected CAD and FAI (tree-ness and leaf-ness) as measures of quantity and CC and PFC as measures of ground cover.

In the case of distributed foliage (such as a crop canopy or leaves within a well filled crown) the cover will depend primarily on the nature of the foliage angle distribution or the way the foliage elements (including leaves, branches and twigs) are arranged in space. In the case of crown cover, the shape of the crowns is a significant factor in the relationship between density and cover. This becomes especially significant when you consider that the projected area of crowns and foliage depends on the direction of the ray that tests the cover. Generally, PFC is much less than crown cover although crown cover can sometimes be easier to measure (e.g.) from photography. It is often difficult to distinguish foliage and shadow in crowns in photographs, and vertical layering makes it even harder to establish the openness of crowns. Even in the field, crown measurements are generally simpler to define and make.

Because the leaves in Australian tree crowns are clumped into modules, the relationship between CF and the amount of leaf area in the crown can be complex. It is also difficult to estimate CF in the field in the face of such variation. Walker and Hopkins (1990) have provided a diagram to help people identify CF in the field. It is repeated here as Figure 2.2. The most important thing to keep in mind for later

consideration is that between the cases of crowns with the same CF it is likely that the leaf area in the crowns will vary quite a lot due to the effects of clumping and leaf hiding.

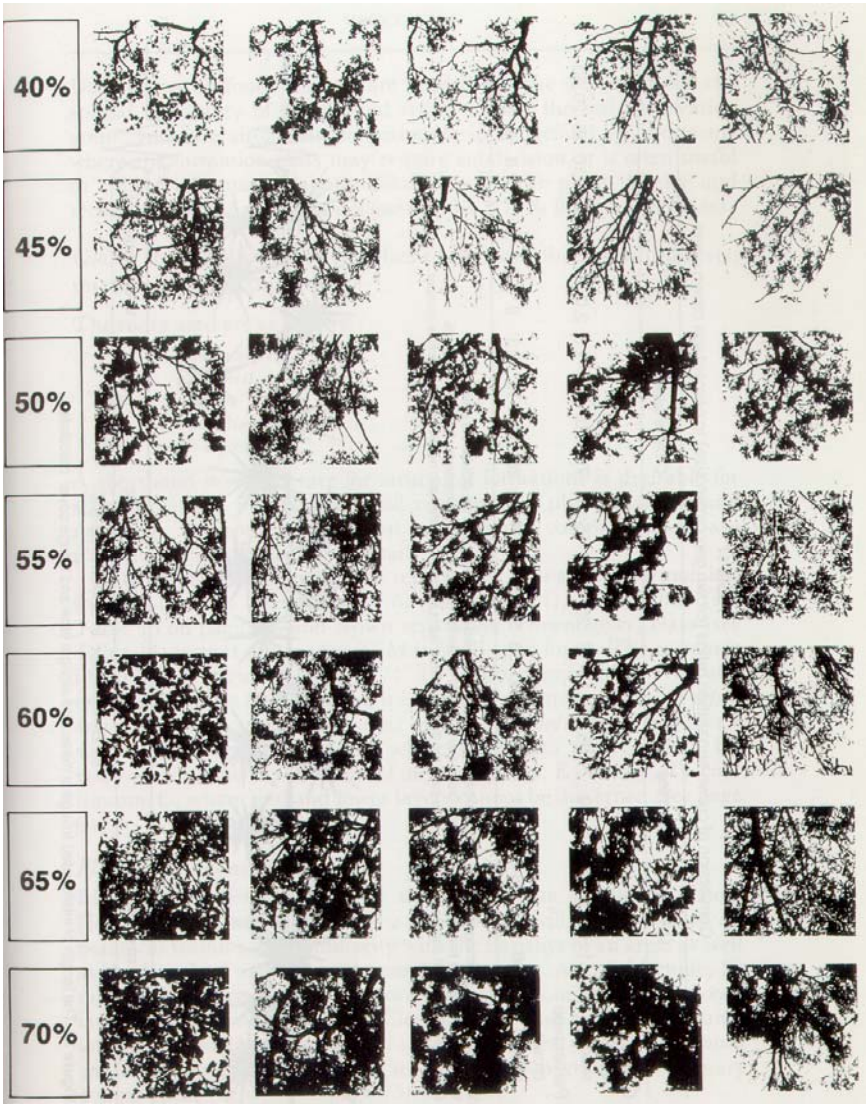

Figure 2.2. Examples of crowns with varying CF provided by Walker and Hopkins (1990). Examples in the rows all have the same CF but possibly varying amounts of leaf and stem.

2.3.5 Horizontally homogeneous leaf canopies

For a simple horizontally extended and non-clumped canopy composed primarily of leaves (such as might be found in crops or for pasture) the gap probability for a simple randomly distributed leaf canopy can be expressed analytically in terms of the leaf angle distribution and the vertical profile of leaf area density.

If the leaves are randomly arranged horizontally, are uniform in properties (but not necessarily abundance) in the vertical and the leaf angles have no azimuthal preference, then for a ray at zenith angle θ_v the probability of a gap in the foliage (i.e.

the probability the ray will pass through the canopy to the ground) is:

$$P_{gap}(\theta_v) = e^{-\int_0^h G(\mu_v, r)F(r)dr/\mu_v}$$

where:

F(r) is the vertical foliage leaf area density profile;
G is the Ross function that depends on the foliage angle distribution and possibly height in the canopy;
μ_v is the cosine of the view or ray zenith angle.

If the leaf angle distribution is uniform throughout the profile then it follows that at the forest floor:

$$P_{gap}(\theta_v) = e^{-G(\mu_v)L/\mu_v}$$
$$PFC = 1 - P_{gap}(0) = 1 - e^{-G(1)L}$$

where:

L is the leaf (more strictly "foliage") area index (or LAI, the total on one-sided foliage area per unit area of ground); and
G(1) is the Ross function for vertical view.

The relationship between the leaf area density and LAI is:

$$L = \int_0^h F(r)\, dr$$

The vertical view will show higher apparent cover for a given L if the foliage is "horizontal" in aspect and lower apparent cover for a given L if the foliage is "vertical" in aspect. The way this changes with view or test ray angle is, of course, valuable information and its use in the analysis of wide angle or hemispherical photography is well known. Based on models such as these, a number of field techniques for the estimation of L and the foliage angle distribution have been developed. These will be described below.

2.3.6 Clumped Canopies – Separating Crown and Foliage Effects

The relationship between Foliage Area Index (FAI) and foliage cover for leaf canopies is similar to that between CAD and crown cover. That is, it depends on the distribution of foliage both vertically and horizontally (Nilson, 1971). For woody vegetation, the foliage is clumped into crowns and the relationship is quite different from how it would be if the foliage were spread uniformly. For this reason, Cover and Cover indices are usually separated into crown and foliage effects.

In natural vegetation covers, the CAD is measured as well as some measure of crown openness or within-crown gap probability so that an approximate foliage cover can be

derived. One simple model we can use is to assume that the foliage within a crown is uniformly distributed in density and angle distribution.

If F is the foliage area per unit volume and G is the Ross G-function for the angle distribution a leaf filled crown will have an effective within-crown LAI or FAI (L_W) defined as:

$$L_W = F\ \bar{s}$$

where $\bar{s}$ is the mean vertical distance through the crown which is a function of the crown shape and depth. If the foliage elements are randomly distributed with Poisson density then the average vertical probability of a gap through the crown is:

$$P_{gap,W} = \overline{e^{-G(1)F\,s}}$$

$$and$$

$$CF = 1 - P_{gap,W}$$

It follows that F (or L_W) can potentially be estimated from CF if the crown shapes and angle distributions of the foliage of the species of vegetation are known. In such cases, the total leaf (or foliage) area for a stand could be found as:

$$FAI = \lambda \bar{A} \times F\bar{s}$$
$$= CAD \times L_W$$

In view of the use of these formulae to infer F from $P_{gap,W}$ in Section 2.6 and the use of the formulae in a simplified but clumped model for Lidar data, the expressions for of s/T (where T is crown thickness as before) and the relationships between CF and F are derived in Appendix 3 for a variety of crown shapes.

Real trees are, of course, highly variable in their structure and within crown foliage distribution. Therefore, the statistical nature of all of these measures must be taken into account and accepted for practical use. Using statistics means sampling and access to sufficient samples. However, in the highly varying covers of Australia it has usually been difficult to take (or afford) sufficient ground samples and difficult even to make effective measurements on a single sample plot. There is need to overcome this limitation and the way it may be helped by Lidar technology is discussed later in the document.

2.4 Vegetation Height

The idea of the "height" of an individual tree might seem well defined. However, the height associated with a plot or stand, or the height associated with a canopy layer or stratum can be defined in a number of ways and may be used in different ways depending on the purpose of the measurement. This needs some attention. Moreover, even the height of a single tree can pose some challenges in the field. It is often found that different people and/or different techniques arrive at different values. This occurs

because crowns are generally "ragged" or open with leaves clumped into modules or shoots and so that the choice of the apparently highest point can be dependent on the position of the person making the measurement and the method of measurement.

One fairly obvious statistic is the mean height of all the trees in a layer or stratum that occur within a plot of specified size (e.g. 20m by 20m). This measure is sometimes used, possibly together with maximum height, to characterise the upper layer where decisions may be easier. This measure assumes layers or strata are defined before the heights are measured. Magnussen and Boudewyn (1998) quote Loetsch *et al*. (1973) in reference to Lorey's mean height. Lorey's mean height is the basal area weighted average tree height in a plot. As trees with large DBH are also often/usually the taller trees this measure will be greater than the mean height and may be well suited for use in a plot of basal area against height. The mean of the "in" trees in Angle Count (plotless) surveys (see Section 3.1.2) is very close to Lorey's mean height and can be used as an alternative.

If height is associated with the mean of an "envelope" touching the tallest trees then neither the mean height over a stand nor the Lorey's mean height will be a good definition to use. In addition, forests are often thinned so that a definition based only on the higher trees may be independent of these and other lower storey modifications. Lewis (1971) defines a quantity called "Predominant height" (PDH) for pines in South Australia. PDH is defined theoretically as the mean height of the 75 tallest trees per hectare. In practice it is not possible to make such a measurement with reasonable effort and a pragmatic definition is accepted as the mean height of a smaller number of tallest trees in some smaller area such as the mean of the single tallest trees in each of four sub-areas of a 0.05ha plot. The base (theoretical) density of the selected trees also varies between states in Australia. Wood and Brack (1999) quote examples of NSW and ACT where it is 40 trees per hectare; 50 per hectare in Queensland as well as the 75 per hectare in South Australia.

In the paper by Garcia (1998), a similar quantity called "top height" is discussed. Top height has been used in a number of countries and is defined (in a similar way to predominant height) as the average of the 100 largest[2] trees per hectare, 10 largest trees per 0.1 hectare (31 m by 31 m plot) or 4 largest trees per 0.04 hectare (or 20 m by 20 m plot). It has been pointed out by a number of authors (by Matern, 1976 for example)[3] that top height defined in this way is a function of plot size so that the plot size must be specified as part of the definition. It is easy to see, for example, that taking the average of the 4 largest trees per 0.04 hectare in 25 plots will not be the same as averaging the 100 largest trees in the complete hectare.

Garcia (1998) notes that in Sweden the standard is taken to be the 10 largest in 0.1 hectare and in the UK it is taken as the largest tree in 0.01 hectare. A variant favoured by ForestrySA (Greg Saunders PC) is the average the largest tree in each of four quadrants of a 0.05 hectare (25 by 20 metre) plot. It is obviously important to be clear on which of the definitions has been used – particularly if the height data have been used to develop and calibrate allometric equations. In the face of such variation,

[2] Note that the use of "largest" in this definition allows for the trees to be selected on the basis of DBH or height.

[3] Briefly, the mean of the "m" largest trees in an area A will be greater than (or equal to) the mean of the largest tree in each of "m" equal and disjoint subdivisions of A.

Garcia (1998) proposed that the definitions always be expressed as means of a number of sample sites of the smallest size (such as 0.01 hectare) in which the tallest tree is selected.

An alternative for ecological measurements is to take the mean height of trees identified as part of a canopy layer as a measure of the mid-point of the layer with the minimum and maximum heights as a measure of the canopy or layer depth. It is possible, however, that maximum height is not a very representative measure and something more like the forester's "predominant height" is also useful in order to obtain a stable height for the top of the upper layer of a stand in environmental and ecological applications. When the highest layer consists of emergent trees above a denser canopy layer (the dominant stratum) the definitions of the predominant height or top height quoted above should capture the emergent layer – but may not. In this case, maximum height will be an additional and useful statistic to include. Obviously, if the layering can be defined it is best to establish the height distribution of the trees within the layers as well. Stratification by species or association is also potentially very useful.

The NVIS system (NLWRA, 2000a) uses a quantity called "layer height" which is defined as the top of the stratum or the bulk of the vegetative material making up the stratum. This is not necessarily based on individual tree measurements and is a canopy or foliage-oriented definition. The NVIS system also defines an average layer height as the average height of the region where the vegetative material lies. Again, this is foliage based rather than tree based. Their definitions of top height and dominant height do not seem to be the same as those of foresters.

Magnussen and Boudewyn (1998) have used terrain Lidar to estimate tree heights. They found that, provided a sufficient density of Lidar shots are made (e.g. at least 1 per $5m^2$ or average spacing of 2.3 m) the quantiles of the vertical hit probability distributions and average plot height can be reconciled quite accurately for some forests. Such data could be related closely to the layer height defined above. However, foresters do normally not use quantiles of the complete height distribution in defining predominant and top heights. Modelling both the terrain and canopy Lidars described later will help resolve some of the differences in approach and findings due to definition as well as the (growth form dependent) biases that exist between Lidar heights and other estimates.

Foresters are interested in the amount of trunk available for sawlogs. To support this they sometimes define a height called "merchantable height" for single trees which is (Brack, 1999) the distance from the base of the tree to the first occurrence of either:

- The highest point on the main stem where the stem diameter is not less than some specified value, or
- The lowest point on the main stem, above the stump, where utilisation of the stem is limited by branching or other defect.

An alternative is the more easily measured "bole height" which is the distance from the base of the tree to the first living branch that forms part of the crown. Lewis (1971) called this the "green level". This height can be estimated from the tree height by using a previously obtained estimate of the crown length ratio (T/h where T is the

crown thickness). It is therefore important for both forestry and ecological studies to have estimates of the vertical crown length as well as tree height.

For stands, height and crown length ratio can therefore be defined and together with crown diameter and DBH define significant parameters for both ecological and forestry measurements.

2.5 The Structure Diagram

The Structure Diagram (or "structuregram", as illustrated in Figure 2.3) is a plot of height against cover (usually predominant height and crown cover). Cover and height are the primary parameters involved in all current structural descriptions of forests used in Australia. Despite this, there are few maps of cover and height classes over most of Australia that have a high level of measurement accuracy. Walker and Gillison (1982) extended the cover and height classification to include the variability associated with different structural categories. It was an important development but it is even harder to measure over large areas.

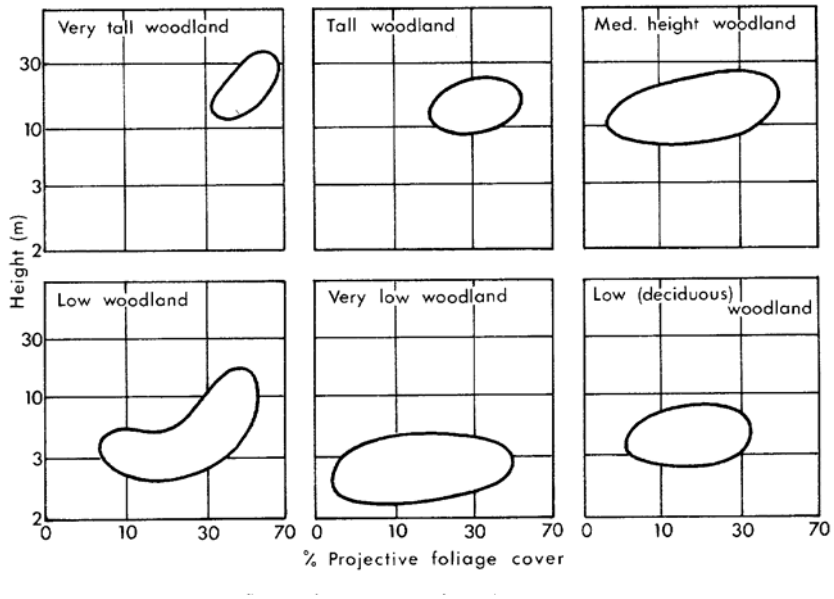

Figure 2.3. Structure diagrams of observed woodland categories (Walker and Gillison in CSIRO DLUR Annual Report, 1979)

The Structure Diagram is the ecological equivalent to the foresters' Stand Height Curve which plots predominant height (or sometimes bole height or the Lorey's height) against DBH or Basal Area. This plot is sometimes used to predict height when only DBH (or BA) is known for input into Volume Tables. A steep slope in the Stand height curve is taken to indicate a young stand which is still sorting out dominance. In older stands the curve becomes flatter. Also, if a site has both high DBH (or BA) and height it is usually a site with high quality for timber. The Structure Diagram provides ecologists with similar kinds information on age and "maturity" in the more complex forest stands of native vegetation areas. In this case, native vegetation classes are generally initially stratified by their location in the Structure

Diagram as illustrated in Figure 2.3 and in the examples taken from data for Australian savanna types in Walker and Gillison (1982 , Page 15, Figure 3).

The NVIS broad classification in terms of Carnahan classes (see Appendix 1) has the form outlined in Table 3, which can provide a way to divide up the compartments of the structure diagram and allocate classes. However, when data are taken in the field, the mean values of cover and height (or predominant height) in the plots within a vegetation stand will show considerable variation between plots in the same stand. This variation is dependent on the plot size over which the measurements were taken. If a plot size is very small, the classification of the sample plots could cover the whole of the above table! Hence, a structure diagram or cover/height classification needs to be accompanied by information on the size of the plot (or length and type of transect) used to obtain the data or over which the cover is assumed to be a measure.

Table 3. NVIS Cover/Height Categories

		Foliage cover (percent)			
		Closed forest	Open forest	Woodland	Non-forest
Height (metres)		>70%	30-70%	10-30%	<10%
Tall trees	>30m	T4	T3	T2	T1
Medium trees	10-30m	M4	M3	M2	M1
Low trees	6-10m	L4	L3	L2	L1
Tall shrubs	2-6 m	S4	S3	S2	S1

This information is also needed for any type of “cover” or “cover”-related data. That is, the variance of cover and height depend crucially on the plot size as well as the density and sizes of the tree crowns. The variation is as much a characteristic of the stand as the mean of the cover and height and the potential existence of “optimum” plot sizes for specific types of information needs more consideration in the future than it has had to date. 20 by 20 metre plots (0.04 ha) or 20 by 25 metre plots (0.05 ha) are commonly used (especially in forestry applications) but they are perhaps still too variable for most native Australian open forests and woodlands. Because of this, traditional Structure Diagrams often show forest and woodland classes as very broad areas of varying cover and height. To reduce the natural variability, Walker and Hopkins (1990) recommend the use of a zig-zag transect. However, if transects are used it is important to establish the effective averaging area to provide a consistent base for data interpretation and comparison.

Like the Stand Height Curve, in a mixed age community the aggregate Structure Diagram will show an increase in both cover and height as sampling moves from cleared areas to mature stands. It is theoretically possible to disaggregate and classify sites on the basis of this diagram and its variance alone. However, there has not been sufficient field data available to make this an operational product or process in environmental forest mapping. To fully implement a detailed structural classification, however, it is also necessary to disaggregate the Structure Diagram into Upper, Middle and Lower layers. The disaggregated Structure Diagrams that result form the primary structural descriptions for the system and in places where such data are spatially distributed it is possible to plot height as a spatial surface with indication of cover. Up to this time, the main limiting factor against the routine generation and use

of such Structure Diagrams – possibly for different plot sizes – has been the difficult and laborious task of collecting the data.

2.6 The (Actual) Foliage Profile

A foliage profile (FP) is a plot of the foliage area per unit horizontal area in a thin layer or "slice" through a canopy as a function of height above the ground (see Figure 2.4). The cumulative sum (integral) from the top of the canopy to the ground is the total foliage area index (FAI). The FP expands the basic structural description of canopies provided by the Structure Diagram (height of dominant stratum and cover) to include multi-layer information for the canopy.

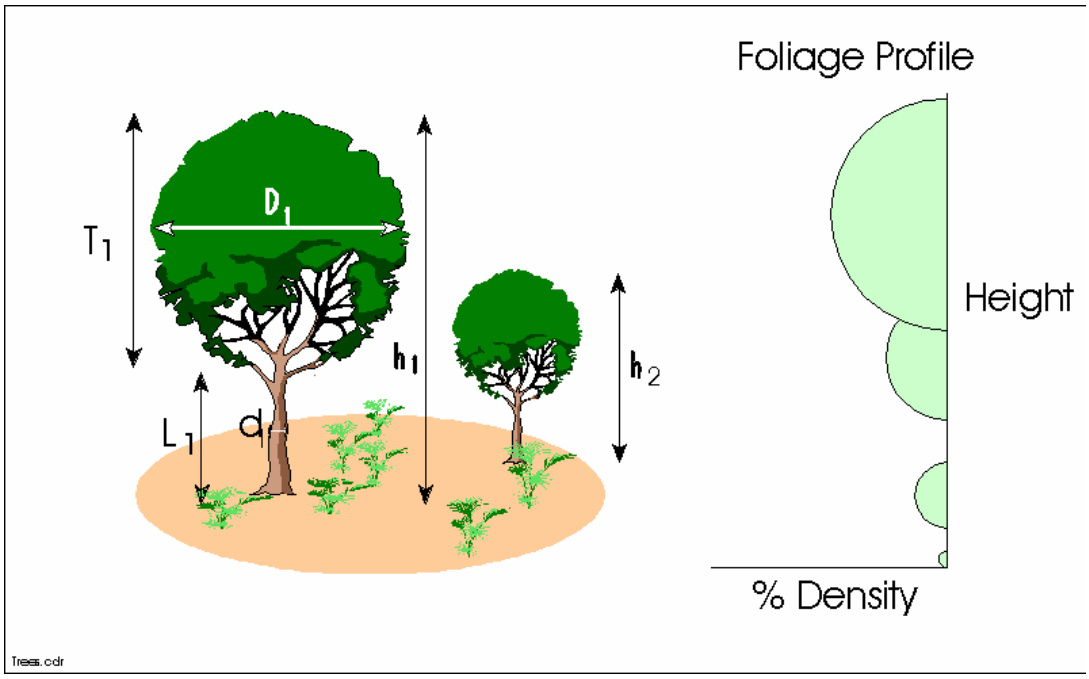

Figure 2.4. Foliage Profile for a multi-layer canopy

The FP is generally seen to provide valuable additional information about a canopy and its structure to that of the structure diagram. The added information is about layering and vertical distribution of biomass. The FP also brings foliage area into the description rather than (just) cover. The relationship between cover and foliage area is s function of the structure made clearer by the FP. The FP can therefore be put to many important uses – such as characterisation of canopy layering, definition of the layer heights and average heights, development of Structure Diagrams for the layers, characterisation of habitats, computation of effective flux resistances and modelling of Lidar returns. Despite these important uses, it is not easy to gather the field data needed for the FP. This has been done in the past only by laborious fieldwork or time consuming stereo aerial photograph interpretation in the past and the sampling involved could rarely overcome the spatial variation encountered. Consequently, the relationships between the FP and foliage area index and the above applications have not previously been fully utilised or developed to an operational tool for vegetation assessment.

Vegetation structure mapping from remote sensing (e.g. multi-view angle data) has been investigated as a tool for obtaining the FP but of the methods available only canopy Lidar seems to offer effective means to derive the FP – and then with some assumptions and collateral information about the canopy. However, the Lidar and also other forms of gap based canopy sounding techniques generally only give us an "apparent" Foliage Profile. In anticipation of this we will call the Foliage Profile the *Actual* Foliage Profile (FP_{act}).

2.6.1 Vegetation Structure Model

The basic structural canopy description used here to derive actual foliage profiles is that described by Walker and Hopkins (1990) with added field techniques described by Walker *et al*. (1987), Walker and Penridge (1987, 1988), Penridge and Walker (1988). This section describes the Walker/Penridge FP and extends it to include within-crown foliage density and hence a full and consistent computation of a FP that sums to an estimated FAI. It is applied later to a data set described by McVicar *et al*. (1996) and the FPs compared with separate measurements of FAI.

The description of the canopy by Walker and Hopkins (1990), like most current structural classifications, recognised three basic strata – an Upper Stratum (U) consisting of the tallest significant growth form, a Lower Stratum (or Ground Stratum) (L) of all vegetation below 1 metre and a Mid Stratum (M) of all vegetation between the upper and lower strata. In this description, the upper stratum (U) contains only one type of vegetation, but L and M (if they are used) can have a number of vegetation types present – including grass. Grass is described only in terms of cover and height.

Vegetation types are basically described by crown shape and include crowns based on ellipsoids, cones or cylinders. The description of a vegetation type consists of mean values for:

- Tree Height (h)
- Crown Width (D)
- Crown Depth (T) or crown length ratio (T/h)
- Crown Factor (CF)

Crown radius (r=D/2) is also used in the formulae listed below.

As described in previous sections, CF can be related to the average probability of a vertical gap through a crown (or within-crown gap probability) as:

$$CF/100 = 1 - \overline{P}_{gap,W}$$

The crown area density (CAD) of each type of growth form in each layer is needed to complete the description. The field techniques used to obtain CAD are not discussed here but themselves provide an area of study and necessary refinement that needs to be addressed in any activities to validate Lidar derived information.

The cover measurements are all affected by the nature of the distributions of trees and the tree shapes and sizes. For example, crown cover, in the sense of the amount of background covered by crowns will depend on the distribution of the trees but in the case where the trees (i.e. stems) are distributed in a Poisson distribution:

$$\begin{aligned} CC(\%) &= 100(1-e^{-\lambda \bar{A}_c}) \\ &= 100(1-e^{-CAD}) \end{aligned}$$

where, as before, the vertical probability of a gap between crowns can be written:

$$\begin{aligned} \bar{P}_{gap,B} &= e^{-\lambda \bar{A}_c} \\ &= e^{-CAD} \end{aligned}$$

The actual cover (projective foliage cover) of the ground by foliage of a single Type, assuming most areas of the ground have at most one tree of the Type vertically above them in any one layer, can be written:

$$\begin{aligned} PFC(\%) &= 100\left(1-e^{-\lambda \bar{A}_c (1-\bar{P}_{gap,W})}\right) \\ &= 100\left(1-e^{-(CC \times CF)}\right) \end{aligned}$$

The Poisson distribution will be assumed for the cases described here and it is assumed that different Types and trees in different layers are independently distributed.

2.6.2 Canopy Foliage Profile (FP)

The within-crown foliage density is needed to generate the FP. If the within-crown foliage density is known then FP is simply obtained by summing the profiles for each of the Types for each layer measured using the above scheme.

Foliage density is defined as foliage area (such as one-sided leaf area or half stem surface area) per unit volume. Consider a thin horizontal "slice" cutting through the trees of a single Type at a given height z. The result will be a set of disk-like slices of foliage with contribution to FAI of:

$$f(z) = \lambda a_c(z)\, F(z)$$

where $a_c(z)$ is the cross sectional area of a slice of the crown at the height z for the Type. Note that a Type is assumed here to have a constant size and shape.

F can change with height (i.e. *z*) in this general formulation but we will not let it vary with height for the derivations in this document. That is, we will be assuming, for each crown Type, that the foliage fills the crown and is uniformly distributed with density F. F can (and normally will) be different for different vegetation Types and Types occur independently within and between layers.

The foliage area index (FAI) for a single Type can be found by summing over these slices so that:

$$FAI = L = \int_0^h f(z)dz$$

where h is the tree height (to the tops of the trees) of the Type.

The expression for *f(z)* depends on the shape of the trees. It is convenient therefore to define shape factors *S(h,T,z)* for different types of crowns in terms of which we can define the FP.

2.6.2.1 Area contribution for Ellipsoids ($S_{ellip}(h,T,z)$)

If the tree Type is ellipsoidal then it follows that:

$$\begin{aligned} a_c(z) &= \pi r^2 \left[1 - \frac{(z-(h-T/2))^2}{(T/2)^2} \right] \\ &= \bar{A}_c \left[1 - \frac{(z-(h-T/2))^2}{(T/2)^2} \right] \quad h-T \le z \le h \\ &= \bar{A}_c \; S_{ellip}(h,T,z) \end{aligned}$$

where *S(h,T,z)* depends on the crown shape and dimensions (e.g. in this case only on the crown length ratio T/h and the relative height above the ground z/h).

2.6.2.2 Area contribution for Cones ($S_{cone}(h,T,z)$)

A second common shape is a cone on a stick. In this case, with h as the tree height and T as cone thickness (with crown diameter D as the base of the cone) it is simple to show that (using the above notation):

$$\begin{aligned} S_{cone}(h,T,z) &= \frac{(h-z)^2}{T^2} \quad h-T \le z \le h \\ &= 0 \qquad\qquad else \end{aligned}$$

again, S depends only on the crown length ratio T/h and the relative height above the ground z/h.

2.6.2.3 Grass contribution

Grass is considered as a layer so that it contributes its F value at each height between the ground and its height h.

That is:

$$S_{grass}(h,T,z) = 1 \quad 0 \le z \le h$$
$$= 0 \quad else$$

Also, by convention we assume that for grass, CAD=1.0.

2.6.2.4 General expression for FP_{act}

Hence, for a given shape of crown:

$$f(z) = \lambda \bar{A}_c \; S(h,T,z)\, F(z)$$
$$= CAD\; S(h,T,z)\, F(z)$$

2.6.3 The Actual FP and Total FAI for a Canopy

The total FP for a multi-layered multi-type canopy is obtained by summing the contributions from each (independent) Type over the independent layers. The sum over all slices is the total FAI for the canopy.

$$FP_{act}(z) = \sum_{i=1}^{ns} \sum_{j=1}^{ntype_i} f_{ij}(z) = \sum_{i=1}^{ns} \sum_{j=1}^{ntype_i} \left(\lambda \bar{A}_c\right)_{ij} \; S_{ij}(h,T,z)\, F_{ij}$$
$$= \sum_{i=1}^{ns} \sum_{j=1}^{ntype_i} CAD_{ij} \; S_{ij}(h_{ij},T_{ij},z)\, F_{ij}$$

where *ns* is the number of strata and *ntype(i)* the number of foliage types in stratum *i*.

For example, Figure 2.5 shows an actual foliage profile generated for a three layer open forest area in Goonoo State Forest from among the examples considered later from the Murray Darling Basin. In the plot, the height (z) is plotted as the horizontal axis and the actual foliage profile value at the height (foliage density) plotted as the vertical axis because it was more convenient for the software involved. The FP plots are often shown with height as the vertical axis.

The total foliage area index is:

$$FAI = \int_0^{h_{\max}} FP_{act}(z)\, dz$$

In this case the total FAI was 1.05 m^2/m^2.

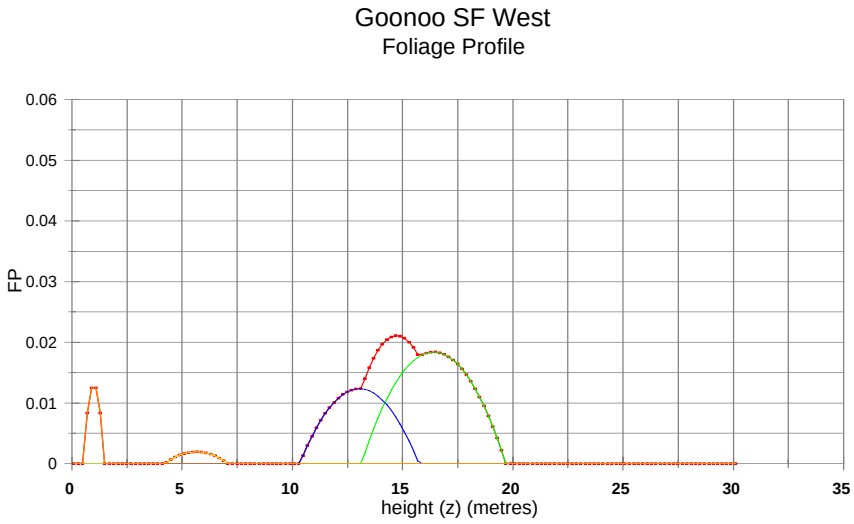

Figure 2.5. Foliage Profile for Goonoo State Forest West

It is also possible to accommodate the heights of the types in the layers being not fixed but having a probability distribution *P(h)* so that:

$$FP_{act}(z) = \sum_{i=1}^{ns} \sum_{j=1}^{ntype_i} CAI_{ij}\ F_{ij} \int_{h_{ij\,\min}}^{h_{ij\,\max}} P(h_{ij}) S_{ij}(h_{ij}, T_{ij}, z)\, dh_{ij}$$

Sometimes, however, the canopy can be described as a single dominant stratum with trees having a height distribution *P(h)*. In this case we could write:

$$FP_{Act}(z) = \int_{h_1}^{h_2} \lambda(h) \bar{A}\, F_p\ S(h, T, z)\, dh$$

$$\lambda(h) = \lambda\ P(h)$$

$$FP_{Act}(z) = \lambda \bar{A}\, F_p \int_{h_1}^{h_2} P(h)\ S(h, T, z)\, dh$$

3 METHODS FOR STRUCTURAL PHYTOMETRY

3.1 Basal Area and Timber Volume

Forestry measurements usually take a "horizontal" view at the floor of the forest to assess timber yield and site quality. The objective, in this case, is to assess the number, diameter and length of satisfactory saw-logs that can or will be extracted from an area of forest. In the case of wood chipping, the foliage and the smaller stems assume greater importance but generally it is the trunk and main stems that contribute most to total biomass. The measurements needed for these two cases will not be identical and assessment for chipping could well use methods more like those of environmental vegetation assessment than those used to assess saw-logs.

Basal Area can be expressed as:

$$BA = \lambda \frac{\pi}{4} \overline{DBH^2}$$

where λ is the tree density and the average DBH is the average of the squares of DBH. This is different, in general, from the square of the mean DBH.

Timber volume (V) in an area is normally defined in terms of DBH, the distribution of DBH (the Stand Table), the height to green level, or Crown Length Ratio (ratio of crown thickness or length to height, T/h) and the "Taper factor" (or "Form Factor") which describes the average shape of the trunks (or effect of the shape on the volume estimate) for the major species being assessed. However, it is an objective of much forest measurement to establish sites and conditions where there are strong relationships between these factors such that V can be estimated accurately with a few key pieces of information. Typically, these are BA, DBH and possibly h.

3.1.1 Site Data and Timber Cruising

Forest assessment is usually done by using one or more of the following sampling schemes.

- Fixed size (including permanent growth and temporary) plots;
- Variable size (usually temporary) plots; and
- Cruising.

In fixed size plot measurement, the site is chosen in some "random" way and a detailed set of data is taken at the fixed size sites.

Typical direct measurements on the primary or dominant stratum in the plots (often permanent growth plots) that are measured in a commercial production forest include:

- Diameter at Breast Height (DBH) and its distribution (or Stand Table)
- Tree density
- Height of dominant stratum (h)
- Crown diameters (D) and thickness or length (T)
- Bole height (an alternative to T)
- Crown length ratio (measured as T/h)
- Basal Area (BA) the area of trunk cross section per ha
- Taper factor
- Log Volume (V)
- Crown Closure or density (CC or CAD)
- Site Index
- Stand height curve (plot of height as a function of DBH or BA)

Not all of these need be taken in practice and estimates of some are often derived from a smaller base set of data. For example, basal area (BA) is sometimes derived from density and mean square DBH; volume is usually derived from stand tables using one or more of BA, DBH and h; and crown closure is sometimes derived from mean crown size and tree density. In fixed size plot sampling the selected measurements are made on all trees in (say) a 20 by 20 metre plot for a number of plots.

Basal Area, tree density, heights, crown length ratio, taper factor (which is usually assumed for a given community) and DBH distribution are all potentially primary information to estimate the number and quality of saw logs in a stand or develop stand relationships such as V as a function of BA and h -or BA alone.

For example, a predictive relationship such as:

$$V = Fh * BA$$
$$Fh = a_1 + a_2 * h$$
$$= \frac{V}{BA}$$

where, Fh is called the "Form Height", can often be derived from the fixed size sites using volume tables and the detailed tree data and extended to as many sites as can be covered by a survey that only estimates basal area and (possibly) height to provide estimates of timber volume at a large number of sites. However, the validity of the relationships will often not persist out of the stands in question or to areas with different species, growth forms, structures or age classes.

Kuusela (1965) expresses the volume relationship in terms of a factor he calls "form factor" (*f*), which is calibrated to take into account tree taper:

$$V = BA \times h \times f$$

The factor *f* depends on the tree type and is regressed on DBH. If stem diameter at two heights is available the sensitivity of the relationship to taper is increased. The form factor is probably more commonly used than form height and on a stand basis

can be derived from theoretical or observed relationships between volume, BA and hight so that:

$$f = \frac{V}{BA \times h} = \frac{Fh}{h}$$

Opie (1976) has developed form factor models for a range of Australian sites and tree types. For example, if tree stems are modelled as cones with base diameter equal to the DBH and height h then the form factor is simply one third (⅓).

Following the development of these and similar models at sites, cruising is then normally used to extend the relationships found between the measurements to other areas. Experienced people, using purely ocular assessments, can make excellent site assessments. On the other hand, it is also common to use portable instruments to make measurements such as basal area and tree height to calibrate relationships with site quality and timber volume as expressed in a general "site-index".

For example, the following Table 4 is after Lewis (1971) and shows a set of seven site quality indices assessed by experienced people at 9.5 years after planting in pine plantations in the SE of South Australia. The monotonic relationship between the different measurements indicates the underlying assumptions that biomass increment drives the growth of all the plant components. It is assumed that site differences are due to site quality and that future growth for the next 20 years is well predicted from knowledge of site index. The accurate mapping of site index is a key objective for any remote sensing. In current surveys, despite the numerical keys in the table, site quality index is mostly assessed visually. The cruising assessors are normally trained (or calibrated) at sites where detailed measurements are taken before the assessments are made.

Table 4. Indices used for Site Quality Assessment (SQA). For *Pinus Radiata* stands in South Australia at age 9½ years

SQ	Vol to 10cm u.b.: m^3/ha	Basal area: m^2/ha		Predominant Height: m	Green Level: m		Maximum Tree Diameters: cm	
		2.5 x 2.5	2.0 x 2.0		2.5 x 2.5 stands	2.0 x 2.0 stands	Ca. 2.5 x 2.5 stands	Ca. 2.0 x 2.0 stands
I...	>226	>42.2	>43.8	>17.0	>6.1	>6.4	22cm Obvious	22cm Few 20 cm Obvious
II..	178 – 226	36.7 – 42.2	39.0 – 43.8	15.7 – 17.0	4.9 – 6.1	5.2 – 6.4	22cm Few ….	22 cm Nil 20 cm Plenty
III.	132-178	31.0 – 42.2	33.7 – 39.0	14.4 – 15.7	3.4 – 4.9	4.0 – 5.2	22 cm Nil 20 cm Obvious	20 cm Few
IV.	85 – 132	25.3 – 31.0	27.3 – 33.7	13.1 – 14.4	1.8 – 3.4	2.7 – 4.0	20 cm Few	20 cm Few 18 cm Obvious
V.	43 – 85	18.6 – 25.3	20.4 – 27.3	11.8 – 13.1	1.2 – 1.8	1.8 – 2.7	20 cm Nil	18 cm Few
VI.	12 – 43	10.3 – 18.6	13.3 – 20.4	10.5 – 11.8	<1.2	0.9 – 1.8	18 cm Few	18 cm Nil 17 cm Obvious
VII	<12	<10.3	<13.3	<10.5	<1.2	<0.9	16 cm Few	16 cm Few

If this Table is assumed to accurately represent such forests then it can be used to summarise measurements for the situation where limited data are taken in the cruise. For example, referring to the form height above, Figure 3.1 shows the relationship

between form height (V/BA) and h which is fitted by the approximation (with an R2 of 0.9997):

$$V / BA = -15.14 + 2.109 \times h - 0.053 \times h^2$$

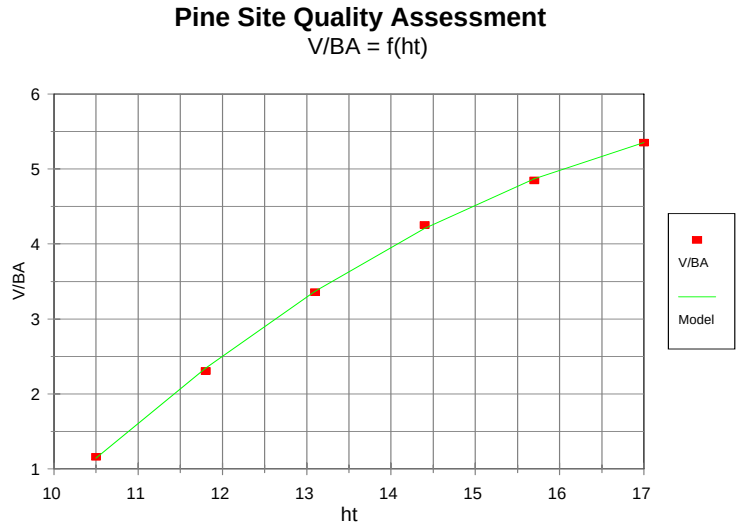

Figure 3.1. Form height based on Pinus Radiata site quality standard data

The form height is similar to, but not quite the same as the green level. The differences are possibly due to factors such as taper factor changing with site quality. This is shown in Figure 3.2 (where the green line represents the green level):

Figure 3.2. Form Height vs Green Level for Pines

However, since forestry is a commercial operation, there are more considerations than just measuring yield. Harvesting costs and survey costs are very important considerations. Assessment of trafficability for harvesting or survey is an important case. The Cruise is often also used to assess such factors and note difficult areas. Any methods designed to replace Timber Cruising will need to define these additional data and find a way to assess them as well as measuring Timber Volume or surrogates for it.

3.1.2 Variable Plot Sampling

A common method for site assessment and (in some places) cruising for broad area timber assessment is the Bitterlich (1948) variable radius, or wedge sampling method (see Grosenbaugh, 1952). The Bitterlich method uses a very convenient set of statistics that occur with the interaction of view direction and view IFOV as follows.

An instrument (such as a Speigel Relaskop or a simple angle wedge) is used which allows the user to view the trees near to a chosen point site to be viewed (Bell and Dillworth, 1988). It provides a field of view in a constant angle "wedge" of fixed size. Trees are tallied "in" if the extent of the view wedge is within the tree trunk area and "out" if it is not.

It can be shown that if the trunks of the trees are randomly (Poisson) distributed then the number of "in" trees is proportional to the Basal Area (BA) up to a constant (the Basal Area Factor or BAF) that depends only on the wedge angle. In fact, assuming the trees are distributed in a near Poisson pattern, the mean and variance of the number of "in" trees can be assessed statistically as part of the field trial.

By undertaking measurements on the "in" trees it is possible to construct effective relationships between variables as was done for fixed size plots. If a consistent relationship is obtained between BA and V then it is possible to use the Relaskop or wedge to move rapidly over an area measuring BA only and making the inference based on the relationships found.

Holgate (1967) provides a very careful discussion of the statistical basis for the Relaskop and the interpretation of its data. He develops expressions for the variance of the estimates and discusses "occlusion" effects. He showed differences between plot counts and Relaskop measurements that had not been resolved at the time he wrote and which will continue to occur due to the underlying nature of the estimates being compared.

Variable plot sampling is a mature technology and the more sophisticated Relaskop instruments allow measurements of tree height, crown length ratio and DBH to be estimated for the "in" trees without moving from the central point. They can also incorporate GPS and ranging to form a very versatile cruising instrument.

3.1.3 Aerial Photograph Interpretation

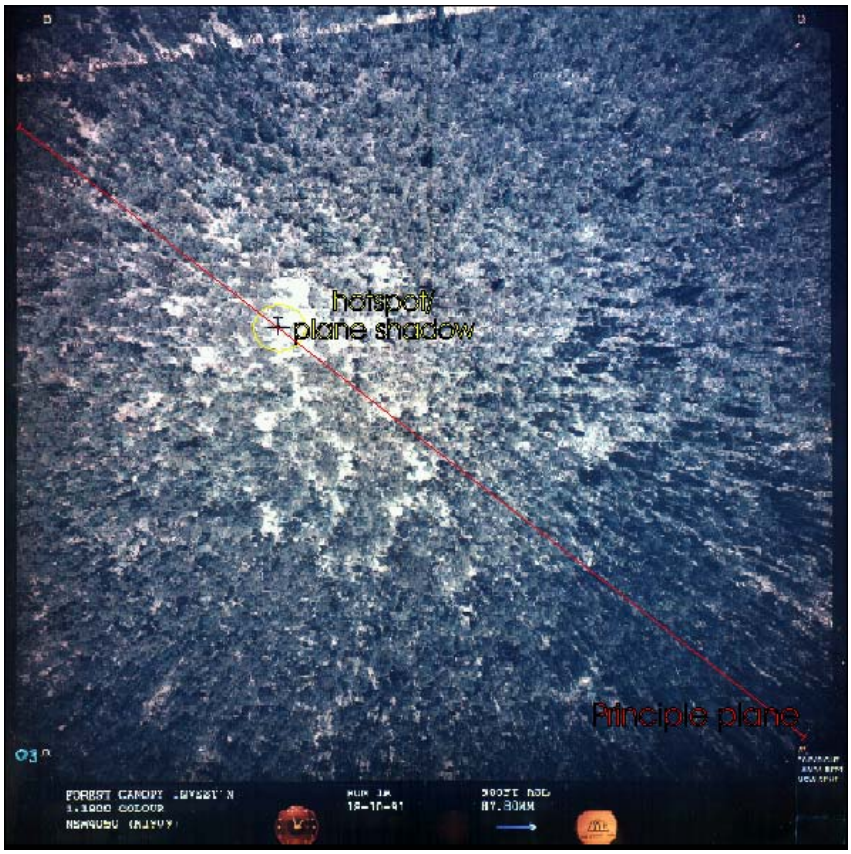

Figure 3.3. Wide angle aerial photograph of a forest canopy

Aerial Photograph Interpretation (API) has been extensively used to extend forest measurement to wider areas. The photography is generally at a fine scale (1:25,000 or 1:10,000) and involves runs where significant overlap between photographs has been obtained allowing stereo comparison and height estimation to be undertaken.

It is well known that if sufficient ground area is visible and recognisable then heights of selected objects can be determined by parallax. Moreover, by delineating crowns it is possible to estimate crown area and crown cover from the photography. Sometimes crown sizes and type are also determined.

Obviously, a Structure Diagram (the plot of height against cover) and estimates of basal area and the stand height curve can be developed as well as some interpretations of species present in the upper layers. Crown closure, stand height and crown diameter together also provide inputs to volume tables and may be calibrated by ground site measurements in some of the photographs.

However, API has its limitations. It is difficult to correct the crown cover for overlap due to shadowing in the canopy depths. Heights of emergent species or trees above the main upper stratum can be measured but not smaller and less dominant tress and shrubs in lower strata. Processing and interpretation costs are also very high and additional to the direct flying costs of low level photography.

3.1.4 Allometric Relations

An allometric relationship provides an estimate for one quantity by using the measurement of another or some others. Such relationships are commonly used in forestry to estimate quantities that are not measured by correlated ones that have been measured.

At the base of such estimation in forestry and ecology (Enquist *et al*. 1998) is the principle that characteristics of plant organs – especially size and mass – are related to total biomass by relationships of the form:

$$Y_i = Y_{i0} M^{b_i}$$

where M is total plant biomass and Y_i is the characteristic under consideration. In a number of cases, the exponent b has very specific forms based on both theory and observation as outlined by Enquist *et al*. (1998).

If this is the case, then for two such characteristics (such as DBH and height or BA and foliage biomass) we would have:

$$Y_i = Y_{0ij} Y_j^{b_i / b_j}$$

allowing the prediction of one from the other.

For example, such allometric relationships can be locally calibrated as in the development of a relationship between basal area and timber volume which is then used to estimate timber volume at sites where the information being inferred (volume) has not been directly or extensively measured but basal area has. That is, if a number of sites are visited where only basal area is measured the application of the equation formed at the sites where detailed measurements are taken provides a means to map the spatial variation in timber volume. Other examples occur where individual tree height, crown leaf area, or foliage and stem biomass are all estimated from DBH or various tree and shrub measurements are inferred from stand DBH, height, basal area and possibly crown length ratio.

The use of allometric relations for predicting height from DBH based on the stand height curve are especially common for the estimation of tree heights. However, in many cases the stand height diagram must be stratified to produce useful equations.

In other cases, allometric relations are often used in models or to derive information that has not been measured by using relationships found in quite different circumstances. Such persistence obviously needs to be carefully tested. For example, in Chen *et al*. (1991) the leaf area of crowns was estimated using a relationship from Gholz *et al*. (1976) of the form:

$$L_W = 8.5\, e^{-3.89+1.89\,LogDBH}$$
$$= 0.1738\, DBH^{1.89}$$

where *DBH* is in cm and L_W is in m^2. Chen *et al*. (1991) use the very different value this allometric relationship derives for site LAI compared with hemispherical and LAI-2000 data (which are described later) to infer that these methods considerably under-estimate LAI. Even given that this underestimation may occur for good reasons, one would have to question the general applicability of the using the above relationship for such a study as well.

Fournier *et al*. (1997) use a stand height curve with an R^2 of 0.5201 to predict height from DBH measurements where height was not measured. In this case the fitted relation was simply a cubic curve in DBH. It is not clear that the locations of the sites where height and DBH were measured were a similar structural or age class to the sites where it was being used. Again, some concern must be had at the consequences of using this kind of indirect estimate.

Wang and Jarvis (1990) also make use of linear allometric relations to predict height and crown foliage area from DBH. They use separate relationships for Sitka Spruce and Pinus Radiata and use the relationships to provide parameters for their MAESTRO model for the absorption of PAR by a canopy.

In a similar way, Landsberg and Waring (1997) use the more general form of allometric relationships discussed above relating biomass of components of a stand (such as foliage and stem) to total biomass – which is then surrogated by DBH. That is they use a range of models stratified by species (in their notation) of the form:

$$W_i = a_i W^{n_i}$$

where, in this case, W is the DBH. They then use their model to compute mean annual increment of biomass, express this as DBH and then use the relationships to distribute the increment among the canopy and stem components.

While these approaches have met with some success, there is clearly scope for the development of much more readily available measurements of canopy components and much more extensive data on the persistence of the relationships between them. The increased use of tree growth modelling and the increased interest in total biomass of vegetated areas have also placed pressure on foresters to improve this aspect of their traditional measurement techniques.

3.1.5 Strengths and Limitations of the Foresters' Approach

There are many well-established forest inventories and monitoring systems in place throughout the world. In many areas, future yield can be predicted to an acceptable accuracy by relatively few periods of measurement of site quality and experienced foresters can quickly and accurately rate sites during timber cruising. The approach can then be successful (see Leech and Correll, 1993) and firmly established in its industry as well as in its areas of prime application. In such areas, the relationship

between assessed site quality and future growth is well established and final yields are generally predictable to an accuracy accepted by management based on many years of experience as well as on established forest management practice.

This success does, however, depend on the degree to which the result is really "acceptable" for forest management and whether the relationships between age, height, diameter, LAI (or FAI) and growth are consistent and predictable at the level of sampling accepted. This situation tends to occur most commonly in well-managed forests with a long history of study, dominant (tree) growth forms and relatively simple vertical canopy profile – or age distribution. In many cases, forest management itself tends to reinforce the strengths of the relationships and correlations.

The underlying model upon which forest measurements depend generally assumes that variations in height and DBH (and crown size) depend on site variation (site quality) and age of the trees. It is assumed that trees of a particular age and at sites of a given quality will tend to follow a predictable overall growth (increasing "size") in all their dimensions over time. Complex forests are seen as mixed age systems in a landscape of varying site quality. For a given site quality, age is seen to be predictable by any of a number of measured quantities such as basal area, (predominant or bole) height or DBH. For a given age class, site quality is also usually seen as being predictable by any of these measurements and these and other canopy characteristics (such as total foliage) are assumed to be predictable by stable allometric relations.

To an ecologist, or forester working in native forests, the effects of succession, competition and disturbance, gap phase evolution (different species move into gaps when they occur) and the development of "niches" for species of different growth form and light tolerance create much greater complexity. They all act to create a forest environment where the simple relationships on which forest mensuration and allometry depend no longer hold or are not consistent.

This, and the different viewpoint of timber resource inventory from that of ecological assessment (which includes biodiversity and animal population ecology), has led to the differences we see between the measurement methods and forest descriptions of (say) the NVIS and the traditional forest measurement. However, both are important and both depend directly on measurements of the structure of forests. With the development and greater utilisation of forest productivity models (Battaglia and Sands, 1998) there is also an increasing need to combine these approaches.

In such forest productivity models (such as IRM, Vertessy *et al*., 1996; or 3PG, Landsberg and Waring, 1997), the environmental conditions and site quality (often parameterised by LAI) are used to estimate the Mean Annual Increment (MAI) of biomass in a forest which is distributed to the canopy components and layers by growth models (IRM) or allometric relations (3PG). The accuracy of predictions from such forest models is being called into question and it is clear that they would benefit greatly from better measurements and better-calibrated models for the distribution of MAI to forest components and the development of canopy structure.

3.2 Foliage and Canopy Measurements and Methods

3.2.1 Site Classification, Measurements & Foliage Profiles

In environmental and ecological studies the foresters' methods (such as the Relaskop as in McDonald, 1993) have also been used to map and classify forests. However, because of the different emphases (such as on foliage and habitat) there have been a number of attempts to develop site characterisation for structure from the ecological view-point.

The underlying statistical approaches of fixed and variable sized plots and "cruising" or transects have also been used. Most differences occur in the activities at the sites and the measurements taken during transects.

3.2.2 The Walker-Hopkins method for structural mapping

The Walker-Hopkins (1990) method is a direct structurally based field technique for describing and measuring sites to provide structure diagrams and foliage profiles – as well as a classification in the style described above for the NVIS system. At the plots, or sample sites, the information described previously is collected. To recap briefly, Walker and Hopkins (1990) recognised the three basic strata continued in the NVIS system – an Upper Stratum (U) consisting of the tallest significant growth form, a Lower Stratum (or Ground Stratum) (L) of all vegetation below 1 metre and a Mid Stratum (M) of all vegetation between the upper and lower strata.

Measurements at fixed or variable sized plots are made after the site is classified into these primary strata and the main species and growth forms established. The measurements usually consist of Tree Height (h), Crown Width (D), Crown Depth (T), and Crown Factor (CF) for either all "types" (species/growth forms) in the strata or for each tree in the plot. CF is visually estimated from vertical photographs of "typical" crowns ranging from 30% (open) to 100% (opaque) at 5% intervals. Some examples of the fixed size plot data are given in the last Section on modelling for a Murray Darling Basin transect (Section 6). Based on these data, DBH, crown areas, basal area, foliage profile, a point on the structure diagram and all of the information we have nominated as important as means to describe and characterise site structure can be obtained – but for just one site.

In the field, Cover (CC) or Crown Area Density (CAD) can be estimated in the fixed size plots by the density and mean crown size of the different types in each main layer. The CF data allows an estimate for PFC to be made provided some idea of the degree of randomness or clumping there is in the tree spacing. Various other methods can be used such as the transect-based Walker and Penridge "Crown Gap Ratio" or the estimation of crown leaf area by the "module counting method". These will be described here as examples of current field procedures. They are not the only ones but they are commonly used.

3.2.2.1 The crown gap ratio method

The crown-gap ratio (*c*) was described in Walker *et al*. (1988) and Penridge and Walker (1988). The statistic is defined as the ratio of average gap (separation distance, denoted G) between crowns to average crown size (diameter D) is estimated in the field. Under a number of conditions it is found that crown area density (CAD), or $\lambda\bar{A}$ is related to the statistic *c* via a relation of the form:

$$CAD = \lambda\bar{A} = \frac{\alpha}{(1+c)^2}$$
$$c = G / D$$

Penridge (Penridge and Walker, 1988) numerically simulated CAD by establishing a number of distributions of points between uniform to random to clustered, computing the Delauney triangulation and obtained the mean over all sides of the Delauney triangulation for the points. For a wide range of distributions they obtained a mean α value of 1.08, which is also the value for the Poisson case. However, it was also clear that α depends on the way the distances and tree sizes are sampled. In a field experiment using transects, a value of 0.789 had been found to fit the data well. Walker and Penridge then simulated a "zig-zag" transect obtaining a mean value over a set of typical Poisson and more or less clumped distributions of 0.806 (or 80.6%).

Looking at this another way, if the distance between adjacent crowns in each case is the nearest neighbour distance and the point distribution is Poisson we would have for the expectation of the ratio:

$$E(G / D) = c \approx \frac{NND}{D} - 1$$

where NND is the expected Nearest Neighbour Distance. Hence,

$$CAD = \frac{\alpha D^2}{NND^2}$$

For the Poisson case, $NND = 1/\sqrt{\lambda}$ so we obtain:

$$CAD = \alpha\lambda D^2$$
$$= \lambda\frac{\pi}{4}D^2$$
$$\alpha(\%) = 25\pi = 78.5$$

This is close to the value selected by Walker and Hopkins and even closer close to the value found from the field data.

The field method preferred by Walker and Hopkins (1990) is neither a complete triangulation nor a subset of NNDs. It is a connected transect through the area with two distances per tree (except at the ends) and may be more much more like the zig-

zag transect simulated by Penridge and Walker (1988). Penridge and Walker (1988) found that the variations in distributions they used caused α to vary between 0.789 and 0.815. It may be useful to revisit this area. For example, it may be possible for the distribution of inter-tree distances or some other statistic derived from the data could be used as added information to select an appropriate value α for a site or region.

The CAD is related to cover in the Walker-Hopkins (1990) method as:

$$PFC \approx CAD \times CF$$

where CF is Crown Factor and PFC here is an approximation to foliage cover.

3.2.2.2 Module counting and other methods

The "module counting method" provides an alternative to the combination of the Crown Factor (CF) measure and Crown Gap Ratio. In the module counting method, trees are counted for density in a fixed size plot by layer and type and then leaf area within crowns is estimated by counting "modules". Most Australian trees have open crowns consisting of clumps of leaves at the end of branches, which are called "modules". The leaf area per module is established by sampling and measurement and total crown leaf area (and hence leaf area density) estimated from the number of modules and crown size measurements.

Alternative methods include using transmittance or some of the other techniques discussed as canopy measuring tools below and applying them to a single crown. However, it is often difficult to reconcile these different measurements taken at sites where the clumping effect is significant. For example, if alternative techniques such as the LiCor LAI-2000 Plant Canopy Analyzer (PCA) or DEMON LAI meter are used together with direct methods such as module counting and CF measurements, the divergence between methods can be very wide in open forests and woodlands - although agreement between methods can be quite good in closed forests as found by Vertessy *et al*. (1994, 1995). There is considerable room, therefore, for techniques that are consistent, objective, repeatable and rapid. It seems important, however, that they take structure into account as well as total foliage amount because, without taking structure into account, it is likely that the total foliage amount will not be reliable or in any way "correct".

3.2.3 Foliage profile by vertical measurements

MacArthur and Horn (1969) described a range of measurements of the vertical foliage profile in a forest that do not separate out individual crowns but treat the canopy as a single entity. The method(s) used were laborious but innovative and provide a forerunner of methods applicable to Lidar data.

The measurements are divided into three types. The first is used for the grass layer and is similar to the Warren Wilson (1960, 1963, 1965a,b) point quadrat method that is described later. That is, the number of grass blades hit by a vertical line below a point estimates grass foliage cover. For low vegetation (shrubs and small trees) a

mesh is used and the distance from the mesh to the first contact leaf or stem above each of 16 points is measured using a camera range-finder. In dense foliage, more lines are added until at least some lines penetrate to the sky. In high vegetation (e.g. >15m) the range and leaves become unclear and the fraction of gap is measured above a dense mesh of points.

The most interesting statistics arise from the intermediate or low vegetation cover. The analysis derived by the authors assumes the foliage is randomly distributed and the measurements at different points of the mesh are independent. Then suppose that by $P_{gap}(z)$ we mean the probability of no leaves in a vertical line of length z from the ground. The probability of the first contact with foliage being at distance z is then:

$$P_{FC}(z) = -\frac{dP_{gap}(z)}{dz}$$

MacArthur and Horn (1969) show that if *f(z)* is the (vertically projected) area density of foliage at height z (that is, the vertically projected foliage profile) it follows that:

$$\begin{aligned} f(z) &= \frac{-1}{P_{gap}(z)} \frac{dP_{gap}(z)}{dz} \\ &= -\frac{d\left\{LogP_{gap}(z)\right\}}{dz} \end{aligned}$$

or

$$P_{gap}(z) = e^{-\int_0^z f(z')dz'}$$

(Actually, MacArthur and Horn (1969) did not discuss the significant difference between f(z) and the foliage area density F(z), the one sided leaf area density at height z. This will be discussed below where hemispherical photography and point quadrat methods are discussed).

The gap probability function is estimated by ordering the samples of first contacts (z_j) and equating:

$$\tilde{P}_{gap}(z) \approx \frac{\#\left\{\ foliage\ hits \geq z\right\}}{N}$$

where N is the total number of samples taken.

Clearly, if there are only a few samples, the spatial variance and other uncertainties will combine to make this a very noisy estimate and create consequently noisy estimates of the foliage profile. However, it is an estimate and neighbouring estimates may be pooled or a parametric model fitted to stabilise the results. This was not done by MacArthur and Horn (1969).

For example, the Weibull distribution as used by Yang *et al*. (1999) and others could be used. This function models the cumulative foliage profile with three parameters (four if the canopy height is unknown) as:

$$L(z) = a\left(1 - e^{-b(1-z/h)^c}\right) \quad 0 \le z \le h$$
$$P_{gap}(z) = e^{-L(z)}$$

which can be fitted to the estimated P_{gap} (e.g. by maximum likelihood) and then used to estimate *f(z)* by differentiation:

$$f(z) = \frac{abc}{h}\left(1 - z/h\right)^{c-1} e^{-b(1-z/h)^c}$$

For the high canopy, assume an estimate of the total gap fraction is made for foliage greater than a height z_{max}. Then:

$$P_{gap}(z \ge z_{\max}) = e^{-\int_{z_{\max}}^{h} f(z')dz'}$$
$$= e^{-L_h}$$

That is, an estimate of the total vertically projected foliage area above the maximum height can be derived from the proportion of gap.

The difficulties with this method have been that it is time consuming and laborious and its results are very noisy in the presence of spatial variation of the type common in forests. In addition, its assumptions of randomness and independence are not acceptable in clumped canopies consisting of trees and shrubs in a number of layers – such as are found in Australian open forests and woodlands. Hence it has not been used routinely in the provision of foliage profiles.

3.2.4 Hemispherical Photography

Hemispherical Photography has been used to estimate P_{gap} for the whole canopy above a camera point as a function of view zenith (and azimuth) angle by estimating the percentage of visible "sky" in small sample sectors over a set of zenith and azimuth angles determined by their position in the hemispherical or "fish-eye" photograph. This is different from the method of MacArthur and Horn (1969) above in its use of varying view angles.

A hemispherical photograph (Figure 3.4) senses the total fraction of gap in canopies at different angles by using the gray-level differences between background sky and foliage to segment a photograph taken from the ground and estimate gap fractions over the "hemisphere".

Figure 3.4. Hemispherical Photograph of a Eucalypt Canopy

The probability that a ray will travel to vertical distance z from a point on the ground in direction μ_v ($\mu_v = \cos\theta_v$) in a random canopy with vertical foliage area density variation *F(z)* is:

$$P_{gap}(\theta_v, z) = e^{-\int_0^z G(\mu_v, z')F(z')dz'/\mu_v}$$

where *G* is the Ross G-function which depends on the foliage angle distribution ($g(\theta_L)$ for zenith angle to the leaf normal of θ_L) and the direction of the ray. Specifically, the Ross G-function is the projected area of unit foliage area in unit volume in the direction of the ray with direction μ_v ($\mu_v = \cos\theta_v$). The gap probability is therefore (as before) dependent on the total projected area of foliage encountered along the ray direction.

If the foliage consists of small, flat leaves where the leaf orientations are fully defined by the zenith angle of the normal to the leaf (θ_L) and the azimuthal and rotational orientations are uniformly random then the relationship between the leaf angle distribution and the Ross G-function can be expressed using Reeves Kernel (Reeves Appendix to Warren Wilson, 1960) as:

$$K_S(\theta, \theta_L) = \begin{cases} \cos\theta\cos\theta_L & (\theta + \theta_L \le \pi/2) \\ \cos\theta\cos\theta_L\left(1 + \frac{2}{\pi}\{\tan\psi - \psi\}\right) & (\theta + \theta_L > \pi/2) \end{cases}$$

The angle $\psi \quad (0 \le \psi \le \pi/2)$ is defined as:

$$\psi(\theta_0,\theta) = \cos^{-1}\left(\cot\theta\cot\theta_L\right) \quad (\theta+\theta_L > \pi/2)$$

Using this kernel the G-function may be written:

$$G(\mu_v) = \int_0^{\pi/2} K(\theta_v,\theta_L)\, g(\theta_L)\, d\theta_L$$

where in this expression the leaf distribution is normalised such that:

$$\int_0^{\pi/2} g(\theta_L) d\theta_L = 1$$

It follows that the model for the probability of a gap through the whole of a random canopy of height *h* is:

$$P_{gap}(\theta_v, h) = e^{-\int_0^h G(\mu_v,z)F(z)dz/\mu_v}$$

where $\mu_v = \cos\theta_v$ and *F(z)* is the vertical canopy profile of leaf density.

The vertical foliage profile (*F(z)*) and any changes in *G* with height in the canopy cannot be derived from a single hemispherical photograph taken at ground level. To interpret such a photograph, it is generally assumed that the canopy is uniform in the horizontal direction and uniform in angle distribution in the vertical direction so that *G* is constant in *z*. In this case, the P_{gap} model may be simplified to:

$$\begin{aligned} P_{gap}(\theta_v) &= e^{-G(\mu_v)L/\mu_v} \\ &= e^{-f(\theta_v)/\mu_v} \end{aligned}$$

where *L* is the canopy LAI and *f* is the projective foliage density per unit length in the direction θ_v.

$$L = \int_0^h F(z)dz$$

In this situation, the photographs allow both LAI (*L*) and some measures of the foliage angle distribution (*g*) to be derived from the gap data through various methods based on solving an integral equation based on the P_{gap} model above or some approximation. (See Miller, 1964; Anderssen *et al*., 1984).

Miller (1967) derived a simple theoretical relationship between the total foliage amount (or LAI) and the projective foliage density (which can be estimated from Fisheye lens photographs) of the form:

$$L = 2\int_0^{\pi/2} f(\theta_v)\sin\theta_v\, d\theta_v$$

However, this is not easy to compute in practice and various approximations have been made to it or else F (respectively LAI) is derived along with foliage angle.

The relationship between the Ross function (G) and the leaf angle distribution for a random canopy with uniformly distributed leaf azimuth can be estimated by solving the previously defined integral equation:

$$f(\theta_v) = \int_0^{\pi/2} K(\theta_v, \theta_L)\, h(\theta_L)\, d\theta_L$$

where:

$h(\theta_L)$ is the foliage area angle distribution function assuming azimuthal independence and symmetry and
$K(\theta_v, \theta_L)$ is Reeve's Kernel function defined previously.

The relationship between $g(\theta_L)$ and $h(\theta_L)$ is simply that:

$$h(\theta_L) = L\, g(\theta_L)$$

Analytical solutions to this integral equation are possible, including an exact form for $g(\theta_L)$ involving higher derivatives of G as shown by Miller (1964) and Philip (1965) where the formulae were used to interpret data from inclined point quadrats that are described below. Anderssen and Jackett (1984) and Anderssen *et al*. (1984, 1985) exploited the analytical inverse equations to develop practical formulae for a number of functionals that can be developed based on the foliage distribution and are applicable to data from hemispherical photographs and also to point quadrat data.

Using the integral expressions, the Miller's Theorem (Miller, 1967) quoted above can also be written as:

$$2\int_0^{\pi/2} G(\theta_v) \sin\theta_v \, d\theta_v = 1$$

Alternatively, a simple parametric model can be used to model the foliage distribution, and hence the Ross G function, and the data fitted to estimate the parameters. One such was the extremophile distribution function with parameter "x" used in Jupp *et al*. (1980). It is based on the foliage being a mixture of only vertical and/or horizontal elements:

$$G_J(\mu_v) = \frac{x\cos\theta_v + \frac{2}{\pi}\sin\theta_v}{x+1}$$

The parameter "x" was originally derived as the ratio of the LAI contributed by the horizontal elements to that contributed by the vertical elements. However, it can also be regarded simply as a fitting parameter. As a simple test of the above expressions it is easy to confirm that Miller's functional, when applied to this approximate G-function is 1.0.

An alternative is the Ellipsoidal distribution approximation due to Campbell (1986) in which foliage is assumed to have an ellipsoidal distribution leading to the expression:

$$G_C(\mu_v) = \frac{\sqrt{x^2 \cos^2\theta_v + \sin^2\theta_v}}{x + 1.702\,(x+1.12)^{-0.708}}$$

In this model, the parameter "x" was originally derived as the ratio of vertically projected canopy area to horizontally projected canopy area – which is similar to the previous model. Also, as with the previous "x", it is generally simply used as a fitting parameter or estimated empirically and tabulated for different canopy types.

Some of the background to approximations to the leaf angle distribution and their application in canopy measurements is discussed in Campbell and Norman (1989). Another study by Goel and Strebel (1984) showed that many measured angle distributions in crops could be modelled by a beta distribution with two parameters. This allows mean and variance of the foliage distribution to be derived. However, the expression for G is not as simple as the previous two.

Any of these expressions could be fitted to the data to obtain L and angle distribution parameters such as x above. In the extremophile and ellipsoidal distributions, the x value will be somewhat different but, in each case, it can be interpreted in terms of a functional on the angle distribution or a measure of the mean leaf angle. In the case of the model used by Jupp *et al*. (1980) the relationship is approximated as:

$$\bar{\theta}_L \approx Tan^{-1}\left(\frac{1}{x}\right)$$

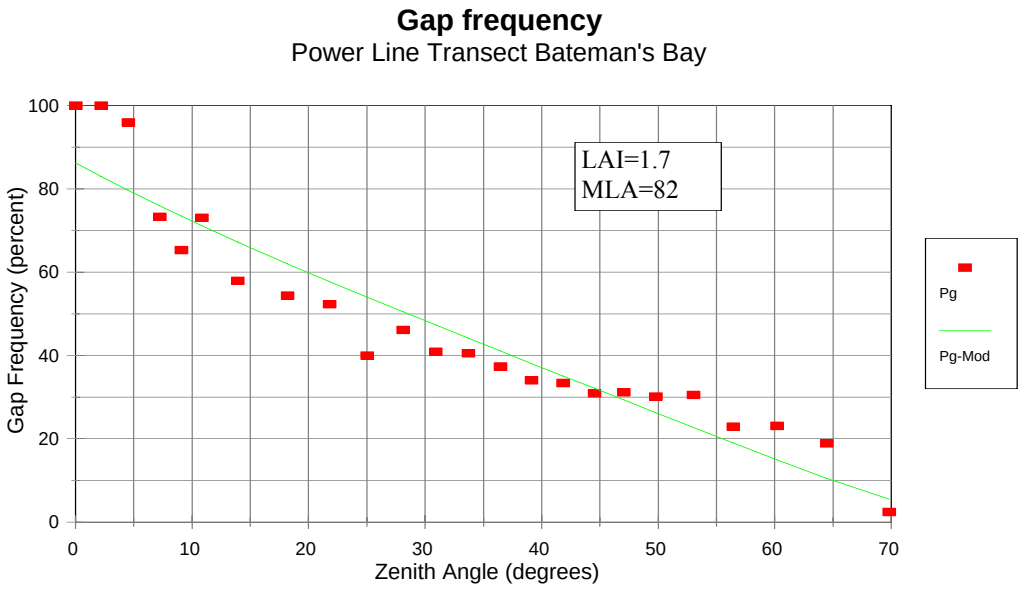

Figure 3.5. Modelled and actual P_{gap} near Bateman's Bay, NSW

For example, Figure 3.5 shows the percentage gap or gap frequency taken from a wide-angle photograph of a forested area near Bateman's Bay in NSW. Also shown is the simple model with an LAI of 1.7 and a mean leaf angle of 82° and used as an

example in Jupp *et al*. (1980). The differences between the model and data include the effects of clumping into crowns as well as spatial variance. As with all of the methods being described in this section, the method suffers from the effects of the high level of spatial variation in forests – and especially in parameters such as leaf angles. However, number of hemispherical photographs at the same and/or different sites in a stand can be averaged to obtain more stable statistics and a number of studies have been made using this technique (e.g. Anderson, 1971; Bonhomme and Chartier, 1972; Smith *et al*., 1977; Jupp *et al*., 1980).

The various papers by Anderssen and Jackett (e.g. Anderssen and Jackett, 1984; Anderssen *et al*., 1984, 1985) demonstrated a variety of functionals that can be generated from the data. This, combined with the advent of digitisers and computer analysis (Rich, 1990) has led to wider use of hemispherical photography in foliage analysis. However, most analyses are based on assumptions of random leaves rather than the structures found in many forested areas. In this case, the results give us "apparent" properties rather than "actual" properties.

It may be possible to infer both *F(r)* and the vertical variation of some parameters of G if hemispherical, or other sets of directional, photographs were taken at a range of heights in the canopy. Published examples of this application include experimental studies by Koike (1985) using a number of small frame directional photographs and Ondok (1984) who used hemispherical photographs. Ondok (1984) used a triangular distribution to model foliage and foliage angle and simplify the mathematics.

However, it should also be possible to undertake more detailed inversions using the work described above. For example, to make the problem better posed it may be assumed that *G* is uniform and only *F(r)* varies or a parametric model (such as the Weibull model introduced previously) could be used. In either case, the data set can be written:

$$P_{gap}(\theta_{v,i}, h_j) = e^{-\int_0^{h_j} G(\mu_{v,i}, z')F(z')dz'/\mu_{v,i}}$$

$$-\mu_{v,i}\ Log\left(P_{gap}(\theta_{v,i}, h_j)\right) = \int_0^{h_j} G(\mu_{v,i}, z')F(z')dz' \quad i = 1, n;\ j = 1, m$$

If a sufficient number of good measurements are taken there may be enough data to solve these equations under varying assumptions of smoothness and parameterisation.

It is also useful to observe that vertical distances to first contact, hemispherical and other multi-view photography may all be used with individual trees as means to estimate within-crown foliage. In principle, a combination of fixed size plot Walker-Hopkins measurements, photography or other gap measurements and some cruising can provide actual foliage profiles in forests and woodlands. However, the techniques are all time consuming, often deliver relatively few data in a very heterogeneous environment and can be expensive.

3.2.5 Two-dimensional (or Inclined) Point Quadrats

A related method, which mostly has only been used for grasslands and crops rather than forests, is the Two-dimensional (or Inclined) Point Quadrat method refined from previous techniques by Warren Wilson and co-workers (Warren Wilson, 1959a,b, 1960, 1963). This technique has been used to estimate foliage area, foliage profiles and vertical distributions of foliage angles as well as derived properties such as sunlit foliage (Warren Wilson, 1967) but has also been limited in its routine application by the same issues of sampling variation as have plagued the previously described methods.

In this technique, a point quadrat (a suitably mounted sharp needle with distance or range gradations) is pushed through a canopy at a fixed angle and the number of foliage elements "hit" within each layer of foliage per unit distance of travel is counted as data.

It can be shown that these data are estimates for the foliage density and angle distribution through the relationship:

$$f_j(\theta_v) = \int_{h_{j-1}}^{h_j} G(\mu_{v,i}, z')F(z')dz'$$

which is similar to the information we could also obtain from hemispherical photography if the photographs were taken in a vertical transect. Effectively, the $P_{gap}(\theta_v, z)$ for various angles and ranges has been sounded by the point quadrat through the contact probability since with the assumptions being made:

$$P_{gap}(\theta_v, h_j) = e^{-\sum_{i=1}^{j} f_i(\theta_v)/\mu_v}$$

In Warren Wilson (1965b), the author also describes the field procedure and interpretation of first contact data. That is, if instead of the number of hits in a single probe between two heights being recorded, the number of first hits within the range is measured over a number of sampling probes then similar information can be derived. This is similar to the method used by MacArthur and Horn (1969) from beneath the canopy but allows a range of angles to be sounded. The first contact method does, however, require many more probes to provide stable data.

Philip (1965) and Miller (1964; 1967) (see also Gates and Wescott, 1984) showed how the integral equations derived from these data could be solved by inversion to obtain the foliage profile and mean foliage angle as a function of height in the canopy. The integral equations are, however, rather poorly posed. This, plus the sampling variance in the data in the face of very high spatial variation, clumping effects and the laborious nature of its collection has limited the widespread use of the method. To give an indication of the problem, Ross (1981) estimated that it would take 10,000 point quadrat contacts to estimate $f(\theta_v)$ to 1% precision.

However, the work done by Philip (1965), and more recently Anderssen and Jackett (e.g. Anderssen *et al*., 1984) can potentially be applied widely to hemispherical photography, point quadrats, vertical profile measurements (MacArthur and Horn, 1969) and (as we will see later) to the interpretation of ground-based or airborne Lidar attenuation in canopies. An extension of the point quadrat method to more structured forest canopies by taking measurements in vertical cylinders is reported in Sumida (1993) but it is also laborious and time consuming and spatial variance is a major problem – as it is with the point quadrat method.

3.2.6 Transmittance based methods

The light climate in a canopy or on the forest floor consists of light that has come through gaps in the canopy and light that has been transmitted through leaves or multiply scattered by leaves and foliage. Areas of direct sunlight on the forest floor are called "sunflecks" which are created by the sun shining through canopy gaps and areas of deep shade (the "umbra") indicate no gaps between the point and the sun.

Many people have attempted to use the structure of the light climate under a canopy to measure the canopy structure. The size distribution and cover fraction of sunflecks was used by Norman *et al*. (1971) to describe the spatial patterns or structure of canopies. Later, Lang (1986, 1987) used the direct sun beam as a means of estimating LAI and mean leaf angles with considerable success.

Basically, the method consists of averaging the light field of the transmitted direct sun beam over a distance under a canopy. Sunflecks provide the intensity of the unattenuated solar beam and deep shade can be used to estimate the diffuse radiation enabling an estimate for P_{gap} to be made. As we noted above:

$$P_{gap}(\theta_s) = e^{-G(\mu_v)L/\mu_s}$$
$$= e^{-f(\theta_s)}$$

where θ_s is the sun zenith angle. By taking readings at different times of day the capacity to invert the models is reached in the same way as for hemispherical photographs or point quadrats.

Lang's DEMON instrument and software are commercially available to carry out this method. It is essentially a better method than a more common approach in which the solar transmittance under a canopy is estimated by the ratio of the total diffuse radiation under the canopy to a similar measurement outside the canopy. However, an instrument called the Sunscan canopy Analysis system (Delta-T) can obtain good estimates by averaging as in the Lang method and recording both diffuse and direct radiation. As with all previous methods, the level of sampling needed to achieve stable results can be very high.

The Licor LAI-2000 is a popular tool for measuring LAI in the field and uses a sensor that records irradiance in 5 rings or segments of the hemisphere (Welles and Norman, 1991). The transmittance in each ring is obtained by readings in and out of the canopy and LAI estimated by a numerical approximation to the Miller (1967) equation:

$$LAI = -2\sum_{i=1}^{5} w(\theta_i)\, Log\left(T(\theta_i)\right)\cos\theta_i$$

where θ_i is the centre angle for the ring and $w(\theta_i)$ is the ring weighting factor. Other formulae are available for the mean leaf angle.

The formula for LAI uses the principle that $T(\theta_i)$ in a ring can be equated to the mean P_{gap} and so:

$$f(\theta_i) \approx -L\log\left(T(\theta_i)\right)\cos\theta_i$$

This approximation is best for uniformly overcast skies and at dawn or dusk and at its worst when the sun is high and there are some clouds in the sky. The quadrature approximation is:

$$\sum_{i=1}^{5} w(\theta_i)h(\theta_i) \approx \int_0^{\pi/2} h(\theta)\sin\theta d\theta$$

Transmittance methods are popular as they can be deployed easily in the field. Yang *et al*. (1999) (for example) used an LAI-2000 as a canopy profiler to measure cumulative LAI as a profile in canopies to very good effect. There can, however, be significant problems with the data if conditions are not right. The light climate in a canopy is highly variable and the irradiance is also highly variable in both space and time. Differences in reflectance and transmittance of foliage components, specular reflections off leaves and stems and penumbral effects at the edges of the foliage make the data less than ideal for interpretation by the theoretical methods described above.

Even more significant (but not only a problem for transmittance methods) is that the foliage is not randomly distributed but is clumped within and between crowns or tussocks. Chen (1995a, 1995b) has analysed this effect extensively showing that LAI as estimated by the equations above will under-estimate LAI in clumped canopies. He developed a technique using his "Tracing Radiation and Canopy Architecture" (TRAC) instrument. This instrument is used to measure gap size distribution as well as gap fraction and allows a "clumping factor" to be developed to compensate for this effect (Chen *et al*., 1997). Nilson (1999) has also introduced a model to account for this effect in terms of crowns rather than empirical "clumping". We will return to this issue later when it is discussed in relation to the interpretation of Lidar data.

3.3 General use of Remote Sensing Technologies

As well as ground survey and aerial photography, there has been a significant activity in using remote sensing from airborne and spaceborne platforms to measure canopy type, condition, cover and structure. In the case of optical remote sensing, some of the opportunities as well as many of the issues discussed above for structural mapping have been outlined in Jupp and Walker (1996). In addition, there has been a great deal

of activity in attempting to derive structure from radar data of various forms and from various platforms.

More commonly in the optical region, remote sensing has been used to map general vegetation type, species associations, current condition, photosynthetic activity and overall cover using spectral data. The recent developments of hyperspectral sensors for use from airborne platforms and the arrival of spaceborne high spectral resolution sensors will provide a general base mapping capability of this type. However, very little of the structural information as described in this document has been obtained from such data.

Possibly the most successful use(s) of remotely sensed data in forest studies has come from its use to measure absorbed PAR and to model the potential for growth in forests. This approach has many uses as foresters move to use growth models to predict yields. Satellite and airborne data can be used for this task and in this approach the changes in canopy structure are allocated when a total increment of biomass has been modelled.

As far as direct structural measurements are concerned, there has been considerable interest in the relationships between the changes in surface radiance with sun and view angles (or BRDF) and structure. Among the most successful approaches to modelling the BRDF of forests and woodlands have been the Geo-optical Models described in Li and Strahler (1986), Jupp *et al*. (1986), Strahler and Jupp (1991) and Li and Strahler (1992). Jupp and Strahler (1991) also described the hotspot or BRDF effect for a leaf canopy – such as a crop. This selection is, however, only one narrow strand of a whole literature of effort. It has been found that the canopy structure is a very strong determinant of the form and strength of the way the brightness varies with sun and view angles (referred to as the Bi-directional Reflectance Distribution Function or BRDF) of land surfaces. In fact, most wide-angle data sets – such as airborne scanners, pointing sensors from space and wide view sensors from the air or space – need some knowledge of the BRDF to provide consistent data for subsequent interpretation. However, while measurements of BRDF certainly have the potential to yield important structural information (such as some ratios of vertical to horizontal foliage distributions) the inversion problem has remained very difficult to resolve.

The Li-Strahler BRDF model (Li and Strahler, 1986) was developed from a model previously used by Li and Strahler to derive forest structural information from image data through using the variance in the data (Strahler and Li, 1981; Li and Strahler, 1985). This approach, which is treated theoretically by Jupp *et al*. (1988, 1989), has not had a lot of operational application but (like the BRDF) shows how canopy structure, growth form, crown size and other structural elements have strong effects in the data (in this case on data variance) but are difficult quantities to derive from the data. On the other hand, the use of spatial statistics in empirical and semi-empirical ways has had some application (e.g. Coops and Culvenor, 2000). In principle, therefore, spectral mean data, multi-view angle data and image variance and covariance together provide considerable information on canopy structure. But in practice this combination is still not used routinely except possibly to provide image statistics.

Radars (e.g. Ulaby *et al*., 1990) also respond strongly to canopy structure. However, most of these techniques seem to have difficulty in deriving the type of structural description we have looked at here and which has been used in Australia for vegetation mapping. An alternative is to use very high spatial resolution images as has been done by Coops and Catling (1997a,b) and Coops *et al*. (1998) using video data. However, the extra image processing, mosaicking and balancing required to pre-process the input data make this difficult or costly to apply to large areas – and there is no vertical resolution of canopy information unless the images can be taken as stereo or multi-view angle images.

In view of this, and in terms of the previous discussions, we believe that in order to:

- derive a sound characterisation of the BRDF for image interpretation;
- achieve separation of crown and foliage effects at regional scales;
- determine layering effects in natural forests and woodlands and
- provide independent information for optical and radar data to complete the mapping task;

we need to be able to resolve the extended gap probability function $P_{gap}(z, \mu_v)$ for a number of ranges (z), a number of view angles (μ_v) and its second order function $P_{gap}(z_i, \mu_i, z_v, \mu_v)$ for incident and view ranges and directions and at a number of scales (i.e. sampling patch size or structuring element size).

That is, we need to determine gap probability as a function of view angle and *range* and at a variety of scales as measured by the solid angle of the "structuring element" or "sieve". To determine range and P_{gap} as a function of range we propose to use Lidar technology and its data as described below.

3.4 Summary of Typical Measurements by Activity

Based on the above discussion of measurement technologies and current activities we can refine the discussion of measurement technologies as follows:

1. Environmental, Habitat and Conservation

   Environmental measurements such as the Walker-Hopkins field method or the various techniques for cover and height described above provide the broad level for the parameters identified for the NVIS. Basically, this means growth form, cover and height for the dominant stratum or (better) the delineation of the three or four main layers and their growth form, dominant species, cover and height by field measurement or API.

2. Forestry

   2.1 Native Forests

   Traditional forest measurements involve detailed measurements at fixed (e.g. permanent growth) sites, calibration of timber volume with

transfer by a simpler set of data such as Basal Area and DBH (and possibly height) and then extension by cruises or API.

Detailed data can include: Diameter at Breast Height (DBH) and its distribution (or Stand Table), Tree density (λ), Height of dominant stratum (h), Crown diameters (D), thickness or length (T), Crown length ratio (measured as T/h), Basal Area (BA), Taper factor, Log Volume (V), Crown Closure (CC or CAD), Site Index, Stand height curve (plot of height as a function of DBH or BA).

2.2 Plantations

Plantations in well established areas use similar techniques to establish site index from which future growth and yield is inferred. Stocking rates (tree density) are assessed and trees thinned. However, it is likely with the increasing use of growth models that data more like the NVIS structural description will be utilised.

3. Carbon

At this time, biomass and carbon are estimated from structural classes. If sufficient biomass data could be associated with the new NVIS classes it is likely that they will provide the basis for future estimates. Therefore, the basic structural techniques such as those outlined by Walker and Hopkins (1990) provide the best available methods. Alternatives suggested have been to use forestry techniques and establish foliage and root biomass by allometric equations. However, the complexity of native forests suggests this may not prove accurate without the development of new allometric equations for different forest types.

4 CANOPY LIDAR MEASUREMENTS OF COVER AND STRUCTURE

4.1 Introduction

The Laser signal returned from various levels of a canopy will depend on the range resolved gap probability function introduced in preceding sections. The return from the earth's surface will depend on the total cover and the timing of first canopy return signals will indicate the height of the upper stratum. The shot-to-shot variation in these data will be a function of the variance in tree sizes and the degree of clustering of foliage into crowns and clumps. However, realising the full benefits of these data with current systems such as the NASA SLICER (Harding, 2000; Harding *et al*., 2000) is not yet complete. One problem is that data taken to date have rarely been calibrated (i.e. accounting for energy and reflectance) and another has been the lack of account for horizontal structure in the interpretations. In addition, current airborne Lidar systems tend to work in the vertical and do not scan at angles to the vertical. This leaves some significant uncertainties in the actual structure of the vegetation being mapped.

The Lidar systems considered here are of two kinds. One, called "ECHIDNA®", is situated on the ground and gives full digitisation of the return pulse for a variety of view angles and beam sizes and shapes in the upper hemisphere and can scan "almucantar" or constant zenith angle scans. The ECHIDNA® is an alternative (with day/night capability) to hemispherical photography and fully supersedes both the informative but laborious Warren Wilson method (Warren Wilson, 1959a,b, 1960, 1963) which can be used for crops and grasslands and (for Forestry) the Speigel Relaskop.

The other is an airborne system, called "VSIS" or Vegetation Structure Imaging System. VSIS is assumed to scan and digitise the full return pulse as a function of view angle near to vertical from the air and normally includes a strong ground return. VSIS is intended as an Australian equivalent to SLICER but will take advantage of newer technology, a design phase appropriate to Australian vegetation and the experience of working with ECHIDNA®. A VSIS may also include multi-frequency and polarisation data. Together, these instruments offer a new dimension in canopy measurements and characterisation at site and regional scales.

4.2 Models for Lidar Returns & Implications for Canopy Mapping

To derive vegetation profiles and other structural information from canopies, the directional gap probability with range function $P_{gap}(z,\theta_v)$ provides an effective base of data for vertical canopy profiles of foliage density and angular variation. The variance associated with this function through the second order function $P_{gap}(z_i,\mu_i,z_v,\mu_v)$ also provides data which are currently unexploited in vegetation canopy analysis – including current Lidar based data.

How these relate to the physical data recorded by the sensor is the subject of the following sections. We use a calibrated digitised trace and develop the appropriate statistics. Data will also be augmented by optical remote sensing data. Collocated spectral data are assumed to provide some vegetation type and association information – at least for the upper and mid-stratum and provide a crosscheck on foliage and background reflectances and overall cover fraction. It is assumed one of the spectral channels is the same as the Laser.

4.2.1 Basic Lidar/Target Reflection – time based equation

If you place a lambertian plane target normal to the laser beam at distance *R* from the laser source, which is large enough so that part of the beam does not fall off the target then the Lidar equation for the response (*E'*) to an impulse signal ($\delta(0) = \delta_0; \delta(s) = 0\ s \neq 0$) at time *s* would be:

$$E'(s)=t_A^2\ \rho\ \frac{C}{R^2}\delta(s\text{-}2R/c)+e(s)$$

where:

ρ is the target reflectivity;
t_A is atmospheric transmittance for the path between the Lidar and target;
C is an amalgamation of receiver optics efficiency, receiver telescope area, quantum efficiency etc.;
e(s) is assumed small and represents background of atmospheric backscatter, natural light etc.

An expression for *C* is:

$$C = \eta\ t_0\ A_R$$

Where:

t_0 is receiver optics throughput;
A_R is effective receiver telescope area (which can depend on distance to the target);
η is detector quantum efficiency

C could also be used to absorb any consistent difference in behaviour of the sender/receiver beam optics from a $1/r^2$ relationship (which assumes the Lidar beam is narrow and the reflected beam is diffused and collected by a telescope with FOV narrower than the diffusion) model above.

The result of the Lidar sending out a finite width pulse shape is to effectively "smear" this impulse pulse in range (actually in time) as a convolution with the pulse shape ($h(s)$):

$$E(s)=h(s)*E'(s)$$

So, the "spike" pulse at the target range becomes a finite pulse over an apparent range when time is converted to an apparent range as $r = c\,s/2$. With this conversion, measured signal *E(r)* will come from "in front of" and "behind" the actual target in apparent range.

For example, the effect of the pulse convolution can be determined from analysing the fully digitised signal from a pulse return off a standard target. Tests were done with an atmospheric Lidar developed by CSIRO Atmospheric Research (CAR). Reflectance from solid targets produced a very consistent representation of the convolution kernel in this case. It is shown in Figure 4.1 along with an analytical approximation to the pulse by the Rayleigh kernel:

$$h(s) = a(s - s_0)_+ e^{-b(s-s_0)^2}$$

a Gaussian kernel:

$$h(s) = a\, e^{-b(s-s_0)^2}$$

and a modified Rayleigh kernel:

$$h(s) = a(s - s_0)_+^c e^{-b(s-s_0)^2}$$

As shown in Figure 4.1, the modified Rayleigh model is a good one for the pulse but does not explain the effects in the pulse tail (above 25 ns). The Gaussian is also a good model in this case – again it does not explain the tail. A stable Gaussian pulse with no effects in the trailing area of the pulse would be an ideal feature of a canopy Lidar.

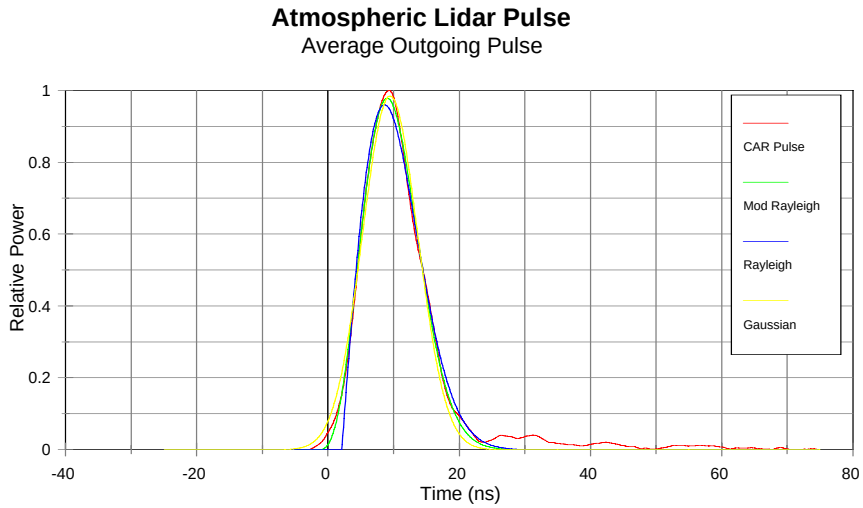

Figure 4.1. CAR Lidar pulse with Rayleigh and Gaussian approximations

The time measure in Lidars is normally taken relative to the emergence of the peak power of the pulse out of the instrument and peak power will be denoted E_0.

4.2.2 Calibration and Signal to Noise

The basic calibrated "remote sensing" problem is to measure range *R* to target and reflectance ρ. If the pulse has a narrow, sharp peak and targets are well separated the task is relatively easy in the range (R) case. But, while more difficult, ρ is still valuable to us and worth pursuing.

The calibration issue is to determine *C(R)* which may depend on *R* – especially in the near range if the signal source and receiver geometry is not (for example) coincident. There have been many theoretical and practical studies (e.g. Halldorsson and Langerholc, 1978; Sasano *et al.*, 1979; Measures, 1992) to describe this geometric form factor. In many atmospheric Lidars it is only at ranges above about 100 to 300 metres where the factor C settles down. For example, the atmospheric Lidar at CAR has an overlap function *k(R)* (where $C(R) = C\,k(R)$) as shown in Figure 4.2 (Stuart Young, Personal Communication).

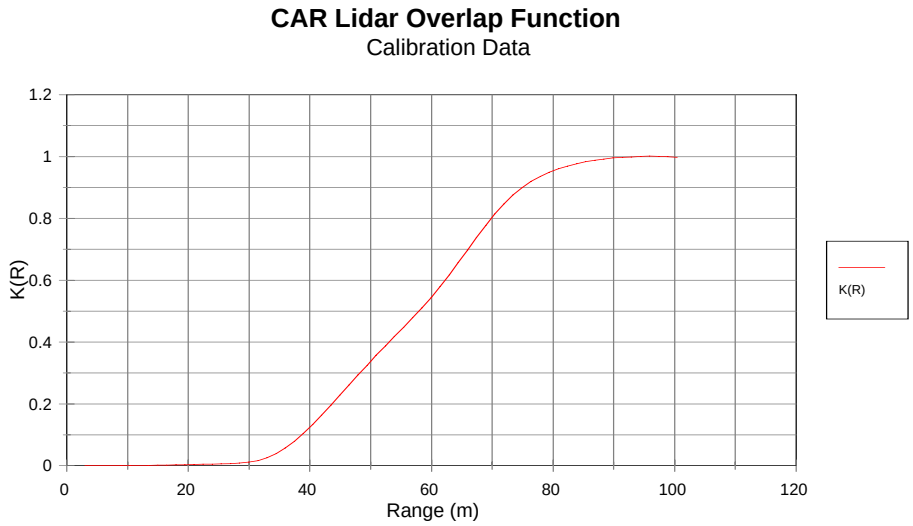

Figure 4.2. Overlap function defining near range calibration for CAR Lidar

This function is created by the fact that the receive telescope and send optics are not aligned. For atmospheric sounding it is not a problem as 100m is not significant for the overlap function to stabilise at 1.0. However, for a ground based Lidar this would be too far and source/receiver alignment must be closer. Even then, there will be a near range effect that must be characterised or removed by engineering. However, the CAR Lidar experiment demonstrated how both *k(R)* and *C* could be determined for such a system.

Obtaining an expression for *C(R)* as well as modelling t_A and *e(s)* allows the data to be converted to a form called the "apparent reflectance". This is defined (in terms of apparent range) as:

$$\rho_{app}(r) = \frac{r^2}{C(r)} \frac{E(r) - e}{E_0\, t_A}$$

For a narrow pulse or system with a deconvolved pulse this is the reflectance of a lambertian target perpendicular to the laser shot that returns the same pulse power as is measured at that range. The handling of pulse width effects will be considered later.

The calibration for *C(r)* can be done in the field as well as in the laboratory. Canvas or spectralon sheets as targets can provide effective calibration with range. Shapiro (1982) describes standard targets of varying reflectivity that were used in calibration and reflectivity studies. In a calibration experiment there should also be some solar radiation instrument(s) to record atmospheric conditions and irradiance and a weather station to record environmental factors (air temperature, humidity, wind speed and solar radiation) for background information.

Signal to noise is a key measure of the instrument capacity and performance. The primary sources of noise in the Lidar signal arise from various sources. Among them are (Measures, 1992):

1. Quantum noise in the photon limited pulse signal
2. Background radiation
3. Micro-turbulence (mainly water vapour) in the atmosphere
4. Dark current noise in the instrument
5. Thermal noise in the instrument (e.g. Johnson, Nyquist)

The role of noise due to quantum statistics and photon limited shots as well as the micro-turbulence in the atmosphere are particular characteristics of these types of measurement.

One aim of any instrument design phase is to estimate the instrument Signal to Noise Ratio (SNR) as a function of signal and system component characteristics so that an equation of a form such as:

$$SNR = (O + G * S)^{1/2}$$

or

$$SNR = O + G * S^{n}$$

for offset O, gain G and signal S can be defined based on selection of system components (including amplifiers and optical systems).

The SNR for a given range can be computed if the apparent reflectance is known or modelled. This provides the means to develop SNR based design studies for the canopies we will be mapping. An example of such a study (from the CLI Lidar ETBD) is presented in Section 6.3. The objective at this point is to model the apparent reflectance and this will be discussed below.

4.2.3 Large Foliage Element Canopy Model

4.2.3.1 Law of the first contact

Canopies attenuate the signal above the background surface and scatter lidar data back into the receiver optics. In a large element plant canopy, if a signal (photon) survives through gaps to a foliage element, the return signal can also retrace the path and so reach the detector. That is, in a plant canopy, the Lidar described above is sounding in the retro-reflection or "hotspot" direction.

More generally, the situation we are modelling is that of a transmissive medium filled by dispersed scattering objects. The transmission of the medium is assumed to be high - such as the atmosphere on most occasions and the objects may not be opaque but may also be assemblages of smaller objects, linked and with different scattering properties. An example is a tree which is an assemblage of branches, stems and leaves but where the leaves are often clumped into "modules" within the general area called the tree "crown".

In such a system, the transmission of a ray is governed by the Gap Probability Function, $P_{gap}(z,\mu)$, which is the probability that the ray will travel to range z in direction μ without contact with an object. It is also known as the length distribution function for rays in the direction μ that do not intersect an object.

In these systems suitably configured ground and airborne Lidars can sense this function as well as the second order function $P_{gap}(z_1,\mu_1,z_2,\mu_2)$ which is the probability that rays in directions μ_1 and μ_2 and ranges z_1 and z_2 will not intersect an object. The estimation of the second order function can be done by using "rays" of various sizes and shapes and ranging in many directions μ.

A laser pulse can be sent in one direction (μ_1) and received at a separate location and from another direction (μ_2). Such a beam will have travelled through gaps in the field of objects to a point specified by μ_1 and μ_2 and the travel time to and from the location at which it has been scattered by an object and returned to the receiver again through gaps in the assemblages of objects. While this general "bi-static" case is a potential tool for analysis, the specific system considered here will be one where the outgoing pulse and the return beam are aligned - the "bore-sighted" Lidar case. Since this operates in the "hotspot" region where all points of objects reachable from the source are also "viewable" by the sensors through the same gaps we have that $P_{gap}(z,\mu,z,\mu) = P_{gap}(z,\mu)$.

In this case, the relationship between the Lidar system measurements and the gap functions is through the "Law of the first Contact". This is the probability that the first contact with an object occurs at distance z and can be written:

$$P_{FC}(z,\mu) = -\frac{dP_{gap}(z,\mu)}{dz}$$

This is basically the intercepting area of scatterers at range z that are reachable from the source.

4.2.3.2 Large object model for Apparent Reflectance

Writing the time based instrument equation of the last section in terms of distance (range) rather than time, and assuming the calibration factor discussed above (C(r)) is known, if $P_{gap}(r)$ is the probability of no collisions from zero to range r then a simple model of the apparent reflectance of the canopy at range *r* is:

$$\begin{aligned}\rho_{app}(r) &= \frac{r^2}{C(r)}\frac{E(r)-e}{t_A^2 E_0} \\ &= \rho_v \, P_{FC}(r) \\ &= -\rho_v \, \frac{dP_{gap}}{dr}(r)\end{aligned}$$

where:

ρ_v is the "effective" hotspot reflectance of foliage elements in the direction of the Lidar (integrated over foliage angle distribution) at the range and may include object orientation and specular effects from foliage facets normal to the beam. Even for lambertian leaves, the effective cross-section of the foliage elements needs to be modelled – especially for the ECHIDNA® where the angular soundings are important to the modelling. Discussion of the effective reflectivity of foliage can be found in Ni *et al*. (2001).

The signal back from the ground will be:

$$\rho_{app}(h) = \rho_g \, P_{gap}(h)$$

where ρ_g is the reflectance of the ground.

It is also useful to *define* a gap attenuation coefficient (or Apparent Foliage Profile):

$$\begin{aligned}l(r) &= -\frac{1}{P_{gap}(r)}\frac{dP_{gap}(r)}{dr} \\ &= -\frac{d\,Log P_{gap}(r)}{dr}\end{aligned}$$

using this definition and terminology:

$$\rho_{app}(r) = \rho_v \, P_{gap}(r)\, l(r)$$

We are assuming there is little or no forward scatter or the individual foliage elements are not very highly transmitting. If this is not so, multiple scattering may cause time delayed signals and signals apparently back from "under the ground". In most cases and at most wavelengths this effect is not anticipated to be very significant and initial modelling seems to support this belief.

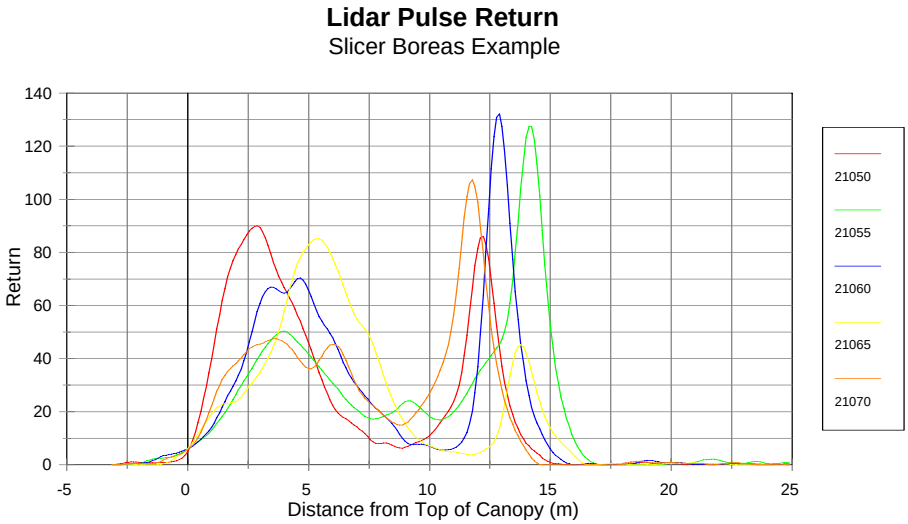

Figure 4.3. LIdar pulse returns from a forest canopy

Figure 4.3 shows a set of five return signals obtained from SLICER sounding over a Boreal forest site. The pulse width is very clear in the ground returns to the right and the attenuation of the signal in the canopy (after rise to a peak return) is also well illustrated. These data have been referenced to the topographic surface and the position of the surface is accurately known. In these data, pre-processing has also been applied to eliminate the basic background noise bias.

4.2.3.3 Effects due to beam and footprint size

The large object model for the Lidar scattering is based on the fact that the derivative of the gap probability function (or Law of First Contact) gives a measure of the density of scattering of the surviving radiation.

In a canopy Lidar, the beam is also spread over a finite footprint. This corresponds to a bundle or cone of "rays" spreading out over a range of angles from the source point. Each of the rays may penetrate the canopy to a different depth and return energy from that point. The effect of this broader beam is thus to create a Lidar "waveform" of returns spread over a number of points of time.

The basic equation based on the first hit probability provides an expected distribution of returns. A single "ray" of near zero width will have a single return which is a drawing according to the Law of the First Contact. Over a finite beam each ray can be thought of as a sample from this distribution allowing the measured first contacts to provide an estimate for the expected return distribution over time as modelled above. To measure this distribution, the system needs to record the Lidar return intensity over time at a high enough density to resolve the returns.

There is a significant interplay between the beam width and the time structure of the returns. A single ray will have a single return from the first hit. Even a finite beam will normally have a single return if the objects are large. For example, even a *very* broad beam will have a single return (spread in time only by the outgoing pulse spread) from a wall perpendicular to the beam.

The time spread of returns is in fact a function of the object sizes and shapes and dispersion as well as the "opacity" of the objects. Objects which are solid will give narrow returns and objects which are assemblages of smaller objects will give dispersed returns in which the "clustering" indicates the object itself. Making use of this response is a significant opportunity in canopy Lidars.

Mathematically, the relationship will depend on the second order (correlation) functions for any range z:

$$h_z(\delta\mu) = P_{gap}(z, \mu_0, z, \mu_0 + \delta\mu)$$

where μ_0 is the direction of the ray at the centre of the beam and $\delta\mu$ traverses the beam and also on the way it "scales".

For example, if the objects are large relative to the beam size with comparable between-object separations, then the waveform will have separated clusters of returns corresponding to these objects. The spread within the clusters will depend on the within-object structure but will often be dispersed. If the objects are small relative to the beam size then the returns will be multiple (or near continuous) and be spread in time in relation to the local density of the objects. An example of the first is tree crowns filled with leaves being sensed by a canopy Lidar and an example of the second is an atmospheric sounding Lidar where the objects (atmospheric particles) are always small relative even to a very narrow beam.

In terrain Lidars, the beam is small so that for many canopies there will be relatively few returns from a single shot. However, the density of coverage needed if the beam is small even relative to leaves and twigs is very high and if the beam is broadened many more time dispersed returns from the canopy will mask the terrain signal.

The time spread of the outgoing pulse, the beam width and the sampling rate of the recorder all need to be carefully modelled to allow the derivation of the canopy structural information or even to effectively measure terrain in the presence of an overstorey. This interaction between the beam width and the structure of the system being sounded is not only a means for averaging the first-hit probabilities but is also key information that canopy Lidars have the potential to obtain and exploit.

4.2.4 "Standard" solutions for P_{gap} and Apparent Foliage Profile

The solution for canopy information proceeds as follows:

$$\rho_{app}(r) = -\rho_v \frac{dP_{gap}(r)}{dr}$$

$$\begin{aligned} H(r) &= \int_0^r \rho_{app}(r')\,dr' \\ &= -\rho_v \int_0^r \frac{dP_{gap}(r')}{dr'}\,dr' \\ &= \rho_v (1 - P_{gap}(r)) \\ &= \rho_v \, Cover(r) \end{aligned}$$

The function H(r) can be computed from the data as a cumulative factor. But, we also know that:

$$\begin{aligned} \rho_{app}(h) &= \rho_g \, P_{gap}(h) \\ &= \rho_g \, (1 - \frac{1}{\rho_v} H(h)) \end{aligned}$$

which provides a consistency relationship for the reflectances and foliage profile. That is:

$$\rho_{app}(h) = \rho_g - \frac{\rho_g}{\rho_v} H(h)$$

To solve this for the gap profile, it is usually assumed that the ratio of the (presumed constant) foliage and ground reflectances is known. For sloping ground the ground reflectance is assumed to be modulated by the cosine of the slope angle. The ground reflectance is then given by the above equation and hence both reflectances are given from the data. With this assumption, ρ_g can be computed and hence also ρ_v.

Note that from this follows that:

$$\begin{aligned} Cover(r) &= \frac{1}{\rho_v} H(r) \\ &= \frac{H(r)}{H(h) + \frac{\rho_v}{\rho_g} \rho_{app}(h)} \end{aligned}$$

so that Cover at any depth can be mapped as can tree height from the start of the foliage returns. Hence, the canopy structure diagram plot can be developed for an area provided a good choice can be made for the ratio of the vegetation to background reflectance.

In fact, it is easy to see that:

$$Cover(h) = \frac{1}{1 + \frac{\rho_v}{\rho_g} \frac{\rho_{app}(h)}{H(h)}}$$

This depends only on the ratio of the reflectance of the foliage to that of the background and shows how this ratio drives the estimate of the overall cover.

Lefsky *et al*. (1999a,b) use the name "Cumulative Canopy Power Distribution" (CPD) for what we are calling "*Cover*".

For the final canopy gap profile:

$$P_{gap}(r) = 1 - \frac{1}{\rho_v} H(r)$$
$$= 1 - \frac{H(r)}{H(h) + \frac{\rho_v}{\rho_g} \rho_{app}(h)}$$

which is easily computed from the data.

The corresponding gap probabilities for the SLICER data shown above shown in Figure 4.4:

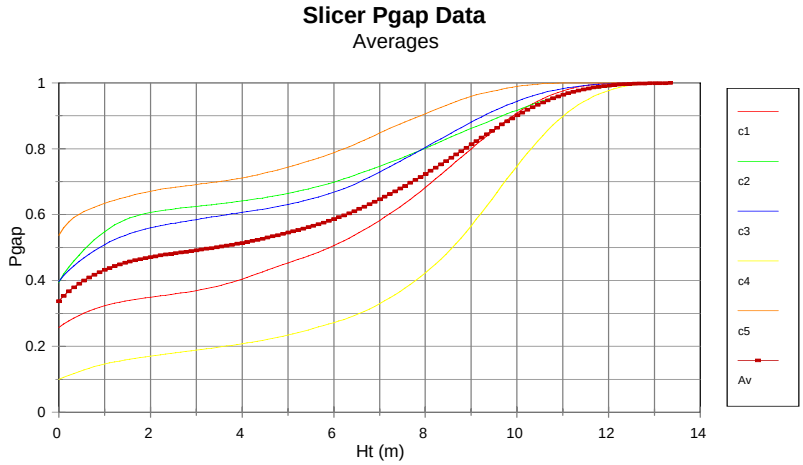

Figure 4.4. Gap probabilities derived from SLICER data

The projected Apparent Foliage Profile (Figure 4.5) can now be obtained by using the relationship:

$$l(r) = -\frac{1}{P_{gap}(r)}\frac{dP_{gap}(r)}{dr} = -\frac{d\,LogP_{gap}(r)}{dr} = \frac{\rho_{app}(r)}{\rho_v - H(r)}$$

However, this direct approach can potentially become unstable in situations where the SNR is low, where the signal being returned is small and where P_{gap} has become small due to attenuation by foliage above the point. This instability must be handled in a satisfactory way by regularisation. Nevertheless, the provision of the gap profile $P_{gap}(r)$ (Figure 4.4) is, by itself, a major outcome and may be used in further canopy modelling as described below.

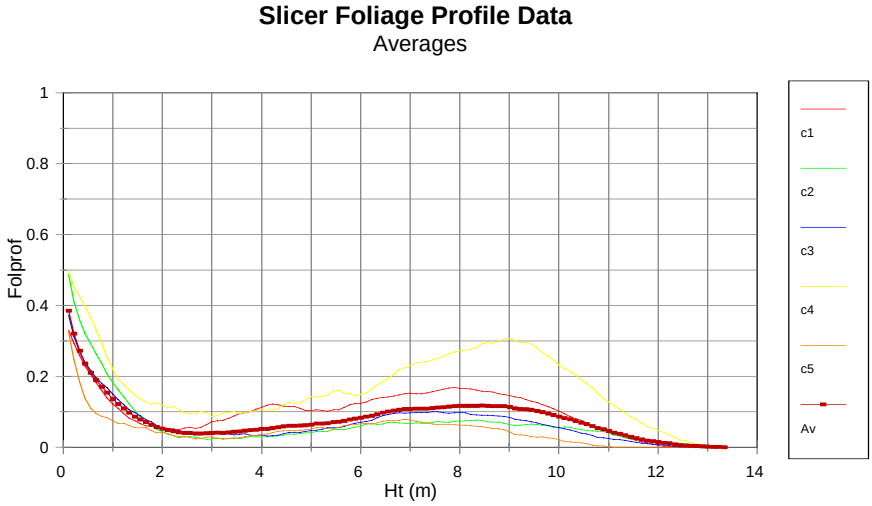

Figure 4.5. Estimated apparent foliage profiles for SLICER data

It can be shown (see Appendix 2) that provided the calibration model in the region of the canopy and ground data can be represented as:

$$C(r) = \frac{\tilde{C}}{r^2}$$

where $\tilde{C}$ is constant, and if it assumed the data are normalised by the outgoing pulse intensity in the units of the data collection (this means measuring the pulse power) then the solution may again be obtained by applying the same method if the reflectance ratios are known and there is a ground return. Therefore the solution is obviously quite practical in most situations. In fact, since for up to 50 metre canopies and 2000 metre flying height, the variation due to normalising by the factor r^2 is small it is often neglected as well – as are background radiation and atmospheric transmission. This is in marked contrast to other cases (such as atmospheric Lidar

modelling and ground based Lidar) where the targets are spread over a very wide range.

From the relationship:

$$l(r) = -\frac{d\ LogP_{gap}(r)}{dr}$$

it follows that:

$$\begin{aligned} P_{gap}(r) &= e^{-\int_0^r l(r')dr'} \\ &= e^{-L(r)} \end{aligned}$$

where *L(r)* is defined by this equation but can be thought of as the cumulative apparent projective cross sectional area of foliage. That is:

$$\begin{aligned} L(r) &= -Log\ P_{gap}(r) \\ &= -Log\ (1 - Cover(r)) \end{aligned}$$

The quantity "*L(r)*" presented here has also been called the CHP or Canopy Height Profile (MacArthur & Horn, 1969) and exploited extensively by groups analysing SLICER data such as Lefsky *et al*. (1999a, 1999b) and Means *et al*. (1999).

Lefsky *et al*. (1999a,b) also define and use a quantity they call "Relative CHP" that (interpreting their definition) can be expressed in the notation of this document as:

$$\begin{aligned} CHP^*(r) &= \frac{-1}{CHP(h)} \frac{d\ CHP(r)}{dr} \\ &= \frac{l(r)}{L(h)} \end{aligned}$$

It follows that:

$$\int_0^h CHP^*(r')\,dr' = 1$$

and Lefsky *et al*. (1999a,b) note that this relative profile is very insensitive to the choice of the ratio of vegetation to ground reflectance. Ni *et al*. (2001) show how this is to be expected and demonstrate it for a range of models.

Since:

$$L(h) = -Log(1 - Cover(h))$$

it follows that *L(h)*, $P_{gap}(h)$ and *Cover(h)* all depend directly on the choice of ratio but the relative distributions do not to as great an extent. All of these factors need to be taken into account in the practical implementation of the models.

4.3 Implementation of the models

4.3.1 Vertically layered random foliage model

A simple model for gap probability is the vertically layered random foliage model. In this case, the foliage profile is simply the Foliage Area Density (total one sided area of foliage per unit volume) denoted *F(r)* and the canopy is assumed to extend uniformly in horizontal directions.

In this case let *l(r)* be the projected cross sectional area of scatterer per unit volume at range r assumed randomly distributed and independently distributed.

Basically,

$$l(r) = \lambda(r)\,\bar{a}(\mu_v)$$

where:

$\lambda(r)$ is the density of scatters at range r and
$\bar{a}(\mu_v)$ is the mean cross-sectional foliage area for the incidence and view angle μ_v (which is nadir view, or $\mu_v = 1$, in this case)

Alternately,

$$\begin{aligned} l(r) &= G(\mu_v)F(r\mu_v)/\mu_v \\ &= G(1)F(r) \qquad (\mu_v = 1) \end{aligned}$$

where G is the Ross G-function.

If foliage elements are assumed to be very small so that occlusion can be neglected, and taking the vertical view direction, we can simply write:

$$P_{gap}(r) = e^{-\int_0^r l(s)ds}$$

$$\begin{aligned} \rho_{app}(r) &= -\rho_v \frac{dP_{gap}}{dr} \\ &= \rho_v\, l(r)\, e^{-\int_0^r l(s)ds} \end{aligned}$$

$$\rho_{app}(h) = \rho_g\, e^{-\int_0^h l(s)ds}$$

If we define *L(r)* as the cumulative projective cross sectional area:

$$L(r) = \int_0^r l(s)ds$$

then:

$$P_{gap}(r) = e^{-L(r)}$$
$$\rho_{app}(r) = \rho_v \, l(r) \, e^{-L(r)}$$
$$\rho_{app}(h) = \rho_g \, e^{-L(h)}$$

In this case, the canopy gap attenuation coefficient or Foliage projected Profile is just the incremental leaf area.

Note that:

$$-Log\ Cover(r) = -Log\ (1 - P_{gap}(r))$$
$$= L(r)$$

That is, as noted above, *L(r)* is identical to the Canopy Height Profile (CHP) used by Lefsky *et al*. (1999a,b) in their analyses of structure of US forests.

In a practical case, the foliage will not be assumed distributed to a point but perhaps in a finite layer. If L_i is the cumulative effective cross sectional area to layer i:

$$L_i = \sum_{j=i_{\min}}^{i} l_j$$

then, the equations become:

$$\rho_{app,i} = \rho_v \, (1 - e^{-l_i}) \, e^{-L_{i-1}}$$
$$H'_i = \sum_{j=1}^{i} \rho_{app,j} = \rho_v \, (1 - e^{-L_i})$$
$$\rho_{app,h} = \rho_g \, e^{-L_h}$$

Note if there are N layers there is a consistency relationship as before:

$$H'_N = \rho_v (1 - e^{-L_N})$$
$$= \rho_v (1 - \frac{1}{\rho_g} \rho_{app,h})$$

If the reflectance ratio is assumed or known, the data can be inverted to get $P_{gap}(r)$ and foliage profile. The issues of pulse deconvolution and regularisation of the foliage profile estimate do, however, need to be addressed.

The horizontally random model has the property that the actual projected Foliage Profile is the same as the Apparent Foliage Profile. However, horizontal gaps and clustering into crowns and foliage clumps affect both the variance profile between different shots and also the relationship between actual and apparent foliage profile. This will be discussed in more detail later.

4.3.2 Beam divergence and scaling issues

The configuration of the Lidar instruments involves both the time resolution of the Lidar pulse and the beam divergence or spot size. Obviously, the bigger the beam divergence the larger the spot size on the ground and the more horizontal canopy averaging that will take place. As described earlier this allows the distribution of first hits to be sensed from a single waveform but may also have disadvantages when the single first hits have special value.

In a flexible system, the Lidar pulse can be made very narrow or be allowed to spread to a wide spot interaction with a canopy. The narrow beam is favoured in terrain (especially to derive a Digital Terrain Model or DTM) applications and minesite mapping applications for a variety of reasons.

The first reason is that for a narrow beam there is potentially only a single return signal from the first scattering event, after which there is considerable attenuation or no signal to return. The signal can be filtered for a peak return and the data confined to range. For a small spot size, the signal will also often penetrate gaps in the canopy to give a clean, unattenuated and distinct surface background signal for DTMs even with a significant overstorey of trees. In most cases, the return will be from a single surface and will not alter the pulse shape significantly. All of these are advantages for the applications mentioned.

For forest canopy mapping, the disadvantage of the small spot size is that the gap probability (or first hit) distribution can only be inferred from a very large number of samples. The spatial variance of returns will often be so high that very large volumes of single shot data will be needed to infer stable canopy parameters at broader scales – such as crown sizes and clumping. If an aircraft is moving relatively quickly it is likely that too few samples will be taken in any one stand to obtain stable parameters. A slowly moving platform, such as a helicopter, taking large volumes of data (including intensity of returns) is therefore needed. Such an arrangement is very expensive and requires large volumes of data to be processed to obtain relatively simple products.

If the Lidar beam is spread into a larger spot size and the receiver optics arranged to collect over the area illuminated, there will normally be a spread of returns arriving at the detector from targets within the canopy as well as from the background. This beam spreading must be combined with a greater density of sampling of the return signal. In the design assumed here for Canopy Lidar, it is assumed that the complete return signal is sampled for intensity as well as range at a rate allowing quite fine modelling of the foliage profile. This may involve nanosecond or even sub-nanosecond sampling.

Larger spot sizes with digitising of the return signal allows relatively stable estimates of the foliage profile and gap probability function to be derived for each Lidar pulse with an optimum spot size dependent in some way on the canopy clump sizes (Means *et al*., 1999). It allows a relatively high flying and fast moving aircraft to map over large areas and hence provides the means to characterise regions at reasonable flying and processing cost. The spot size should optimally be chosen as a function of the land cover. There is some merit in making it of similar size to the average crown size in an area. It should not, however, be so large that the return signal becomes a heterogeneous mixture. It is anticipated that spot sizes at the canopy top of between 5 and 25 metres will be sufficient to cover all practical scales and that this can be achieved with a combination of (variable) beam spread and flying height.

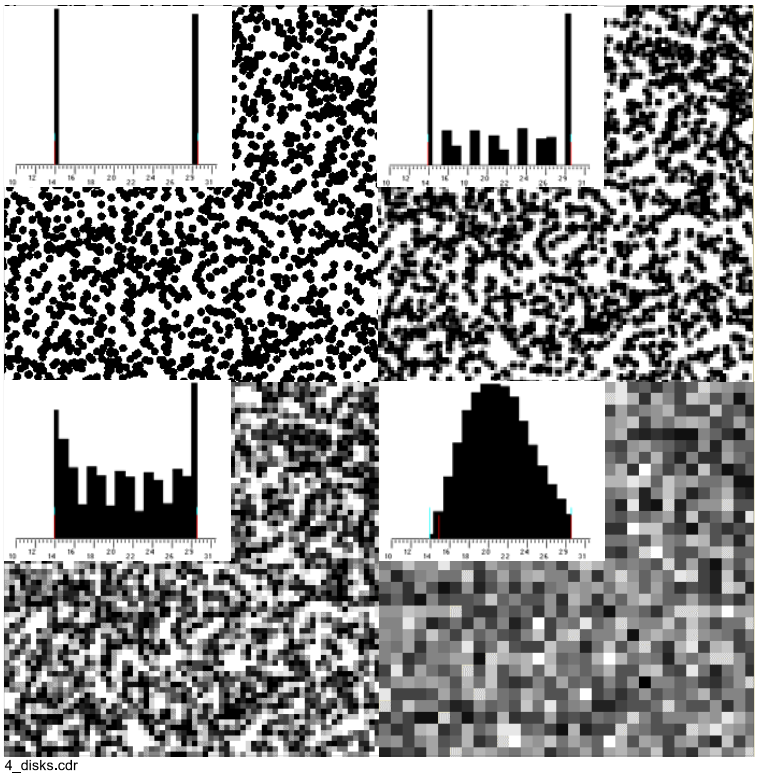

Figure 4.6. Effect of spot size (beam width) on estimated cover

The effect of increasing beam size on the signal and on the sensing of cover is well illustrated in Figure 4.6 where small black disks on a white background are used to simulate trees and (one minus) the cover is simply the mean value of the image data over the increasing pixels. The reduction in variance and convergence to a single peak representing "cover" is characteristic of the tree sizes, cover and also the way the averaging occurs. Incidentally, this diagram clearly demonstrates the change in spread that occurs in a structure diagram when the plot size changes. The effects can also be modelled and an example of the modelling will be described later.

Using larger spot sizes and signal digitising reduces the variance, reduces the data volume per hectare and makes regional mapping feasible. However, its down-side trade-off is that the signal becomes a mixture and (in particular) the signal from the soil background:

1. Becomes weaker and mixed with canopy returns; and
2. Can change its shape depending on local micro-relief, slope and near surface corner reflections.

The need for greater care in identifying, positioning and interpreting the signal from the background is the reason that larger spot sizes are not popular for DTM work and suggests any practical system may need to vary the spot size and even possibly combine narrow pulse data with a larger scanning data set to allow the necessary subtraction and normalisation that the background signal is used for.

4.3.3 Pulse Width and Deconvolution

If the background were a flat, lambertian surface then the return signal from it would mirror the shape and width of the Lidar pulse. The width of a Lidar pulse varies with instrument and the FWHM (Full Width Half Maximum) determines the range resolution of the instrument. That is, the lidar has difficulty in resolving targets separated by less than the range equivalent of the FWHM. With the proposed VSIS, this range is aimed to be one half a metre or a pulse width of about 3 nanoseconds. The digitising of this signal can be down to one half a nanosecond.

The width and shape of the return signal from the ground can be modified significantly by micro-relief and also by slope. The slope effect is larger for a bigger spot size, which is another reason that small spot sizes are favoured for DTM mapping Lidars. For example, if the slope angle is θ and the spot size is d metres, the width of the pulse (in range units) will be increased by:

$$w' = w + d\ Tan\theta$$

That is, if d is 25m a slope of 1:10 will increase the width significantly.

Figure 4.7 shows an arbitary set of ground returns from SLICER data (legend labels are shot number). The SLICER pulse shape is not claimed to be very stable – however, there is a significant shape consistency in these plots which also include a Rayleigh as a model for the pulse shape plus an "asymmetric" Gaussian:

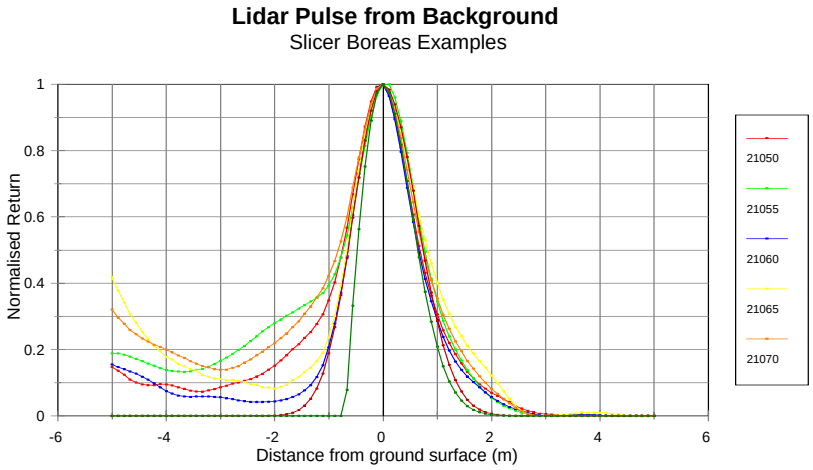

Figure 4.7. Ground pulses from SLICER normalised to unit at ground

Despite the need to remove the broad shape of the pulse at the ground and its "mixing" in the canopy signal, very little has been done with signal deconvolution. This, together with recognition of the ground signal that takes into account the pulse shape changes expected from the micro-relief is an important area needing attention for operational use of canopy Lidars.

By "deconvolution" is meant the inverse of the "convolution" of the signal that would be acquired by a very sharp pulse with the waveform of the actual pulse. Deconvolution can be carried out in the frequency domain by Fourier transform or the time domain by least squares. At this time, a time domain method has been the one given attention.

That is, as we wrote above, if the zero time is taken as the peak of the Laser pulse, the signal (after removal of background noise) can be modelled as:

$$P(r) = h(r) * S(r)$$

where:

h(r) is the pulse shape function and
P(r) is the actual measured return power.

For example, we have seen that for the CAR Lidar used for initial experiments, a modified Rayleigh model for h was reasonable of the form:

$$h(s) = a(s - s_0)_+^c e^{-b(s-s_0)^2}$$

The Fourier approach uses the result that:

$$\begin{aligned} \Im(P(r)) &= \hat{P}(\omega) \\ &= \hat{h}(\omega)\, \hat{S}(\omega) \\ S(r) &= \Im^{-1}(\hat{S}(\omega)) \\ &= \Im^{-1}\left(\frac{\hat{P}(\omega)}{\hat{h}(\omega)} \right) \end{aligned}$$

This looks straightforward and is improved if the pulse shape is known analytically (or by analytic approximation as above) but suffers because:

- The useful digitised signal series is quite short (e.g. 70 nanoseconds in a canopy)
- The digitising step is not very small (e.g. 1 nanosecond is at the edge of technology)
- A discrete fourier transform must be used
- The finite pulse becomes an infinite function in the fourier domain.

The digitising step and length limit the fundamental frequency and Nyquist for the discrete fourier representation of the data and hence the finite pulse is heavily aliased.

Finally, the transformed pulse will be small in the high frequency part of the spectrum and the deconvolution will be unstable unless some regularising is applied.

The "quadrature" approach to the time domain version finds a filter such that to a good approximation:

$$P_i = [h * S](r_i) \approx \sum_{j=-k}^{k} h_k \; S(r_{i+j})$$

where r_i is the i'th sample range.

If it is enforced that the actual signal S is zero above the canopy and below the ground then this can be written as a set of equations which may be solved for S.

$$H \; S = P$$
$$S = H^{-1} P$$

The solution for S is also not free of noise and the reasons are actually much the same as in the fourier domain. So, some regularizing can be applied.

One method of regularisation is to only estimate a convolved S with the new convolution function having a much smaller width (e.g. 1 nanosecond rather than 10 nanoseconds). This acts to filter out very high frequency effects and will stabilise the solution. If this convolution is written as K this means estimating KS so that:

$$KHK^{-1}(KS) = KP$$
$$(KS) = (KHK^{-1})^{+}(KP)$$

where the operation of K on P acts as a prefilter for high frequency noise and the "plus" indicates a generalised (possibly regularised) inverse.

A major advantage of the time domain approach is in the finite representation of h and the control over the quadrature approximation to the convolution. More control over the regularisation is also possible. For example, to regularise the above solution you may require:

$$L(KS) = \left\| (KHK^{-1})(KS) - (KP) \right\|$$

to be small and some regularisation such as KS or some derivative of KS to be small.

There are a number of time domain approaches to developing the filter weights $\{h_k\}$ and solving the equations. In its general form, the inverse convolution (or de-convolution) problem is to estimate a function *s(t)* from an observed function *p(t)* satisfying:

$$p(t) = \int_{-\infty}^{\infty} \varphi(t' - t)\, s(t')\, dt' + \varepsilon(t)$$

where $\varphi(t)$ is a known function – the Lidar pulse in this case and $\varepsilon(t)$ is the noise.

An approach that has been used to good effect is to use interpolation functions such as splines with regularisation.

Let *s(t)* be approximated by an interpolating spline for a set of time points (the spline knots, $\{t_i \mid i = 1, n\}$) and represented by its Cardinal series of functions $M_j(t)$ satisfying:

$$M_j(t_i) = \delta_{ij}$$

It follows that *s(t)* can be represented as:

$$\tilde{s}(t) = \sum_{j=1}^{n} s_j M_j(t)$$

Let

$$\tilde{\varphi}_j(t) = \int_{-\infty}^{\infty} \varphi(t' - t) M_j(t') dt'$$

then the result is the least squares solution to a problem that can be regularised by using a reduced number of spline knots or by a smoothing function of the form:

$$\tilde{p}(t_k) = \sum_{j=1}^{n} \tilde{\varphi}_j(t_k) s_j + \varepsilon_k$$

$$= \sum_{j=1}^{n} h_{kj} s_j + \varepsilon_k$$

The key elements here are the analytical convolution, the imposition of zero returns outside the estimated bounds of the top of canopy and ground (as previously) plus regularisation. However, the weights (h_{kj}) may not be positive and there can be high frequency effects to remove by post filtering. The key element to success is careful and adaptive regularisation based on the noise statistics.

4.3.4 Design and Specification of Lidar Systems by SNR Modelling

As noted above, calibrated Lidar systems can be converted to "apparent reflectance" or the reflectance a flat standard (lambertian) target at the given range would have to produce the same return signal. Similarly, the models described above can be defined and discussed in terms of the apparent reflectance as well.

The apparent reflectance for a range of different land covers or modelled land covers and forests can provide a means to specify and design the Lidar systems needed for airborne or ground based measurement and mapping. The airborne system will be discussed here.

As described previously, an instrument can be characterised by testing or modelling in terms of its ratio of signal level to noise, or Signal to Noise Ratio (SNR). Both the noise and the SNR depend on the signal level so that for a given power across the receive telescope field of view there will be an SNR value and by division of the signal level by the SNR there will be an RMS noise level computable as well.

For an aircraft flying at a given altitude at a given time of day with specified atmosphere there will be well defined atmospheric transmittance and background radiance so that the signal arriving for the range to the canopy will depend only on the apparent reflectance level and (hence) there will be an SNR value for each value of apparent reflectance at that range.

It follows then that if the flying time, height and atmosphere are specified and a model for SNR as a function of apparent reflectance is given (modelled) such as by:

$$SNR = a + b\ \rho_{app}^{n}$$

then for every model canopy it is also possible to plot SNR and RMS noise as a function of height above the ground.

This will provide a useful analysis of our capacity to resolve layers in the canopy – especially in the presence of dense overstoreys.

However, it is not providing a direct analysis of the resolvability of the information in the canopy. To do this, we will use the model for the inversion to apparent foliage profile:

$$\begin{aligned} l(r) &= -\frac{1}{P_{gap}(r)}\frac{dP_{gap}(r)}{dr} \\ &= \frac{\rho_{app}(r)}{\rho_v - H(r)} \end{aligned}$$

By making some approximations it is possible to show that the RMS error for the inverted apparent foliage profile has the form:

$$RMS_l(r) = \frac{\rho_{app}(r)}{\rho_v\ P_{gap}(r)\ SNR}$$

In the last section of this ATBD (Section 6), a set of models for Australian land covers will be presented and their Lidar returns simulated. A number of SNR models for typical instruments have been used to plot these measures of performance and define the needs for an effective instrument to map the lower layers of Australian forests.

4.4 Advanced Products – indices, layers and spatial variance

The models and methods described above represent a base set of products for mapping vegetation canopies from airborne Lidars. These types of model have been used with SLICER data to assess and investigate many ecological and forest sites in the US with very impressive results (e.g. Lefsky *et al*., 1999a,b).

However, as discussed in previous sections, there are many factors that an airborne Lidar is "blind" to in the canopy. These include foliage angle distributions, the clumping of foliage into crowns and the relationships that exist between stem and foliage. Inference of these, or of important canopy parameters despite these, can be done where the forest system shows high levels of correlation between vertical (apparent) foliage profiles and the significant parameters. The relationships that are developed are similar to allometric relations used by foresters. Alternatively, advanced modelling may be used to unravel some of these factors.

4.4.1 Canopy indices

There is considerable scope for developing indices based on Lidar waveforms, gap probability curves or apparent foliage profiles. In a very early example of such indices, MacArthur and MacArthur (1961) developed an index they related to bird species diversity. If l_i is the apparent foliage in the i'th layer then they defined:

$$p_i = \frac{l_i}{\sum_{j=1}^{N} l_j} = \frac{l_i}{L}$$

The foliage height diversity (FHD) index was defined as:

$$FHD = -\sum_{i=1}^{N} p_i \, Log \; p_i$$

MacArthur and MacArthur (1961) divided the foliage profile into three layers, 0-2', 2-25' and over 25'. They then found a relationship for their study area existed between the index and bird species diversity (BSD) defined similarly on the distribution of birds among a large number of species. (In fact, they found that $BSD = 2 \times FHD$ fitted the data well).

In effect, this is expressing the idea that a single tree layer will only attract a few species whereas a multi-layer canopy will attract many. This may come about as different species make use of the different layers. Whatever its ecological significance, however, it does express an important fact about the diversity of the structure. It fits well with the general structural categories of the NVIS and may be an interesting product – even if it does not always predict bird species according to the above equation!

Lefsky *et al*. (1999) define a quantity they call "quadratic mean canopy height" (QMCH) defined as:

$$QMCH = \left(\sum_{i}^{\max h} p_i \, h_i^2 \right)^{1/2}$$

where p_i is as before except that here the foliage "bins" are 1m thick and the h_i are the mid-points of the layers. They also use maximum, mean and median canopy height defined in a similar way relative to the fractions of apparent foliage at different levels of the profile.

More recently, Dubayah *et al*. (1997) have been directly deriving an index as the median height above the ground in the Lidar waveform (including the ground return). Obviously, the lower the cover the lower the index. In some ways, this index is related to height multiplied by cover which again is often well correlated with height times basal area – or timber volume. However, there is obviously considerable complexity integrated into the index as well.

The derivation and utility of indices will develop as data increases and experience grows. Nevertheless, an interpretation of the data in terms of modelling and inversion is attractive and the options we have for such products will be examined as the final discussion of this ATBD.

4.4.2 Recognising and mapping canopy layers

The provision of samples of the gap probability and initial (possibly regularised) foliage profiles can be seen as an initial step in data interpretation. Interpreting the data as a random and independent layered canopy with the foliage profile as the measure of its vertical LAI distribution is clearly inadequate in the real world of discontinuous canopies and mixed trees and shrubs as they occur in most Australian native vegetation covers.

In a clumped canopy, attenuation between the units of clumping (e.g. modules in crowns or crowns in stands) will be low and within the units will be high. As a result, the Apparent Foliage Profile will usually be lower in foliage amount than the actual profile due to foliage being "hidden" at depth by other foliage in a clump. It is therefore important to retrieve as much of the crown and clumping properties of the canopies as is possible from the data to estimate the amount of foliage correctly.

Another consequence of canopy heterogeneity is the variance of the data, which arises from the clumping of foliage into modules, modules into crowns and trees into clumps. This means groups of Lidar shots must be combined to provide an interpretation. But aggregated data also tends to remove the distinctions between a vertically layered canopy and a more realistic model with tree crowns and layering by trees rather than by foliage. Hence, the combined use of spatial variation and individual vertical shots seems to provide the best strategy in heterogeneous canopies.

An empirical approach to the definition of layers and their extraction from the Lidar data would be to aggregate shots from apparently homogeneous areas (as defined by other forms of remote sensing, such as a simultaneously obtained multi-spectral image) and fit functions describing each layer. The layers could then be fitted to each shot to get local variation in layer intensity.

One such function is the Weibull distribution as used by Yang *et al*. (1999) and others. For a single layer of maximum height H, and moving to height above the ground (z) rather than range, this function models the cumulative foliage profile as:

$$L(z) = a\left(1 - e^{-b(1-z/H)^c}\right) \quad 0 \le z \le H$$
$$P_{gap}(z) = e^{-L(z)}$$

which can model a single profile of l(z) with a single peak by exact differentiation:

$$l(z) = \frac{abc}{H}\left(1 - z/H\right)^{c-1} e^{-b(1-z/H)^c}$$

By choosing a number of layers, this group of functions can model most profiles – but after one or two it usually becomes ill posed to fit these functions. For example if there are N layers:

$$0 \le H_1 \le H_2 \le \ldots \le H_N = H$$

then the model can be written (where $t_+ = 0 \quad if\ t \le 0$):

$$L(z) = a\left(1 - \sum_{i=1}^{N} q_i e^{-b_i (H_i - z)_+^{ci}}\right)$$
$$q_i \ge 0 \qquad \sum_{i=1}^{N} q_i = 1$$

The recognition of layers obviously needs some care and involves mixed linear and nonlinear modelling. However, applying this method to aggregated data over an area or stand to establish an effective two or three layer description like the Carnahan or NVIS structural model could lead to an initial overall description of the canopy into major stands and layers which could be interpreted locally as a second step.

That is, *a* and the q_i values can be inverted for single profiles with constraints that they are non-negative. These can then be used to interpret layer cover. This is possible because the Weibull distribution has a useful interpretation in terms of the work we have described in previous sections. If we consider a single layer and look at $P_{gap}(0)$ for the Weibull distribution we find:

$$P_{gap}(0) = e^{-a(1-e^{-b})}$$

It is possible to equate:

$$a = \lambda \bar{A} = CAD$$
$$CC = 1 - e^{-CAD} = 1 - e^{-a}$$
$$b = G(1) L_W$$
$$CF = 1 - e^{-b}$$

Here, CAD is Crown Area Density, CC is Crown Cover and G(1) and L_w are discussed in the Appendix 3.

With these identifications, the data can be interpreted in terms of both crown cover and projected foliage cover. Although these associations should not be pushed too far, once the models are fitted, important information products such as layer height and layer average height can be derived from them.

For example, using the same data set as in the previous examples, stable gap profiles can often be obtained by averaging over SLICER shots. Repeating the previous Figure 4.4 as Figure 4.8 for local reference, we have:

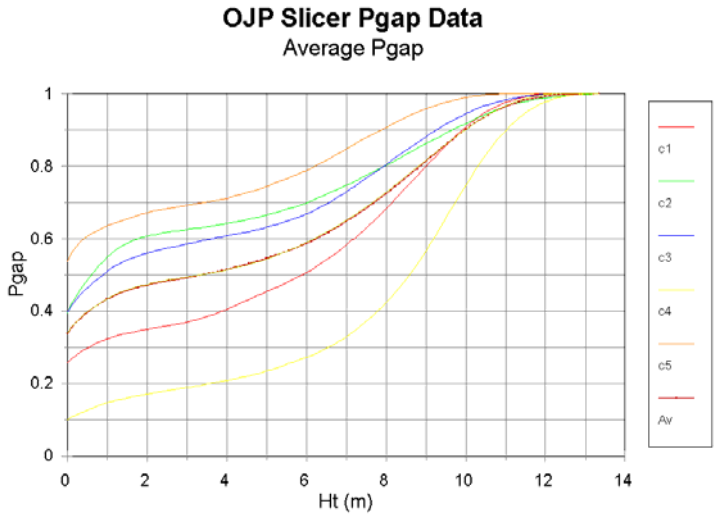

Figure 4.8. Line and total Average SLICER P_{gap} Profiles

There is a considerable variation between these lines in terms of both layering and cover. However, to illustrate the method we will only fit the overall lumped average profile.

Figure 4.9 shows the results of fitting three Weibull functions to the data presented and plotted in Figure 4.8:

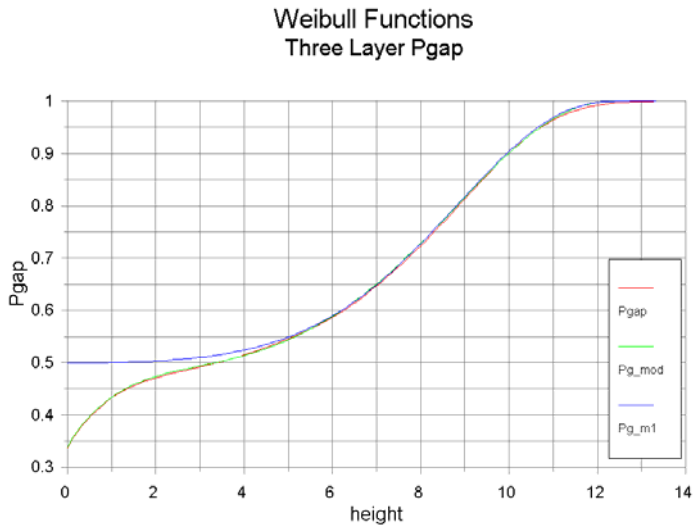

Figure 4.9. Gap profile for fitted Weibull model

The profile labelled "Pg_m1" is a single Weibull model fitted to the upper canopy. Clearly it does not provide a good model for the understorey. However, the graph labelled "Pg_mod" uses three Weibull functions and fits the data well.

Figure 4.10 shows the Weibull functions involved which together approximate the accumulated foliage profile L(z):

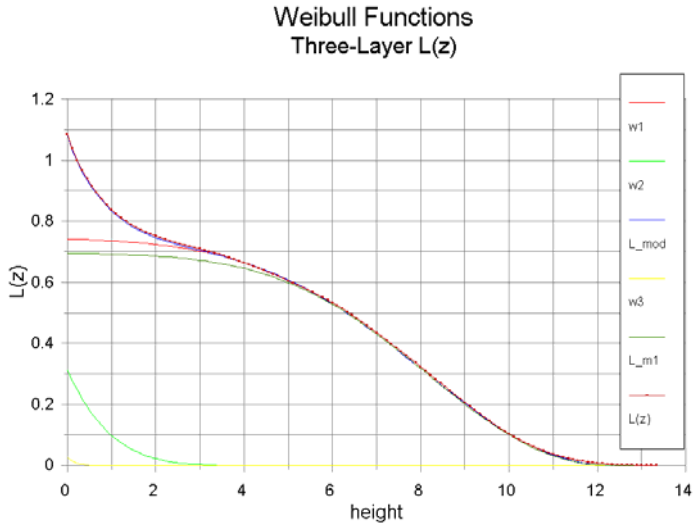

Figure 4.10. Fitted Weibull function components

The three components (w1, w2, w3) are shown plus the single Weibull function optimised to the upper canopy only (L_m1). The small near-ground component is assumed to be an artefact of the profile not being well corrected for the influence of the ground pulse by deconvolution. The composite Weibull model (L_mod) fits the data very closely.

Figure 4.11 shows the resulting apparent foliage profiles.

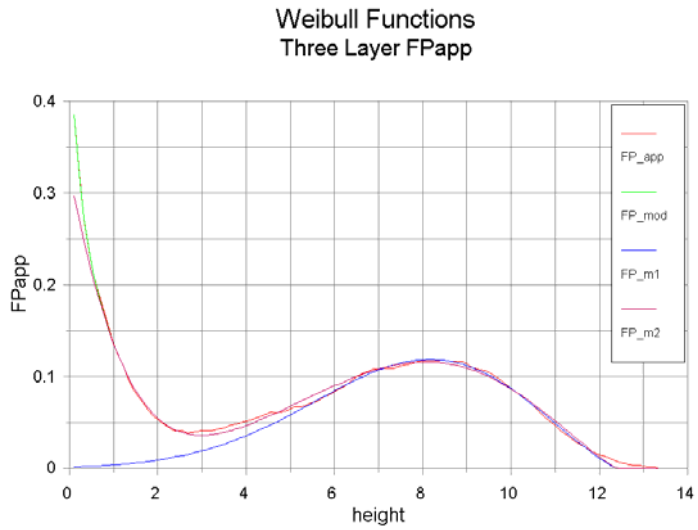

Figure 4.11. Fitted Weibull Folaige Profile Models

The curve labelled FP_m2 is the combined model excluding the small near-ground component thought to be an artefact of the ground pulse. The curve labelled FP_m1 is the optimised to the upper canopy single Weibull model.

Clearly, the model fits well. It would be possible to add two more components (one small density of emergent trees and another mid-canopy layer). These are present in the current data set due to the aggregation of quite different shots. In practice, data from similar spatial areas (Lidar estimated stands) will be used to establish the layering.

Using the above associations between the Weibull model and the traditional structural information results in the following Table 5:

Table 5. Parameters identified from fitted Weibull models

	CAD	CC(%)	CF(%)	H	L(0)	PFC(%)
L1	0.747	52.6	99.9	12.39	0.742	53.3
L2	6.72	99.9	4.7	5.21	0.313	26.5
L3	20.19	100	0.1	1.99	0.027	2.0
L1’	0.696	50.1	99.8	12.42	0.695	50.0

It seems that the interpretation for the major layer (L1 or L1’) is sound but for the other two (L2 and L3) the PFC would be a main output with a and b being relatively unstable. L3 is most likely not vegetation. Note, however, that this approach does not provide any information on crown size and density and other methods must also be used to obtain them.

The estimation of discontinuous properties, such as crown size, layering, height statistics, relative abundances of growth form and cover by layer and tree type is obviously a much more significant effort than the provision of structure diagrams and apparent foliage profiles. There is every reason to anticipate that stand properties such

as gappiness, clumping and crown sizes by layer are achievable for regional areas. In particular, the data will provide statistics of clustering and gappiness as a function of height. This is very strong data for image variance studies. The relationship between variance as a function of height as well as foliage density as a function of height is particularly valuable information for interpretation of clumping.

4.4.3 Use of gap models for discontinuous crown canopies

Either as a second step following layer recognition, or directly from the data, a more detailed crown based model may be provided by either simple Boolean models or the Li P_{gap} model which has been described elsewhere (Ni *et al*., 2001). It can take into account the clustering of foliage into crowns and variation of tree heights. However, it is based on a very simple canopy structure and this model must still be extended and enhanced to be able to describe gap probabilities characteristic of the types of discontinuous canopies common in Australia. At this time there are two main gap models being used with Lidar data. A brief description of these follows.

4.4.3.1 Simplified whole layer Gap model (Jupp et al., 1986)

A simple gap model was proposed by Jupp *et al*. (1986) based on a layered canopy as measured in the field using the Walker and Hopkins (1990) description of a canopy. In this simple model it is assumed that a test ray will hit at most one crown in any layer and that the layers can be treated independently. This is reasonable for woodlands and open forests and near vertical view angles but not for dense, tall canopies at oblique look angles.

For simplicity, suppose that there is just one layer of trees above the ground and that the density of tree "centres" projected on the background is λ_C. Also, assume the tree crowns are so dense that they are effectively opaque and that the mean projected area of a crown on the background from direction μ is $A(\mu)$. Then for the whole canopy:

$$P_{gap}(\mu) = e^{-\lambda_C A(\mu)}$$

Where:

$$A(\mu) = A/\mu'$$

Where A is the vertically projected crown area and:

$$\mu' = \cos\theta'$$
$$Tan\theta' = Tan\left(\frac{T}{D}Tan^{-1}\theta\right)$$

with T as crown Thickness and D as crown Diameter.

This shows that for such a canopy, it is not the leaf angle distribution that is deciding the gap probability but the crown shape. (T/D). Obviously, however, crowns are

generally open and "filled" with leaves rather than opaque. The simple extension used in Jupp *et al*. (1986) was to write:

$$P_{gap}(\mu) = e^{-\lambda_C A(\mu)(1-e^{-\lambda_L A_L(\mu)})}$$

where λ_L is projected density of leaves in a single crown and A_L is the mean projected area of a leaf on a horizontal surface from the direction μ.

A more general way to write this model is:

$$P_{gap}(\mu) = e^{-\lambda_C A(\mu)(1-P_{gap,W}(\mu))}$$

where $P_{gap,W}(\mu)$ is the probability of a gap within (*W*) a crown in the direction μ. This extends the vertical view results derived before. If the crown is modelled as a volume filled with leaves with volume density of leaf area *F* we could hope to write as a first approximation:

$$P_{gap,W}(\mu) = e^{-G(\mu)F\bar{s}(\mu)}$$

where G is the Ross function and $\bar{s}(\mu)$ is the mean distance through a crown in the direction μ.

More correctly (but more difficult to derive as illustrated in Appendix 3) the model should be integrated over the "shadow" of the crown on the background as:

$$P_{gap,W}(\mu) = \int_{\text{Silhouette}} e^{-G(\mu)Fs(\mu)}\, p(\mu, s)\, ds$$

where $p(\mu, s)$ is the distribution function for lengths through a crown in the direction μ and the "silhouette" is the "shadow" area of the crown on the background in the view direction. Expressions for this mean are derived for the vertical view in Appendix 3 where it is also clear that the result can differ significantly from simply using the mean distance through a crown.

This simple model of leaf filled crowns as opaque crowns with "holes" in them illustrates how the gap probability is a function of the clustering into crowns, the shape of the crowns and the amount and angle distribution of the leaves in the crowns. This can easily be extended to multiple separated layers of independent trees and coincides with the previously discussed model for PFC when the view is vertical.

As the model was proposed, however, it provides an approximate model for the whole canopy gap (such as may be used for a ground based hemispherical photograph) but does not provide P_{gap} as a function of position (i.e. range) in the canopy (except by major layer). Its main limitation is therefore that it applies only to the whole canopy – or only to a canopy by layers. In order to extend the model it is necessary to take into account the possibility that the path is through only those parts of a crown above the given position in the canopy and the above integral needs to be carried out over the projected "shadow" of the partial crown. The task is quite complex.

4.4.3.2 Generalised Gap model (Li and Strahler, 1988; Li et al., 1995)

Another approach to deriving the more general probability function is to model the length of a path to a certain depth in the canopy from a specific direction that will be within crowns. This was done by Li and Strahler (1988) and extended as described in Li *et al*. (1995) to provide an effective model for a single layer of trees of constant size but varying heights. In the extended model, the canopy is assumed to be described as an assemblage of randomly distributed tree crowns with spheroidal shape having horizontal crown radius *r* and vertical crown radius *b* and centred between heights h_1 and h_2 as the lower and upper bounds of crown centres above the ground. The crown count volume density λ_v is equal to:

$$\lambda_v = \frac{\lambda}{h_2 - h_1}$$

where λ is the stem count density.

Within the crowns there is supposed to be a random distribution of foliage so that the gap probability is separated into two effects depending on the between crown gaps and the within crown gaps. That is, a test ray will penetrate to a given depth either by not hitting a crown volume or else by hitting at least one crown but passing through the within crown gaps.

For a Boolean model (crown centres distributed as the Poisson distribution) the between crown gap probability can be written:

$$P(n = 0 | h, \theta_v) = e^{-\lambda_v V_\Gamma}$$

where:

n=0 indicates that the number of crowns "hit" is zero
h is the depth to which the ray penetrates
θ_v is the view zenith angle or zenith angle of the test ray and
V_Γ is the beam projected cylinder volume with radius r from the top of the canopy to h

The within crown gap probability is complex as the path length through crowns is random and may be through or into more than one crown. If the length of path in crowns is denoted s and the within crown attenuation is modelled as a Boolean model (Serra, 1982):

$$P(s) = e^{-\tau(\theta_v)s}$$

where:

$$\tau(\theta_v) = k(\theta_v) F_a$$

where:

$k(\theta_v)$ is the leaf area projection factor for view angle θ_v and
F_a is the foliage volume density.

The within crown gap probability can be written in terms of path length and attenuation as:

$$P(n>0|h,\theta_v) = \int_0^\infty P(s|h,\theta_v) e^{-\tau(\theta_v)s} ds$$

The path length probability and a range of approximations to the integrals is discussed in Li *et al*. (1995). It follows that for this special case of a crown and foliage model an approximation to the gap probability function may be made. This may be used in the analysis of hemispherical photography or the penetration of sunlight or the effects of canopy structure on albedo – as well as in the interpretation of Lidar data.

However, there are a number of extensions to this model that should be considered. One is to divide the canopy into layers as has been done in the mapping of Australian vegetation and a second is to consider the trees and shrubs in the layers (or the middle layer at least) to be one of a number of morphological types. A third extension may be to allow the crown sizes to be random as well and a fourth to allow more general height distributions for the trees. With these in place – at least the first two – a complete model for gap probability which is compatible with the Australian structural description of vegetation will be available and which will better summarise the data obtained by the field work discussed above.

4.4.4 Shot variance as a function of range and spot size

From shot to shot there will be natural variation as well as noise. It is possible to explain some of the natural variation and its relationship to the spot size using the Boolean model of Serra (1982) and the work reported in Jupp *et al*. (1989). This variation may also be used to derive advanced canopy parameters.

The estimated gap probability function can be used to provide the probability of gap between and hitting of foliage in a thick "slice" at range r. The proportion of pore or gap in a slice at range r can be written:

$$q(r) = e^{-l(r)}$$

and $1 - q(r)$ is the projected proportion of foliage in the slice scattering the light back to the instrument.

In a canopy of trees and shrubs the foliage will be clumped into crowns so that for any given shot the "slice" will consist of disk like clumps of foliage. The proportion of foliage therefore intersected by the Lidar spot will vary and be a function of the tree density, crown sizes and the spot size.

Fortunately, models relating to these variations have been developed and presented in Jupp *et al*. (1989). It is shown in that paper that for the same average amount of foliage, the clumping into a few large crowns per unit area will generate higher variance than if the foliage were randomly dispersed or clumped into a large number of small clusters.

Of course, the variance for slices at different levels will not be independent. Hence, the vertical and horizontal spatial correlation (or variogram) and the variance it induces in Lidar data provide a strong indicator of the clumping effects of trees and shrubs in the various layers.

In the example below, the effect of spatial averaging is presented assuming it is explained solely by the variance induced by the clumping. In the future, the use of spatial variance to estimate the clumping factor and hence to correct for the differences between actual and apparent foliage profile will provide advanced products. However, some research is needed before this is a proven product.

Nevertheless, a key innovation in the processing described here is in its use of the changing data that is collected by flexible and varying beam width instruments. The larger beam width of the canopy Lidar is not just about averaging or reducing spatial variance. The change that occurs with varying beam size and shape provides information and parallels the fundamental operations of mathematical morphology – but in hardware.

4.4.5 Limiting Case: Interpreting the Terrain Lidar Data

In the limit of very small spot size the variance in both vertical and horizontal directions will be very high. However, this variance is eagerly sought in the case of the terrain Lidar which is used to map topographic elevation where as many shots hitting the ground as possible are used to plot the trace of the land surface and create a Digital Terrain Model (DTM).

Terrain Lidars generally have a small spot size and pulse at very high rates to get a very high density of narrow beam samples over a given patch of ground. To obtain the high density, such instruments are often flown on helicopters with accurate GPS and INS systems to locate the spots on the earth's surface. Generally, the terrain Lidars record the first and last significant return without calibration. The range can be estimated from the peak of the return since individual returns are generally separated and discrete.

The topographic surface is measured by estimating the "envelope" under the last significant returns, eliminating anomalous values and then interpolating the data to a DTM. Alternatively, a "prior" estimate of the DTM may be used to eliminate anomalous data and home in on an accurate surface model. In the vertically oriented and open canopies of Australian Eucalypts it is a reasonable expectation that many ground returns will be available and you would be able to estimate an accurate DTM, even under quite dense forest canopies in terms of crown cover.

Many of the first returns of the terrain Lidars operated in forests are scattering events from canopy elements. This has led to the investigation of the data for the purpose of canopy measurements. If canopy cover, height and structure can be inferred from terrain Lidar data it could well add value to surveys that are primarily aimed at creating DTMs. In Australia these opportunities are under study as described by Tickle *et al*. (1998), Fraser *et al*. (1999) and Witte *et al*. (2000) although these studies do not take as much advantage of other work such as that by Naesset (1997a,b), Magnussen and Boudewyn (1998), Magnussen *et al*. (1999) or MacArthur and Horn (1969) as they might.

Altimeter data of this kind have significant disadvantages for vegetation mapping. Among these are:

- The high spatial variance in horizontal and vertical extents;
- Range walk and other instrumental effects;
- Lack of calibration of the data;
- Speckle effects due to specular facets;
- High data volumes to process per hectare covered.

Speckle, for example, is created by small reflecting facets that act as Fresnel reflectors and provide apparently high energy returns from a low density of scatters. Such effects in understorey create very difficult decisions for interpolation of the DTM. As serious, or more serious, is the burden of processing of the large volumes of data per hectare in order to map quite small areas for vegetation information.

One means to interpret and use such data was reported by Blair and Hofton (1999) in which the return pulses over a local region are convolved with a simple model of return intensity and summed. They found that the resulting "pseudo-waveforms" were very similar to those obtained by the larger footprint LVIS data in the same region. However, this may have been due to the area considered and it seemed that the foliage profiles the different data sets would give rise to would vary more than the modelled waveforms.

An alternative method of interpreting these data for vegetation height, cover and structure goes back to the original methods described by MacArthur and Horn (1969). It must, however, be preceded by some pre-processing of the DTM. Specifically, let's assume the following processing has been done:

- Ground returns (usually from last return) identified;
- DTM interpolated to every point;
- Baseline shifted for ground level at zero height.

In this case, the first return data can be separated into those shots that come from canopy elements and those that come from the ground. The ratio of ground returns of the first return to the total shots is an estimate of the total canopy gap fraction – however, it is a biased estimate.

Estimation proceeds by choosing a set of resampling points, creating a window or plot around the central point of the sort of size you might use for a canopy Lidar and finding all shots falling in the window. An estimate (assuming the shots provide

independent data) for the gap probability through the foliage from the aircraft above the point *z* in the canopy is obtained as:

$$\tilde{P}_{gap}(z) = 1 - \frac{\#\{canopy\ returns \geq z\}}{N}$$

where N is the total number of shots within the window.

In Magnussen and Boudewyn (1998), quantiles for this distribution are used for 20 by 20 metre patch sizes to estimate mean height over patches of the same size. Canopy models suggest a correction for the observed bias between Lidar quantiles and observed mean height.

Given the level of noise and speckle in the data, the estimated gap probability is best modelled to provide stable results. This can be done in a number of ways – such as by the Weibull distribution where:

$$\begin{aligned} P_{gap}(z) &= e^{-L(z)} \\ &\quad with \\ L(z) &= a\left(1 - e^{-b(1-z/H)^c}\right) \quad 0 \leq z \leq H \\ &= \int_z^H l(z')\, dz' \end{aligned}$$

In this case, the estimated *H* is the height, ($1\text{-}P_{gap}(0)$) is the cover and *l(z)* provides an initial estimate of the foliage profile for the data within the moving window. Other distributions (such as the triangular distribution) may be used and it is important to use a simple parametric model due to the limited degrees of freedom in these data.

Magnussen *et al*. (1999) have investigated a number of such models, both parametric and non-parametric as well as the statistical estimation of parameters in this type of modelling. One of the models used was the Weibull and it was found to retrieve the canopy height distribution very well. Such approaches could well become normal practice in areas where altimeter data are taken for DTM mapping. However, if vegetation information is the prime objective of the survey it is likely that this level of processing – like the density of data – will come with too high a cost.

There are also many ways to regularise such estimations (such as by choice of variable transformations) but they will not be pursued here. For serious, cost effective and operational regional canopy mapping we will assume we can use variable spot sizes, obtain calibrated data and digitise the complete returns.

4.5 Multi-view models for the ground based ECHIDNA® Lidar

4.5.1 Multi-angle effects and models for an ECHIDNA®

If the Lidar is ground based it is possible to sound the canopy using both multi-angles and varying beam size. Multi-angle laser systems have been used to measure total canopy gap (like a hemispherical photograph) but the ECHIDNA® instrument being considered here is assumed to digitise the full return pulse, scan flexibly in the hemisphere and in "almucantar" scans and (significantly) to sound with variable beam width and shape. Obviously the ability of such an "ECHIDNA®" system to characterise the canopy angle distribution separately from foliage profile is very high and much greater than an airborne system. For this reason, the development of hardware for both an ECHIDNA® and an airborne Lidar system has been proposed to provide tools for detailed local characterisation as well as regional extrapolation.

Even for a random canopy of foliage elements the foliage profile you would obtain from an airborne system is NOT the foliage profile you want but rather a projective foliage profile which depends on the foliage angle distribution and the pointing direction of the Lidar beam.

For a leaf canopy, this can be modelled as follows. If $\overline{a}_L$ is the mean one sided area of a leaf:

$$\begin{aligned} LAI(z) &= \int_0^z \lambda(z')\,\overline{a}_L(z')\,dz' \\ &= \int_0^z F(z')\,dz' \\ L(z,\mu_v) &= \int_0^z \lambda(z')\,\overline{a}(z',\mu_v)\,dz' \\ &= \int_0^z l(z')\,dz' \\ &= \int_0^z G(z',\mu_v)F(z')/\mu_v\,dz' \end{aligned}$$

Hence, *LAI(z)* could be inferred from the ground, air or space by knowing $G(z,\mu_v)$ since:

$$LAI(z) = \int_0^z \mu_v l(z')/G(z',\mu_v)\,dz'$$

The resolution of the uncertainty must be through the use of other knowledge or the use of multiple angles for Lidar sounding that provides ways to measure $G(z,\mu)$. The use of multi-angle Lidar sounding is the basis for the ECHIDNA® and provides a very powerful extension of the methods used in the analysis of hemispherical photography enabling such information to be derived.

As discussed before, the probability of a gap from the ground to height z (vertically above the ground) in the direction μ_v is simply given as:

$$P_{gap}(z,\mu_v) = e^{-\int_0^z G(z',\mu_v)\lambda(z')\bar{a}_L\,dz'/\mu_v}$$
$$= e^{-\int_0^z G(z',\mu_v)F(z')dz'/\mu_v}$$

where:

$G(z,\mu_v)$ is the mean cross-sectional area (or Ross Function) in the sounding direction and
μ_v is used here as the cosine of the zenith angle

The ECHIDNA®, with proper choice of beam width, knowledge of the foliage reflectance and a scanning strategy can provide samples for the function $P_{gap}(z,\mu_v)$ for a range of look angles and over a set of ranges. Taking logarithms:

$$-\mu_v Log\left(P_{gap}(z,\mu_v)\right) = h(z,\mu_v)$$
$$= \int_0^z G(z',\mu_v)F(z')\,dz'$$

Then:

$$\frac{\partial h(z,\mu_v)}{\partial z} = G(z,\mu_v)F(z)$$

which, for sufficient look angles μ_v normalising conditions on G, use of parametric models and/or regularisation allows the estimation of G and F for each level. Assuming G is the same for the whole canopy also simplifies and stabilises the modelling.

As described previously, for a canopy of randomly distributed foliage elements, the relationship between the Ross G-function and the foliage angle distribution at any level in the canopy is:

$$G(\mu_v) = \int_0^1 K(\mu_v,\mu)\,g(\mu)\,d\mu$$

where:

g(μ) is the foliage angle distribution function assuming azimuthal independence and symmetry and
$K(\mu_v,\mu)$ is the Reeve Kernel function defined in Section 3.2.4.

Anderssen *et al*. (1984) have provided methods to solve this rather ill-posed equation. The integral equation also has an analytical inversion, as shown by Miller (1964) and Philip (1965). With effective regularisation, the (apparent, but angle corrected)

vertical canopy profile, estimates for the Ross G function and foliage angles could also be derived from ECHIDNA® data for one site or the composition of data from a number of sites.

As observed by Warren Wilson (1965), (see the plots in Section 2.2.2 of the Warren Wislon paper) an Almucantar scan near an elevation angle of 32.5° (or zenith angle of 57.5°, or $Tan\,\theta_v = \pi/2$) will allow *F(z)* to be derived virtually independently of the angle distributions. A more empirical estimate is an elevation of 31.25° or zenith of 58.75°). It is also possible to design the hemisphere scan for the ECHIDNA® to include this Almucantar and a spiral sampling to maximally invert the angle distribution as a function of height in the canopy.

A particularly important property that will often be derivable from the combination of foliage profile and angle profile will be the point (and its existence) where the canopy moves from foliage to vertical stem and trunk. This provides an estimate for the mean crown length ratio. The extensions needed to resolve foliage and trunks or major stems from the data go beyond the theory previously used for hemispherical photography but are straightforward extensions of the methods illustrated here.

4.5.2 Horizontal Scans for the ECHIDNA®

In its horizontal scanning mode, an ECHIDNA® can derive more of the traditional forestry data.

4.5.2.1 Tree Density

If the ECHIDNA® scans horizontally and records trees (using variable beam widths and software recognition) then the cumulative plot of number of trees against distance will provide both density and a check on the validity of the assumed random distribution of trees. These data improve with number of plots.

Strictly, if the number of trees that can be sounded within a distance r of a random point are counted and (for better results) aggregated over a number of sites in a stand then, using Steiner's Theorem, the data provide unbiased estimates of the number of trees apparently within radius *r* (Masuyama, 1953):

$$n(r) = \lambda\bar{A} + \lambda\bar{U}\, r + \lambda\pi\, r^2$$

where:

λ is the tree density
$\lambda\bar{A}$ is the Basal Area; and
$\bar{U}$ is the mean circumference of the trees.

For trees with disk-like cross sections we could write:

$$\lambda \bar{A}_c = BA = \lambda \frac{\pi}{4} \overline{DBH^2}$$
$$\bar{U} = \pi \overline{DBH}$$

and the difference between the mean DBH and mean square DBH may provide an estimate of the variance of the tree DBH and hence the size distribution. Plotting the data as a function of r should (if the underlying distribution is close to Poisson) result in a quadratic relationship and estimates for the coefficients (to obtain basal area, density and DBH) could be obtained by regression.

Despite the promise in this kind of approach approach, it is not likely to be very stable by itself. For small values of r the sampling variance will be high and it is better to use this in the asymptote for larger values of r to get a stand estimate for the tree density than to use it for basal area and DBH. However, using it in combination with the data and analyses described below provides an opportunity to obtain the important forestry parameters of density, size, size distribution and basal area.

4.5.2.2 Attenuation

Using a broader beam width and the same principles as for canopy sounding from either the air or within the canopy, the gap probability for gaps from an arbitrary point to range r can be derived. If there are no obvious boundaries, this may be averaged over all directions. It can be shown (Serra, 1982) for a forest with well-defined trunks and little understorey at the height being scanned:

$$P_{gap}(r) = e^{-1/\pi \lambda \bar{U} r}$$
$$= e^{-\lambda \overline{DBH} r}$$

Hence, knowing density from the previous data provides mean DBH and knowing $\lambda \bar{U}$ helps to make the estimation of BA from 1 above more stable as well.

4.5.2.3 Basal Area

Using similar principles to the Relaskop (Steiner's Theorem and the Boolean Model, see Serra, 1982), if a scan with a very precisely defined angular wedge with angle ω correctly identifies the "in" trees (N_ω trees for which the trunk fills the wedge) then the number of "in" trees provides the basal area where:

$$BA = BAF_\omega N_\omega$$
$$= \lambda \bar{A}_c$$
$$= \lambda \frac{\pi}{4} \overline{DBH^2}$$

In principle, the difference between mean DBH obtained previously and mean square DBH obtained here can provide an estimate of variance of DBH. However, since the Lidar instrument will also measure DBH of the "in" trees this distribution has many opportunities to be resolved.

As with the Relaskop, the assumption of Poisson distribution of trees can be tested by the variance of in-trees and (if accepted) allows inference of timber volume by allometric relations. The assumption of a lognormal distribution for the DBH means it can be fully characterised by these methods when the assumption is reasonable. This allows estimation of timber volumes and densities for trees above a given DBH. However, unlike a Relaskop, the provision of ranges to "in" trees and the analysis of these data as a function of a "sieve" of Lidar pulses of differing size and shape (ω) has opened up the information on both density distribution and size distribution from the same data set.

In practice, a Lidar instrument will measure the range to trees and their angular width and so it can act as a "Relaskop" with variable wedge size. As with the Relaskop method, the effects of occlusion and hiding of trees by the closer trees is a potential problem but is also an opportunity for the range of geometric probability methods being applied. The "tree hiding" is related to tree trunk size and density and combined with varying wedge sizes may be as useful to the measurement as the simpler Relaskop estimates.

The combined use of these various types of measurement based on geometrical probability can provide better data than any one. Note that, in particular, if the mean and variance of Log(DBH) and density are solved for simultaneously with density for the different types of measurements and both for each plot and for pooled plots in areas assumed to be the same stand then more stable estimates will ensue.

4.5.2.4 Beam size and shape

The use of Steiner's Theorem and the "sieve" of beams of increasing sizes as well as the effects of shape provide a powerful set of tools for analysis of canopies.

For example, the change in number and distance distribution of "in" trees with beam size and the attenuation of anisotropic beam shapes can sense the most obvious anisotropic feature of forests – the trunks of the trees.

However, the examples given here are just a few of the tools enabled in a single instrument by the combined flexibility of:

- Sounding range with a Lidar Pulse
- Using beam size control
- Using beam shape control
- Digitising and recording the return at high density

Exploring the range of analyses this combination has opened up is a serious research and development area to explore in the coming years.

4.5.3 ECHIDNA® as a "calibration" for VSIS or other Lidar systems

In the introduction and throughout this ATBD we have mentioned the underlying 'blind spots" that systems that range, but have limited view angles or sounding strategies, will have. These were summarised as:

- The trade-off between scatterer density and reflectivity;
- The effects of foliage angle distribution;
- The effects of clumping of foliage.

The sections above provide evidence that stem statistics, forest layering, clumping, foliage angle distributions and even reflectivities are all accessible and resolvable by an ECHIDNA® at a fixed site but become less resolvable as you move to airborne and spaceborne Lidars (including topographic and canopy Lidars) or to other sensors such as VisNIR and hyperspectral sensors.

Foresters often use the strong correlations that exist in local and specific areas of forests to estimate (for example) timber volume from spatially distributed measurements of (say) basal area. This allows efficient sampling designs to be produced (such as the 3P system, Bell and Dillworth, 1988) based on information from detailed plots being extended to forest stands through correlated measurements (such as the basal area as a surrogate for timber volume). In the same way, information obtained by the ECHIDNA® provides the means to unravel the blind spots of (say) an airborne Lidar survey by assuming general age classes, types and factors such as Ross G-functions for the crowns are consistent throughout a specific region or forest block.

Specifically, the steps would follow in a similar way to:

1. Use staged and stratified sampling methods to select number and placement of ECHIDNA® plots;
2. Infer stem, canopy and foliage properties by layer at ECHIDNA® plots using algorithms described elsewhere;
3. Infer profile information accessible from the airborne or spaceborne systems by modelling with the models described elsewhere;
4. Establish strength of allometric relations between ground information (e.g. volume or biomass) and profile information (e.g. profile statistics, cover and height);
5. If strong enough, apply to airborne or spaceborne data in areas of similar profile "type" to sites of the ECHIDNA® plots.

This combination provides scaling and a high level of measurement capability to the advantage of airborne and spaceborne platforms. Without such "calibration" these systems are limited in their interpretations and assessments. The same effect will apply to more traditional remote sensing – such a Landsat, Spot or hyperspectral data. Knowing the structure and the underlying structural parameters can lead to better interpretation. The reason for this is that they all sense the light climate as an indication of the structure and condition of the canopy. But it is only when structure is known that condition becomes easily interpreted.

In forestry applications, the gain can be as great. The correlations between stem and canopy measurements are already used to simplify survey and timber resource assessment. This approach provides a new tool and potentially many more options for such resource estimation.

The integrated use of the ECHIDNA® with airborne systems like VSIS (or other airborne systems) and even with spaceborne systems promises to be a major use of the techniques described here – only matched by its use as a stand-alone tool for detailed forest measurement.

4.5.4 Sounding individual trees

The previous sections dealt with the use of an ECHIDNA® to measure statistics of plots and the extension of these or independently derived information over larger areas or forest blocks by an airborne system.

Often, statistical information is desired on an individual measure tree. Lidar rangefinders have been operationally used for such data for some years. However, there is advantage in the use of variable beam width and shape systems like ECHIDNA® to scan single trees and obtain statistics on the vertical and horizontal sizes, stem densities, trunk/crown relationships and other single tree information.

The models of Appendix 3 may be used to derive crown factor from vertical data or extended to include angular variation for more detailed statistics and the hierarchical nature of the within-crown variation may be used to design effective beam sizes to obtain spread time traces allowing this information to be derived from one or more soundings of a tree.

Individual trees have been sounded by photography and sonar data for a number of years but information can be difficult or laborious to derive. The use of ECHIDNA® for this task at the same site as plot and stand measurement provides an added advantage to the ECHIDNA® system.

4.6 Conclusions

The generation of the structure diagram for areas of vegetation and the generation of gap frequency functions for landscapes seems to be feasible as long as the angular effects can be taken into account. The development of a multi-angle ground based instrument (the ECHIDNA®) and an airborne instrument VSIS which uses calibrations obtained by the ECHIDNA® to map large areas seems a well posed approach to canopy and biomass mapping.

The practical development of these instruments must try to maximise SNR and take careful account of pulse width and lidar footprint in the design of the systems. The signal processing needs to establish how feasible it is to deconvolve the signal and separate the ground return from the foliage returns. The ground return contains very significant information on micro-relief expressed in the broadening of the Lidar pulse.

However, this makes it harder to recognise and separate the ground return. Slope effects add to this processing complexity.

Nevertheless, a system based on these principles and including both a ground based multi-angle and airborne scanning system is possible and will have a significant role in regional vegetation mapping. A research-based system also offers the potential to develop the use of polarisation, multi-frequency and advanced processing techniques (such as image spatial variation and gap analysis) within its base framework of canopy structure maps. Unlike many remote sensing tools, there is an immediate product as well as an R&D pathway to advanced products.

4.7 Summary of Lidar Based Measurements by Activity

Based on the above discussion, our analysis of the activities of forest measurement may be updated in terms of measurements that can be derived from the Lidar technology as follows:

1. Environmental, Habitat and Conservation

   Provided sufficient ground Lidar or other data are available to calibrate an airborne system it is possible to map the three main layers of vegetation cover and provide cover/height diagrams for each one at scales from 1:20,000 to 1:50,000. At this stage, information on the structure (such as crown sizes, crown length ratio and growth forms) is not being provided as products. However, combined with current video or scanner technology – or with current satellite data – the VSIS comprises a complete system for achieving much of the data needs for NVIS mapping.

2. Forestry

   2.1 Native Forests

   The ECHIDNA® can provide layer stratified BA, DBH, density, FAI as a function of height, mean foliage angles and (possibly) crown length ratio and crown sizes. These can be packaged into a portable system for accurate measurement at a number of forest sites. The VSIS can extend these data over a wide area of similar forest community at scales between 1:20,000 and 1:50,000.

   Specific Products are planned to be:

   Diameter at Breast Height (DBH), Tree density (λ), Height of dominant stratum (h), Crown diameters (D), thickness or length (T), Crown length ratio (measured as T/h), Basal Area (BA), Log Volume (V), Crown Closure (CC or CAD), Stand height curve.

2.2 Plantations

The products are the same as for native forests but the intensity and scale is more detailed. The availability of the ECHIDNA®/VSIS combination or simply ECHIDNA® provides an extensive inventory with more detail than current inventory uses. The impact on yield determination and sawmill operations needs to be studied.

3. Carbon

The ECHIDNA®/VSIS combination will provide effective structural data of the kind sought for biomass estimation. The combination provides the opportunity for new data relations but must be combined with site data on above ground biomass and root biomass. The level of the NVIS hierarchy that must be reached for effective and accurate inference of biomass and carbon has not yet been established.

5 CANOPY LIDAR CASE STUDIES USING SLICER DATA

What follows is a demonstration of how raw lidar data can be processed to describe vegetation canopies. This demonstration is based on raw data from a NASA experimental instrument (SLICER) as interpreted by the algorithms described above. The SLICER instrument was flown over several sites between 1994 and 1997. The data used here are from flights over the BOREAS study area in Canada during 1997 (Harding, 2000). The flight paths were over areas of coniferous forest like that shown in the aerial photograph in Figure 5.1.

Figure 5.1. BOREAS southern study area, old Jack Pine

5.1 Extracting the vegetation signal

The raw data returned by the Lidar is the relative intensity of light reflected as a function of time after the outgoing pulse. By translating time into range, we can derive the relative height at which the reflections occurred. Once the ground pulse has been identified, the reflected waveform can be interpreted in terms of height above ground. This is shown in Figure 5.2. The background noise level has been estimated and subtracted from the data shown here. The narrow pulse centred on zero is the reflection from the ground. The asymmetry of this pulse is due to the shape of the outgoing laser pulse. This was designed to have a rapid rise time and asymptotic decay and can be modelled as a Rayleigh distribution as described in an earlier Section.

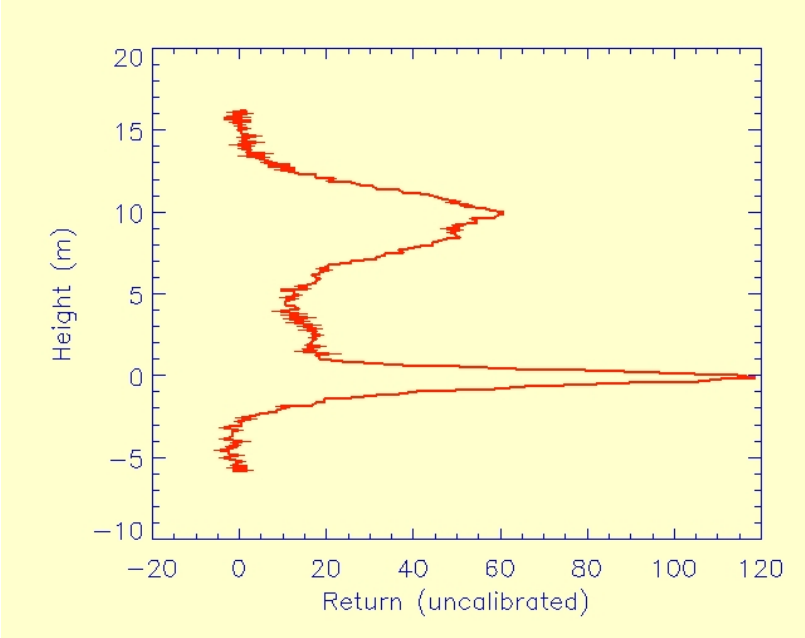

Figure 5.2. SLICER Lidar Waveform (BOREAS Data)

The ground return pulse must be removed in order for the vegetation return to be studied. This can be done by fitting a pulse of the expected shape and subtracting this from the waveform. Figure 5.3 shows the same waveform with an asymmetric gaussian subtracted to remove the ground return pulse.

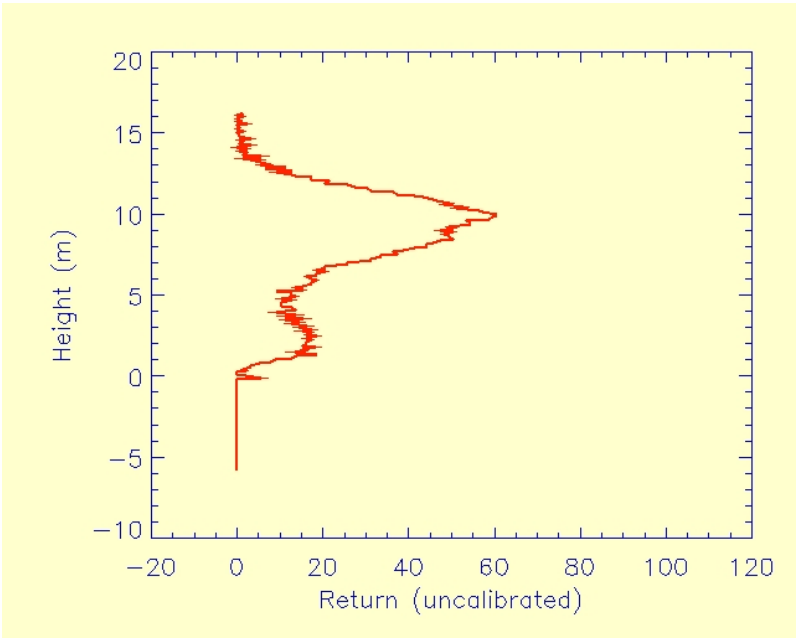

Figure 5.3. Lidar waveform corrected for ground pulse

This figure shows the reflected light over a single spot of about 8m in diameter. The first return above noise level tells us the highest point in the canopy within this circular area (about 13m above ground) which corresponds reasonably with the definition of top height introduced previously. The shape of this waveform suggests a

concentration of foliage (needles and branches) around 10m and an understorey of 2-3m in height. This is a plausible result for a coniferous forest.

The spot size of the SLICER instrument is similar to the crown size of the trees, so we expect to see considerable variation in the shape of returns from shot to shot. If trees are clumped i.e. there are groups of trees and gaps between the groups, there will be some areas where the only reflection comes from small plants (such as grasses) and the ground. Also, we expect that the return profile would be quite different for broad leafed canopies (such as eucalypts) which have both different shaped leaves and canopies.

5.2 Interpreting the Lidar profile

For each Lidar shot we can derive the fractional cover (the fraction of the vertical view that is occluded by foliage) over the area of that spot. This is calculated as the cumulative sum of returns to each height, divided by the total reflection from foliage and ground. The ground return must be scaled by the relative reflectance of the ground and vegetation. Fractional cover is plotted here in Figure 5.4 against height in the canopy.

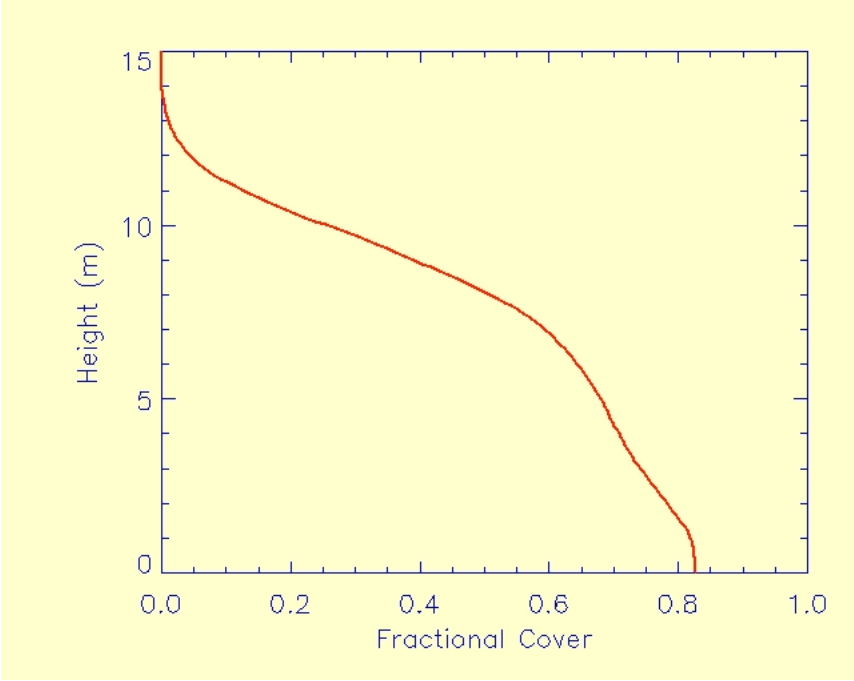

Figure 5.4. Fractional Cover as a function of Height

This plot shows a fractional cover of 0.82 over the spot sampled by this Lidar shot. Looking up from the ground, only 18% of the sky would be visible in vertical view. The shape of this plot tells us something about the shape of the trees. About 60% of the cover lies below 10m, so the top part of the trees must be sparse as cone-shaped coniferous trees are. Also, there is very little contribution to the cover below 2m, so the understorey is also sparse.

Fractional cover leads to gap probability. This is simply 1.0-fractional cover and so represents the fraction of sky visible when looking up through the canopy from

different heights. Gap probability is plotted in Figure 5.5 in red, the blue line is fractional cover as shown above.

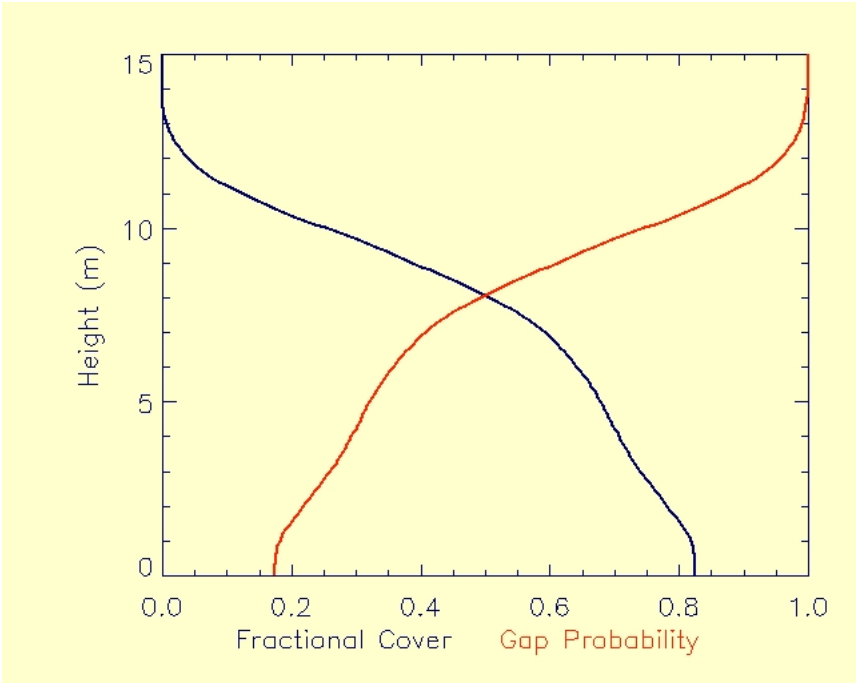

Figure 5.5. Fractional Cover and Gap Probability

Gap probability (P_{gap}) at different heights through the canopy leads to the apparent foliage profile, or foliage area per unit area at each height through the canopy (Figure 5.6). This is the vertically projected foliage profile.

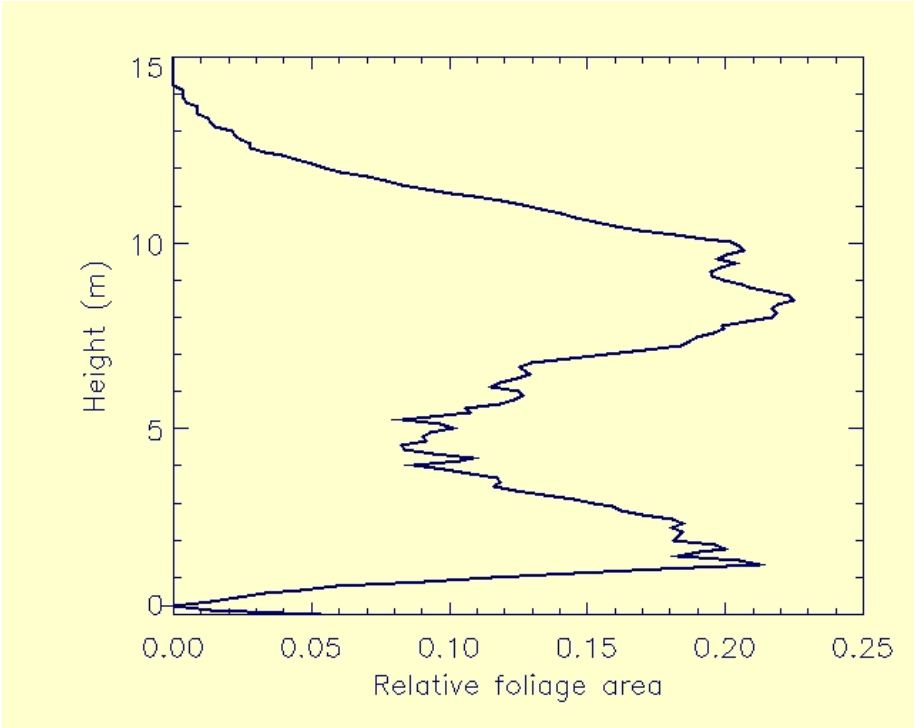

Figure 5.6. Apparent Foliage Profile

The actual foliage profile depends on the distribution of the foliage elements (leaves, branches etc) in space. Our calculations assumed a random foliage distribution, which is an acceptable but not accurate description of the distribution of foliage elements in real trees. The resulting apparent foliage profile (FP_{app}) is shown above in Figure 5.6.

5.3 Horizontal extension of the vertical description

The above analysis shows the main steps in processing Lidar data from a single shot. The small spot size of the SLICER instrument relative to tree size results in significant shot to shot variation. To understand the whole area sampled, it is useful to summarise the results as a series of histograms and scatter plots. We will now show examples from three contrasting sites (Figure 5.7).

Young Jack Pine | Old Jack Pine | Old Aspen

Figure 5.7. Photographs of three sites

The young Jack Pine site is an immature plantation. The old Jack Pine plantation consists of mature trees, but with little understorey, while the old Aspen has a tall canopy and an understorey.

The contrast between these sites is very clear in the following histograms of canopy height (Figure 5.8). The majority of the young Jack Pine site has canopy heights of 3-8m with a minor population of taller trees. The histogram for the old Jack Pine site reveals two distributions. The dominant one is centred around 12-14m and there is another minor peak at 2-4m. This indicates the proportion of clearings with regrowth or low understorey plants, the minor peak, relative to the taller forest canopy. The old Aspen site has one population of tall trees.

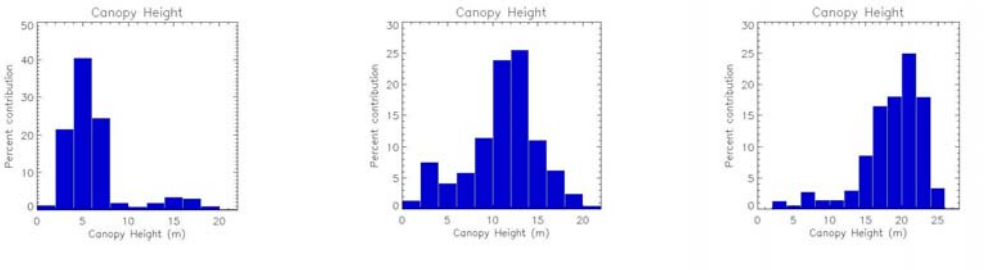

Young Jack Pine | Old Jack Pine | Old Aspen

Figure 5.8. Canopy height distributions at the three sites

Foliage cover histograms are shown in Figure 5.9. The distribution of fractional cover sampled is also bi-modal for both Jack Pine sites, showing a significant proportion of spots with fractional cover less than 0.1 (10%). The old Aspen site has very few areas of low cover with most lidar spots recording cover greater than 0.7 (70%). Areas of

low cover in the older sites may be cleared areas or gaps within the canopy, perhaps associated with treefalls. This issue could be quantified by using a Lidar with a variable spot size. It must be recognised that the area of the Lidar pulse/shot determines the accuracy and spatial coherence of all subsequently derived variables. It is important to choose a spot size appropriate for the purpose for which data are being collected.

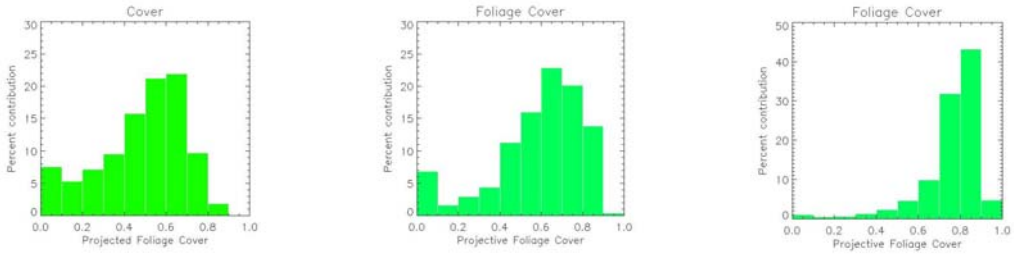

Young Jack Pine Old Jack Pine Old Aspen

Figure 5.9. Foliage cover histograms for the three sites

A common way to display canopy structure data is a structure diagram, which is a plot of canopy height against cover. These are shown for the three sites in Figure 5.10. Again we see two populations in the Jack Pine sites and one main population with some scatter for the Aspen site. The variation within the canopy population could indicate local growing conditions or the disturbance history.

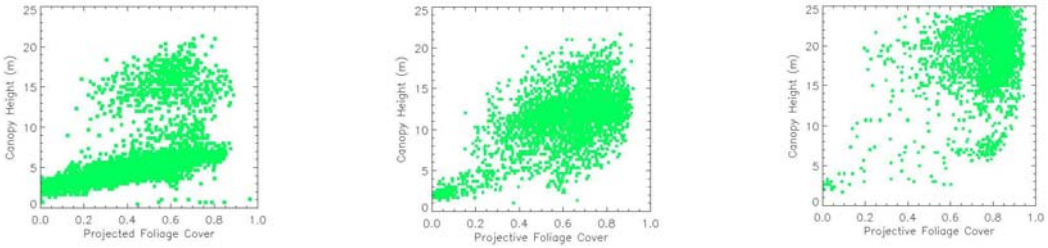

Young Jack Pine Old Jack Pine Old Aspen

Figure 5.10. Structure Diagrams for the three sites

The main (young) population in the Young Jack Pine site is found to lie in a linear formation in the structure diagram of growing trees where cover is proportional to height. This may suggests a range of site quality or emerging age class is present at the site. In this young population, a stand height curve would be an effective forestry tool enabling height to be predicted from basal area or DBH. In this plot, a distinct, taller population is also present which is likely to be a section of older growth Jack Pine adjacent to the area of young trees.

The Old Jack Pine site has a range of covers and heights as well as some cleared and regrowing areas that match the linear structure of the Young Jack Pine. The central area may be a third stratum in this area. The Old Aspen is a mature stand with apparently few large gaps allowing regeneration. However, this is speculation and the main feature of these plots is the powerful stratification it provides of forest types.

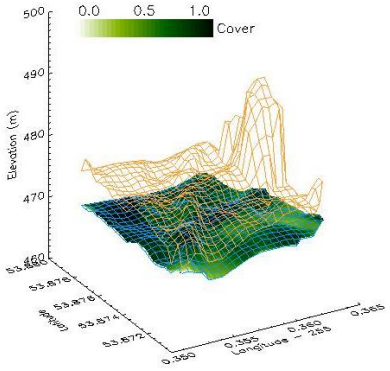

Young Jack Pine

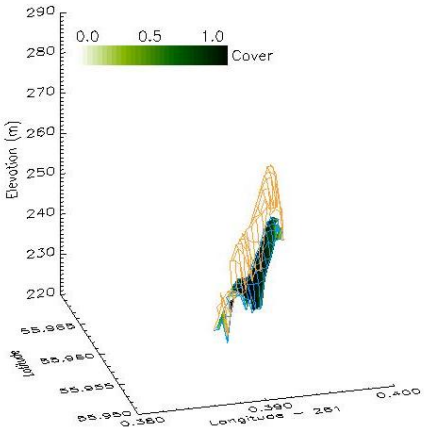

Old Jack Pine

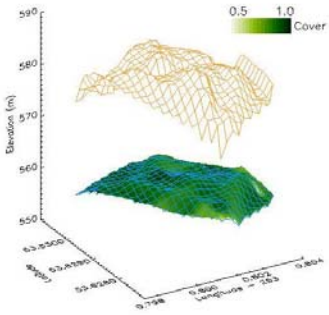

Old Aspen

Figure 5.11. Spatial distribution of cover and height for the three sites

The spatial data provided by the scanner also allows these data to be presented and visualised in a variety of ways. For example, the transects corresponding to the previous structure diagrams are presented in Figure 5.11 which displays ground topography (blue mesh) shaded according to projective foliage cover with tree height shown by the overlaid orange mesh. The image of the old Jack Pine site was generated from a single transect, while data from several intersecting transects have been combined and interpolated to generate the other two images.

These images help to resolve some issues of spatial distribution. The canopy height surface at the young Jack Pine site reveals that the population of taller trees is a distinct stand adjoining the younger plantation. The old Jack Pine site shows an area of low cover and low canopy height at one end of the transect while the canopy height at the old Aspen site is more uniform over the whole sample area.

5.4 Variance and Spot Size

We have noted in earlier discussion that the variance in measured or derived parameters is a function of plot (or in the case of Lidar, spot) size. We have investigated this with the SLICER data by first sampling the shots with views closest to vertical and then aggregating these by averaging over nine spots in a 3x3 configuration. The structure diagrams below in Figure 5.12 show the aggregated data corresponding to a sample size of approximately 30m square.

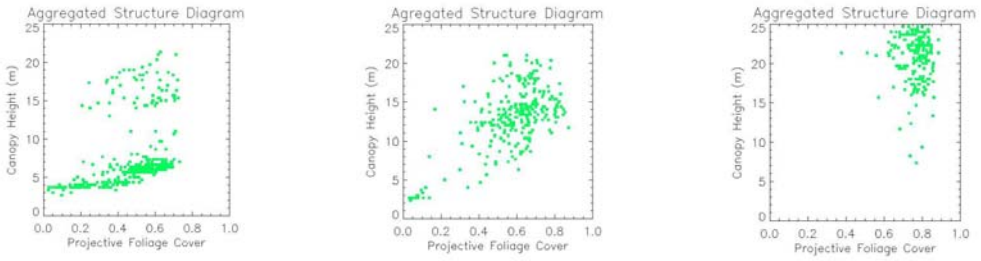

Young Jack Pine Old Jack Pine Old Aspen

Figure 5.12. Structure Diagrams after 3x3 aggregation

The Jack Pine sites still show two separate populations, demonstrating that the minor population is distributed in coherent areas of at least 30m^2 within the sites (as shown above in the 3-dimensional images). The low cover spots from the old Aspen site are not present in the aggregated data, so they may be gaps, possibly due to isolated tree falls.

The way that the variance of cover changes with the spot size can be modelled as described in Jupp *et al*. (1988) and with the assumption that the cover within a spot varies as a Beta distribution with the mean and variance computed using the disk models of the reference. For the old Jack Pine site, it may be shown that if the spot size were 25 metres then the spots would be allocated to the M3 Carnahan code in most cases. It is likely that Australian forests will be even more variable due to larger crown sizes and crown openness. In future research the derivation of the crown sizes

or leaf "clumping" from the second order statistics used as a function of range (and not just in terms of the total cover as discussed above) will be an important topic.

Figure 5.13 shows the relationship between the actual and modelled distributions of cover for the old Jack Pine site for an assumed crown size of 3m. The plot estimating the effect of a 25m spot size illustrates our claim that most of the site is M3:

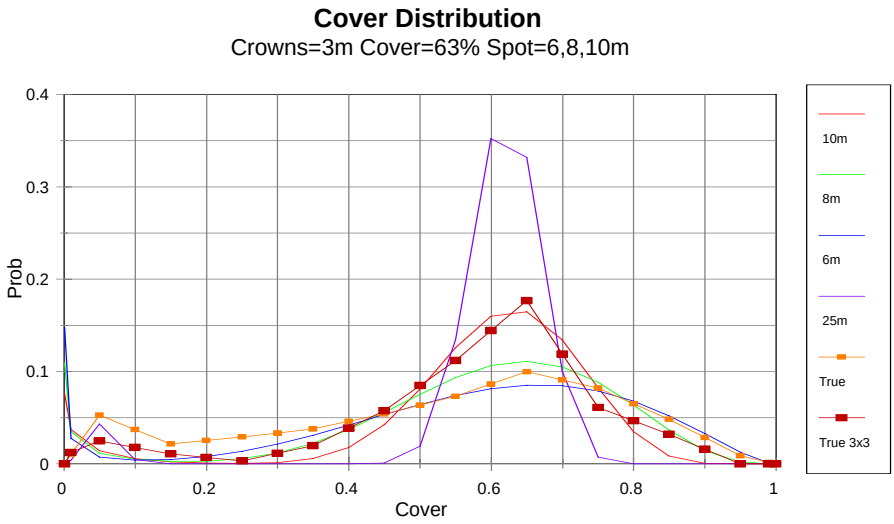

Figure 5.13. Cover as a function of spot size

However, investigations of the more significant converse of this exercise – that the behaviour of the data as the spots are aggregated is an indication that the crown sizes are 3m and not 2m or 4m will be left to a later document – as will the discussion of these histograms as a function of level in the canopy.

5.5 Accuracy of forest parameters derived from lidar as reported in published articles

Field measurements were taken at the BOREAS sites and the recent paper by Ni *et al.* (2001) describes the capacity of a canopy model to describe the SLICER data. However, this is not a test of the accuracy of derived parameters and even in the BOREAS case, some heights were inferred from the Lidar data rather than the field data.

It is important, therefore, to have a clearer idea of the likely accuracy of products from canopy Lidars than has been shown from the previous product description. To provide some measure of this, the following Table 6 summarises a range of published articles and discusses their results on measurement accuracy. In some cases the measurements are direct (as in tree heights) and in some cases the results are reported as correlations. The correlations often indicate that the measurement biases are due to different definitions of properties and point to a need to better understand the relationships between the data types.

However, overall, the published record from 1985 to the present from the use of terrain Lidars and SLICER provides clear evidence of the potential for accurate height

measurement and effective cover measurement. The assessment of layering and forestry data has been less easy but there are clear and persisting correlations that provide a basis for pursuing forest survey based on Lidar data.

Table 6. Summary of accuracies found for airborne Lidar in the literature

Article	Description of measurements	Accuracy
Aldred, A.H. and Bonnor, G.M., 1985	Two different pulsed lasers were used to measure stand height and individual pulse heights. Crown cover calculated using the ratio of number of single peak returns to number of ground returns	Stand canopy height measurements biased by –0.7 to –8.4m depending on type of tree and beam divergence. Individual pulse height measurements biased by –0.2 to –6.6m depending on type of tree, beam divergence and threshold set. r^2=0.93 for 85% threshold Crown cover estimated to within ±15% (95% conf)
Maclean, G.A. and Krabill, W.B., 1986	Terrain Lidar – first and last returns, 70cm footprint. Best results found with exclusion of returns within 10m of ground and with stratification by species.	r^2=0.921 for ln(timber vol) vs returns stratified by species and a 10m exclusion level.
Nilsson, M, 1996	Variable beam divergence, spot sizes 0.75-3.0m, mounted on hovering helicopter. Plot-based measurements. Digitised waveform, but processed to extract peaks only (up to four peaks, or just first and last). Stand volume estimated using the mean product of waveform area and height.	Mean tree height underestimated by 2.1-3.7m Vol= 17.5+0.00372*$\sum$(a*h)/n r^2=0.78

Article	Description of measurements	Accuracy
Naesset, E, 1997a	Airborne scanner, max scan 20º, footprint, 13-16cm, separation 2.8-3.3m. DEM mode i.e. last return only. Mean stand height, h_{15} = mean of largest heights in 15m square grid cells. Stand volume was regressed against two models (A) a function of h_{15} and laser canopy cover density; (B) a function of h_{15} and the mean of all laser heights.	Mean difference between h_{15} and Lorey's height: -0.4m to 0.1m Regression results for 2 sites: Model A, r^2=0.472, 0.838 CV=42.7%, 20.9% Model B, r^2=0.456,0.887 CV=43.3%, 17.2%
Naesset, E, 1997b	Airborne scanner, 13-16cm footprint, last returns. Spruce and Scotch Pine in Norway.	Laser mean height underestimated mean measured height by 4.1-5.5m. Height-weighted mean underestimates true height by 2.1-3.6m Arithmetic mean within grid cells has bias –0.4-1.9m
Lefsky, M.A., 1997	Thesis not sighted but results referred to by Lefsky *et al*., 1999.	Max height: r^2=0.76 Median height: r^2=0.68 Quad. Mean height: r^2=0.78 Possible bias, but not statistically significant from 1:1 relationship.
Lefsky *et al*., 1998	SLICER waveforms processed using the canopy volume profile algorithm to identify filled and empty volume. Biomass predicted from total filled volume and number of waveforms taller than 55m. LAI predicted from total filled volume and open gap volume.	r^2=0.9 for predicted vs observed biomass r^2=0.88 for predicted vs observed LAI

Article	Description of measurements	Accuracy
Magnussen, S. and Boudewyn, P. 1998	Terrain lidar used to measure height of canopy in plots of conifer plantation. Height is under-estimated by lidar. Percentile height of aggregated returns in grid pattern used to estimate mean canopy height. Comparison with measured mean heights, Lorey's height (basal area weighted mean) etc. Statistical tests used to test for difference between lidar-measured and field-measured samples.	Strong correlations between laser percentile heights and field measured heights: $0.6 \leq r \leq 0.85$ which give $P(r=0) \leq 0.01$. Laser estimates underestimated field measurements by an average of 0.7m (3%). Discrepancies were up to 5.7m in some plots. NB These correlations depend on the correct choice of sample percentile – i.e. prior knowledge of the forest, or of a similar stand is needed.
Tanaka, T. *et al.,* 1998 Measurement of forest canopy structure with a laser plane range-finding method – development of a measurement system and applications to real forests. Agricultural and Forest Meteorology, 91, 149-160	Laser range finder used horizontally and vertically (from above and below) in a forest to create 3D reconstruction and deduce range to trees, diameter of trunks, vertical foliage distribution – comparison only visual, no comparative measurements taken. Laser used at night.	Horizontal imaging -> good linear correlation with measured distances to trees and trunk diameters – no measure of fit.
Lefsky *et al.,* 1999a	Used SLICER data to derive height, cover, QMCH, canopy height profile (FP_{app} in our terminology), canopy volume profile (open gaps, closed gaps, filled volume etc). Various forest parameters modelled via stepwise multiple regression. PSME=Douglas-Fir TSHE=Hemlock	Parameter r^2 Total biomass 0.91 Total basal area 0.87 PSME basal area 0.79 TSHE basal area 0.78 Shade tolerant stems 0.52 Mean DBH 0.61 Stdev DBH 0.85 Stems >100cm 0.85 LAI 0.75
Lefsky *et al.,* 1999b	Calculated basal area and biomass from SLICER-derived height indices using relations derived from field measurements	r^2=0.7 for QMCH with BA r^2=0.8 for QMCH with biomass

Article	Description of measurements	Accuracy
Fraser, C., Jonas, D. and Turton, D.A. 1999	Terrain Lidar trial in Australia. Vegetation height data obtained at some sites.	Pine forest: Mean discrepancy=2.5m Standard error=2.2m Max discrepancy=14.3m Eucalypt forest with brushy undergrowth: Mean discrepancy=2.5m Standard error=4.1m Max discrepancy=9.9m
Magnussen, S. *et al.*, 1999	Terrain Lidar measurement of the same plots as previous paper. Two types of model used to correct the bias of lidar measurements. A) Probability of laser hitting a crown above a certain height is proportional to the horizontal extent of the crown at that height. Heights corrected by removal of PPS (probability proportional to size) effects. B) Model canopy depth based on difference between max measured height and max canopy penetration. Bias is assumed proportional to canopy depth.	Correlations with ground measurements ~0.6 for all methods. Median absolute deviations ranged from 1.1 to 2.9m
Means, J. *et al.,* 1999	SLICER data aggregated over plot sizes. Regression relations derived for a variety of forest parameters. Some forest parameters were modelled by more than one relationship (involving different lidar derivatives). Sample size is 26 except in 9, 10, 12 and 13 where it is 10, 11, 21 and 21 respectively.	Parameter r^2 RMSE 1 H 0.95 3.8 2 BA 0.88 13 3 BA 0.92 11 4 BA 0.96 9 5 TotBio 0.90 132 6 TotBio 0.94 103 7 TotBio 0.96 88 8 FolBio 0.84 2.0 9 FolBio 0.67 1.3 10 FolBio 0.81 1.5 11 CanCov 0.94 0.08 12 CanCov 0.53 0.06 13 CanCov 0.69 0.05

Article	Description of measurements	Accuracy
Tickle, P. *et al.,* 2000	Laser range-finder deployed from helicopter for transects over Qld forest. Canopy height estimated from max height of each crown. PFC estimated from proportion of vegetation hits (above 2m). Two estimates, second eliminating area of dense regrowth as beam divergence thought to be significant over the height of the canopy. Crown Cover also derived (method not clear). Regrowth, mature and total stocking estimated and regressed.	$H= 0.6381 + 1.0278*H_{Laser}$ $r^2=0.97$ PFC (all) $PFC=1.4955 + 0.6518*PFC_{Laser}$ $r^2=0.82$ PFC (subset) $PFC=1.8192 + 0.656*PFC_{Laser}$ $r^2=0.934$ $CC = 18.187 + 0.66046*CC_{Laser}$ $r^2=0.903$ Regrowth stocking: $r^2=0.85$ Mature stocking: $r^2=0.85$ Total stocking: $r^2=0.895$
Davenport *et al.,* 2000	Terrain Lidar used to measure height of crops from the standard deviation of heights in a field.	$R^2=0.892$ for linear fit of σ vs measured height Mean error 8.2cm or 20% of crop height Max error 20cm
Witte, C. *et al.,* 2000	Airborne laser scanner, 30cm spot, field sites in Qld.	$PFC = 20.057+0.7748*PFC_{Laser}$ $R^2=0.92$ Highest laser return vs tallest trees: $r^2=0.9$

5.6 Conclusion

The results presented here demonstrate some of the possibilities of Lidar to measure forest characteristics including a literature study of the expected accuracy of retrieval for the parameters. We have shown the capacity to sample foliage elements vertically through the canopy, which is not possible with most other remote sensing technologies. The Lidar measurements have been used to produce broad scale statistics of the forest and we have demonstrated the importance of spot size and variation in the mean values of cover and height in characterising the forest. We believe that these products and the accuracies reported are available from a suitably configured airborne canopy Lidar for operational applications and that a wide range of more advanced products can be developed from the material in this ATBD for airborne and ground based Lidar systems.

6 LIDAR SIMULATIONS OF AUSTRALIAN OPEN FORESTS

6.1 Murray Darling Basin Transect

In McVicar *et al*. (1996), a Transect of data is described which traverses the Murray Darling Basin. The sites of the transect were measured in the field using the Walker/Hopkins Type and Stratum method and Foliage Profiles (FP_{act}) were constructed based on these data. In addition, independent Site estimates of LAI were made by a different method (the module counting method). Among these sites were a diverse range of covers and layered structures that are typical of open forests but certainly much richer than the broad classifications of the Carnahan categories suggest. Four of these (see Table 7 and Figures 6.1 and 6.2) were chosen to illustrate the simulation studies that have been made to ensure that hardware selected for VSIS and ECHIDNA® can map Australian forests.

Table 7. Basic data for the four selected MDB sites

Site	Height (m)	Width (m)	Depth (m)	Shape	CC %	Crown Factor	Stratum	Carnahan Class/**FAI**
3. Goonoo SF West	19.70	6.89	6.56	O	23.9	55.0	U	eM3Z **1.05**
	15.75	4.56	5.40	O	13.2	55.0	M	
	7.10	1.30	2.89	O	1.30	50.0	M	
	1.50	1.00	1.00	O	3.00	50.0	L	
5. Warung SF East	29.25	13.62	14.25	O	58.0	55.0	U	eM2G **1.55**
	19.50	6.75	7.50	O	8.70	55.0	M	
	8.00	2.00	2.00	O	7.00	50.0	M	
	3.50	1.50	1.50	O	12.0	40.0	M	
	0.50	0.00	0.00	G	50.0	0.00	L	
12. Siding Springs OB	30.60	6.85	6.50	O	42.9	55.0	U	eM3Z **1.03**
	25.00	5.00	6.50	O	6.1	55.0	M	
	14.80	2.60	4.40	O	7.0	50.0	M	
	1.00	0.80	0.80	O	3.0	40.0	M	
	0.30	0.00	0.00	G	1.0	0.0	L	
19. Canbelego West	25.00	13.00	10.00	O	50.0	40.0	U	eM1wpL **3.62**
	12.00	4.00	8.00	A	55.0	60.0	M	
	2.00	1.00	1.00	O	30.0	45.0	L	

Table 7 lists the canopy data from McVicar *et al*. (1996) that is based on the Walker/Hopkins description for four of the sites. It also lists the Carnahan code for the site obtained from the general map of Australia provided by Auslig.

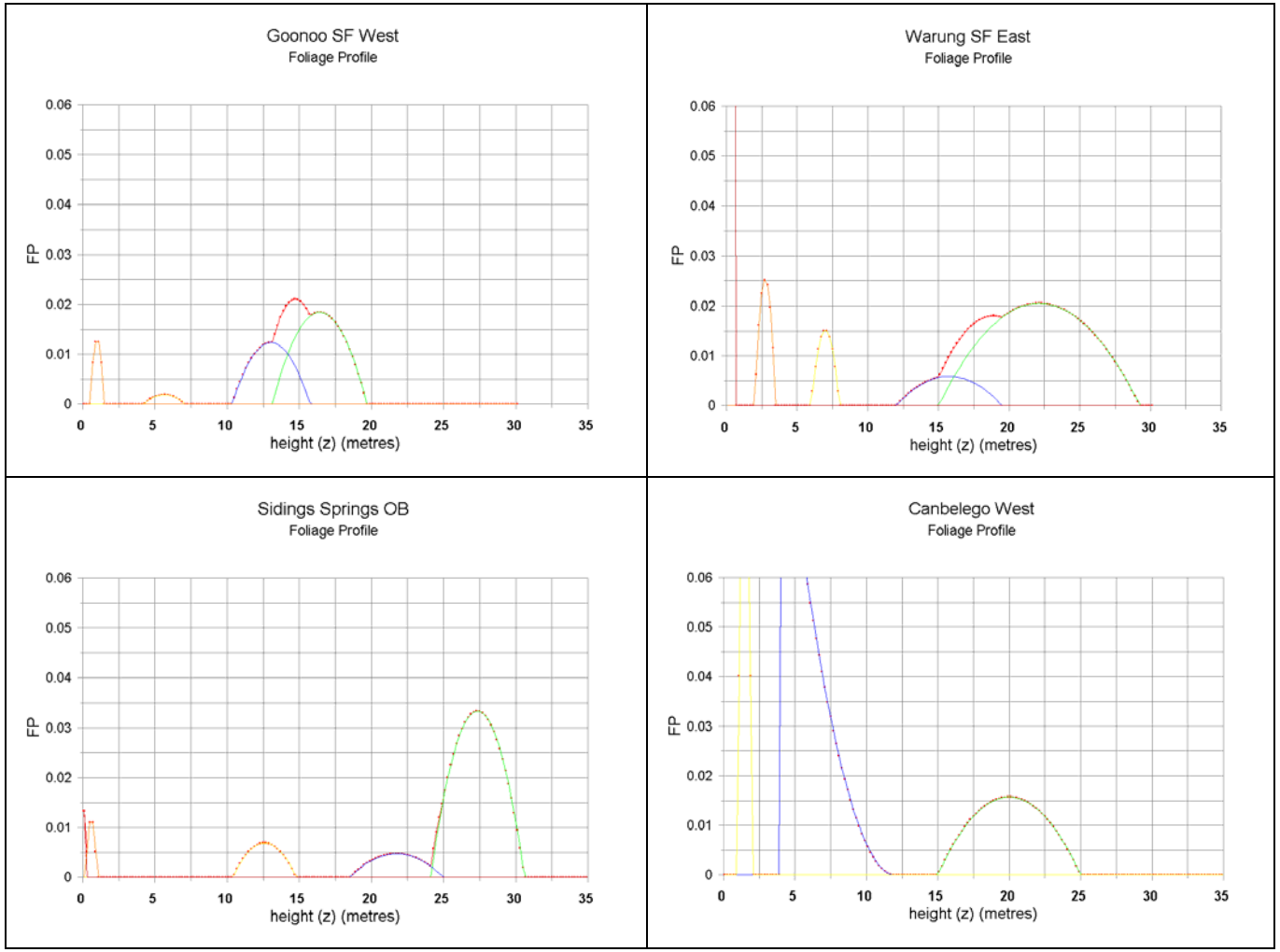

Figure 6.1. Foliage Profiles for Four Sites in the MDB

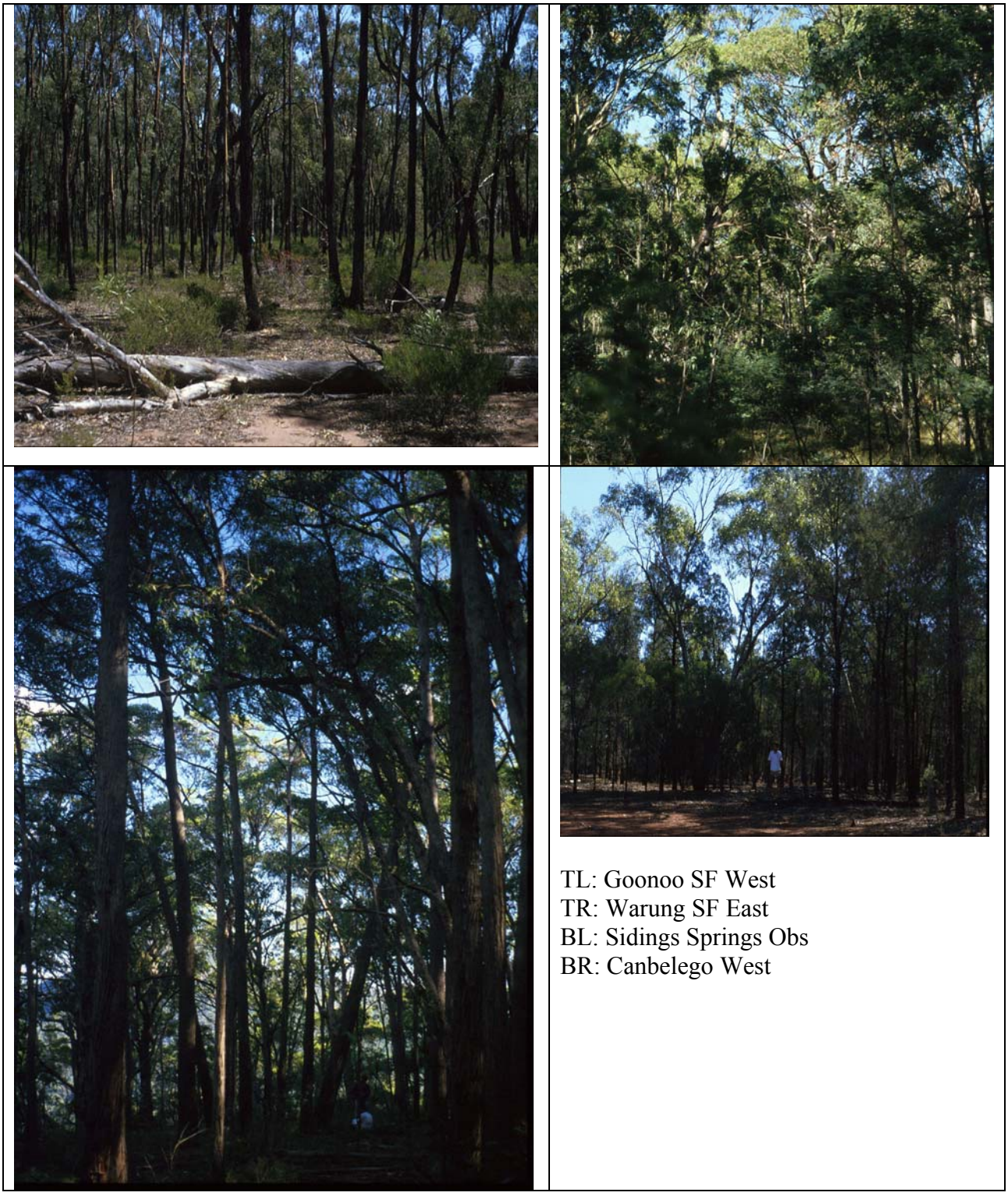

Figure 6.2. Photographs at the four sites to illustrate structure.

6.2 Foliage Profiles

At the time it was written, the Foliage Profile program (FOLIG, Penridge, 1987) did not provide total FAI for sites so that they were recomputed for this ATBD using the field-observed CF to estimate foliage density as described in Appendix 3.

The information obtained from the sites is illustrated in the actual foliage profiles and selected photographs of the sites in the following pages. The total FAI accumulated over the profile is listed in Table 7.

From the foliage profiles and photographs the most obvious features of the sites are:

1. Goonoo State Forest West is a site with a main Eucalyptus layer of trees and not much in the lower part of the canopy.
2. Warung State Forest East has a generally sparse but tall and large crown size upper layer over a dense near-ground shrub layer and a high density of grass on the forest floor.
3. Sidings Springs Obs has a tall upper story of Eucalypts over a less developed understorey.
4. Canbelego West has a sparse upper Eucalyptus canopy over a very dense understorey of callitrus (conifers).

6.3 Apparent Reflectance & Inversion Error

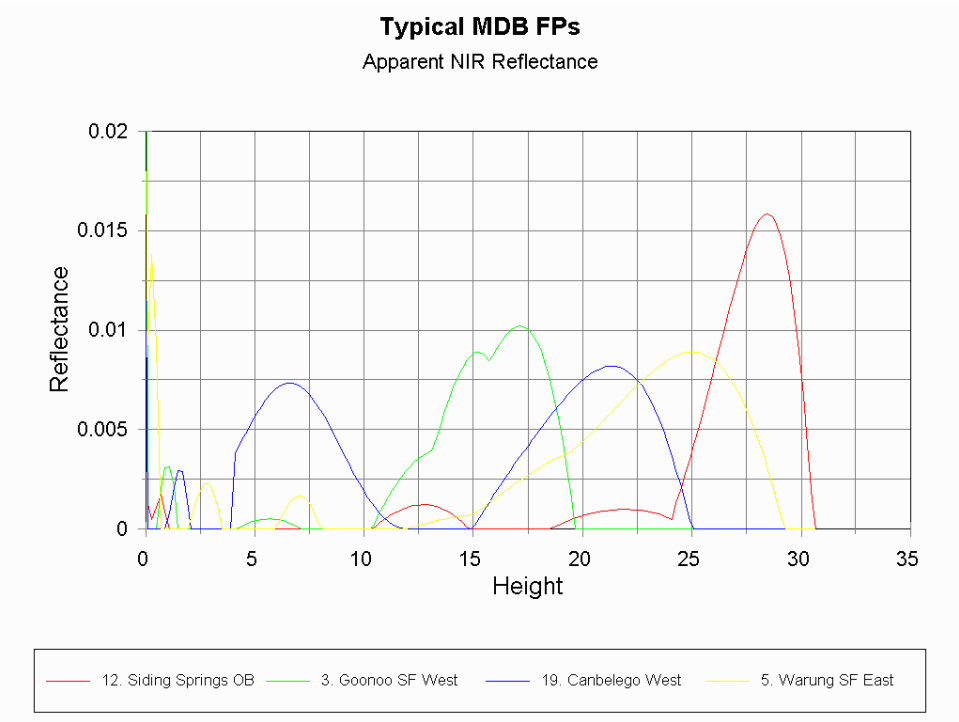

Figure 6.3. Apparent Reflectance Models for the four sites

The FAI and FP_{act} information can be used to provide initial tests of the design criteria for the canopy Lidar. First, using the models from this ATBD the simulated

Lidar returns from each of these sites can be computed as apparent reflectance. The process may be "inverted" as well to give apparent foliage profile from the simulated Lidar data. The apparent reflectance values are shown in Figure 6.3.

For a given instrument SNR model, the SNR as a function of height can be computed from the apparent reflectance as can the expected error in the inversion to the apparent canopy profile. The models may thus be used to investigate how well understorey layers of selected canopies can be inverted from the data. For example, the following plot of SNR as a function of apparent reflectance is taken from the CSIRO CLI ETBD for an approximation to the SLICER instrument. The SNR was modelled (see Figure 6.4) for convenience as:

$$SNR = 5471 \times \rho_{app}^{0.865}$$

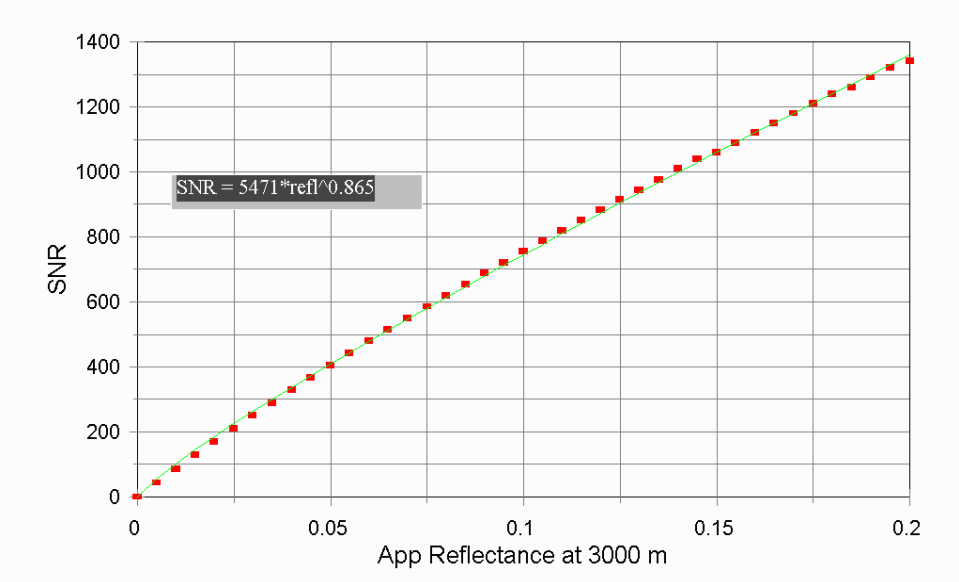

Figure 6.4. SNR model for SLICER Instrument

If the plots of apparent reflectance and this SNR model are combined it is possible to estimate the error at each level and plot the 2σ variation of the inverted apparent foliage profile as described and derived previously. This is shown in Figure 6.5.

Clearly, the 2σ level of variation in the inverted apparent foliage profiles is not able to accurately retrieve the understorey biomass in these cases. This means an actual VSIS will need a much higher power or seek other methods to increase SNR. The design criterion for VSIS has been set at 1000:1 at a 0.1 apparent reflectance and 3000 metres flying height. The example was obviously not at this level.

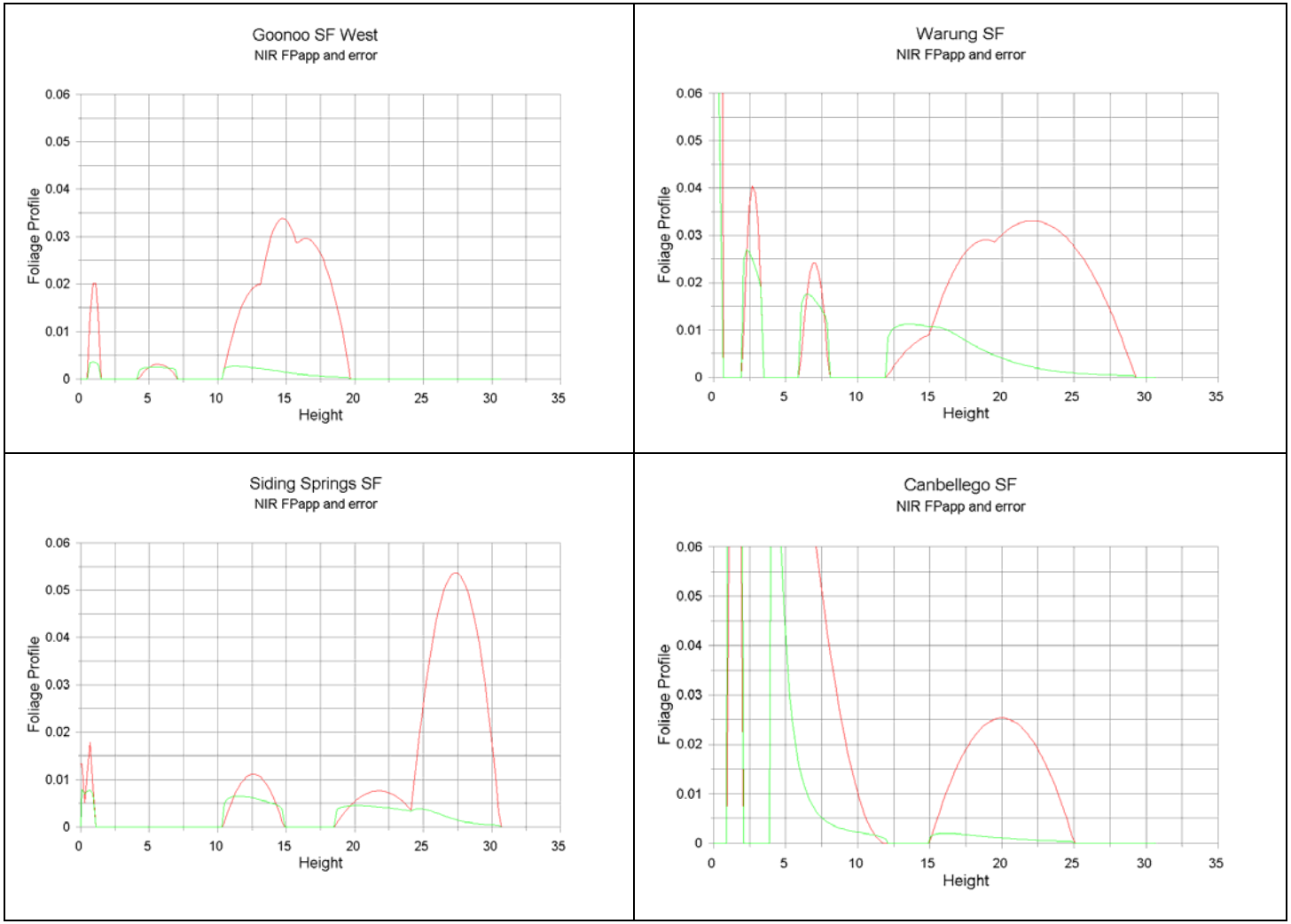

Figure 6.5. Error in Apparent Foliage Profile inversion

Following this exercise it has become possible to model and simulate Lidar returns for any Australian forest type where such data are available. Spot size and pulse width can also be varied and variance from spot to spot computed. The last will be used in operations to assess whether a region is structurally homogeneous.

It is also possible to use growth models such as 3PG (Landsberg and Waring, 1997) or the Integrated Resource Model (IRM, Vertessey *et al*., 1996) to grow a forest (or another land cover) using various levels of real and modelled data, then simulate the Lidar data (and possibly data from other sensors) to predict the capacity of a given instrument combination to monitor components of the land surface (such as understorey) in a range of environments.

An exercise collecting all cases of Walker/Hopkins or equivalent structural descriptions plus a set of "reasonable" models covering most Australian forest types is planned to provide a base for analysing potential or proposed instrument performance during the design and build phases of VSIS and ECHIDNA®.

7 CONCLUDING SUMMARY

In this ATBD we have outlined:

1. Background definitions and descriptions of forest structure as it relates to both forestry, ecology and hydrology;
2. Selected historical and current methods for measuring such structure in the field;
3. Algorithms that enable canopy Lidar data to exploit this history and also provide advanced products from ground and air (and also space) based platforms;
4. Examples of such data analysis and simulation.

The most critical part of the analysis is in the determination of the Lidar instrumentation, its data and its data analysis that will open the way for the full exploitation of this base of analysis. The greatest power in such analysis is obtained in the ECHIDNA® data. However, such data can also be used to calibrate and interpret VSIS and other airborne or spaceborne data over wide areas.

Much of the work in this ATBD does not refer to new work but it has collated and brought together the relevant and significant approaches and methods to enable the Lidar tools to be used effectively to provide advanced measurements of forests. In one important aspect, however, it leads to an innovative basis for commercial exploitation. At base, the Lidar tools measure range (or length) in different directions and with a different spot size in canopies. The Lidar beam spot size, shape and the variation of the intensity over the leading edge of the beam describe a set of "structuring elements". Exploiting the measurements these soundings provide is an innovative and potentially commercial opportunity in the CSIRO Canopy Lidar Initiative.

The ideas contained in the exploitation of beam size, shape and angle in conjunction with digitisation technology and the benefits of combinations of airborne and ground based Lidar system have been the subjects of the following Patent Applications:

Patent Application to Australia, New Zealand, US, Canada, Japan, China and the EC: LIDAR SYSTEM AND METHOD (ECHIDNA), 9 February 2001, Number PR3014;

Granted Australian Petty Patent 1: LIDAR SYSTEM AND METHOD (ECHIDNA), 21 February 2001, Number 23163/01

Granted Australian Petty Patent 2: LIDAR SYSTEM AND METHOD (ECHIDNA & VSIS), 21 February 2001, Number 23164/01

Granted Australian Petty Patent 3: LIDAR SYSTEM AND METHOD (PRODUCTS), 17 April 2001, Number 35196/01

The collation and selection of ideas and the specific derivations and developments described in this document are ones on which any group wishing to exploit Lidar technology could and possibly should base their products.

8 ACKNOWLEDGEMENTS

Nicholas Coops of CSIRO Forestry and Forest Products provided internal CSIRO review of the original internal document and made many valuable comments that were incorporated fully. Dean Graetz of the CSIRO Earth Observation Centre offered both advice and comments that were greatly appreciated. Glenn Newnham of CSIRO EOC read the public version and helped progress it to publication and Joe Walker of CSIRO Land & Water provided comprehensive external review of this public version for which we are very grateful. There are materials used in this study that we are very grateful to have had access to. These include the SLICER data made available to the public by NASA (http://denali.gsfc.nasa.gov/research/laser/slicer/slicer.html), materials used from other publications, especially the Figure from Walker and Hopkins (1990) in Section 2.3.4, Figures 1.1 and 1.2 from NASA as well as access to the CSIRO Atmospheric Research Lidar and its data for investigations into the possibility of the ECHIDNA® instrument.

9 REFERENCES

Aldred, A.H. and Bonnor, G.M. (1985). *Applications of airborne lasers to forest surveys*. Petawawa National Forestry Service, Canadian Forestry Service, Agriculture Canada, Information Report PI-X-51, 62p.

Anderson, M.C. (1971). Radiation and crop structure. In *'Plant Photosynthetic Production/Manual of Methods'*, Edited by Z. Sestak, J. Catsky, and P.G. Jarvis. The Hague.

Anderssen, R.S. and Jackett, D.R. (1984). Linear functionals of foliage angle density. *J. Aust. Math. Soc. Ser. B*, **25**, 431-440.

Anderssen, R.S., Jackett, D.R. and Jupp, D.L.B. (1984). Linear functionals of the foliage angle distribution as tools to study the structure of plant canopies. *Australian Journal of Botany*, **32**, 147-156.

Anderssen, R.S., Jackett, D.R., Jupp, D.L.B. and Norman, J.M. (1985). Interpretation and simple formulas for some key linear functionals of the foliage angle distribution. *Agricultural & Forest Meteorology*, **36**, 165-188.

Ansmann, A., Neuber, R., Rairoux, P. and Wandinger, U. (Eds) (1997). *Advances in atmospheric Remote Sensing with Lidar*. Selected Papers of the 18th International Laser Radar Conference (ILRC), Berlin, 22-26 July, 1996.

Barson, M.M., Randall, L.A. and Bordas, V. (2000). *Land Cover Change in Australia. Results of the collaborative Bureau of Rural Sciences – State agencies' project on remote sensing of land cover change*. Bureau of Rural Sciences, Canberra.

Battaglia, M. and Sands, P.J. (1998). Process-based forest productivity models and their application in forest management. *Forest Ecology and Management*, **102**, 13-32.

Beadle, N.C.W. (1981). *The vegetation of Australia*. Cambridge University Press, London.

Beadle, N.C.W. and Costin, A.B. (1952). Ecological Classification and nomenclature. *Proceedings of the Linnean Society of New South Wales,* **77**, 61-82.

Beard, J.S. (1976). *Vegetation map of Western Australia: map and explanatory memoir*. Applecross WA, Vegemap Publications, 1976: 27 vols, illus, maps.

Bell, J.F. and Dillworth, J.R. (1988). *Variable Probability Sampling. Variable Plot and Three P*. O.S.U. Book Stores Inc., Corvallis, Oregon.

Bitterlich, W. (1948). Die Winkelzahlprobe. *Allg. Forst –u. Holewirtsch. Ztg.*, **59**, p45.

Blair, J.B., Coyle, D.B., Bufton, J.L. and Harding, D.J. (1994). Optimization of an airborne laser altimeter for remote sensing of vegetation and tree canopies. *In Proceedings of IGARSS'94*, Pasadena, Ca, Vol II, pp 939-941.

Blair, J.B., Rabine, D.L. and Hofton, M.A. (1999). The laser vegetation imaging system; a medium-altitude digitisation-only, airborne laser altimeter for mapping vegetation and topography. *ISPRS journal of Photogrammetry & Remote Sensing*, **54**, 115-122.

Blair, J.B. and Hofton, M.A. (1999). Modelling laser altimeter return waveforms over complex vegetation using high-resolution elevation data. *Geophysical Research Letters*, **26**, 2509-2512.

Bonhomme, R. and Chartier, P. (1972) The interpretation and automatic measurement of hemispherical photographs to obtain sunlit foliage area and gap frequency. *Israel Journal of Agricultural Research*, **22**(2), 53-61.

Brack, C. (1999). Forest Mensuration. http://www.anu.edu.au/forestry/mensuration.

Bufton, J.L. (1989). Laser altimetry measurements from aircraft and spacecraft. *Proceedings of the IEEE*, **77**(3), 463-477.

Campbell, G.S. (1986). Extinction coefficients for radiation in plant canopies calculated using an ellipsoidal inclination angle distribution. *Agricultural & Forest Meteorology*, **36**, 317-321.

Campbell, G.S. and Norman, J.M. (1989). 1. The description and measurement of plant canopy structure. In Russell, G., Marshall, B. and Jarvis, P.G. (Eds), *Plant canopies: their growth, form and function*. Cambridge University Press, 178p.

Carnahan, J.A. (1976). Natural Vegetation. In *Atlas of Australian Resources*, Second Series, Department of Natural Resources, Canberra.

Carnahan, J.A., Bullen, F., Deveson, E. and King, I. (1990). Vegetation. In *Atlas of Australian Resources (3rd Series, Vol 6)*. Canberra; Australian Survey & Land Information Group.

Chen, J.M., Black, T.A. and Adams, R.S. (1991). Evaluation of hemispherical photography for determining plant area index and geometry of a forest stand. *Agricultural and Forest Meteorology*, **56**, 129-143.

Chen, J.M. and Cihlar, J. (1995a). Quantifying the effect of canopy architecture on optical measurements of leaf area index using two gap sixe analysis methods. IEEE Transactions on *Geoscience and Remote Sensing*, **33**, 777-787.

Chen, J.M. and Cihlar, J. (1995b). Plant canopy gap size analysis theory for improving optical measurements of leaf area index. *Applied Optics*, **34**, 6211-6222.

Chen, J.M., Rich, P.M., Gower, S.T., Norman, J.M. and Plummer, S. (1997). Leaf area index of boreal forests: Theory, techniques, and measurements. *Journal of Geophysical Research*, **102**, 29,429-29,443.

Coops, N.C., and Catling, P.C. (1997a). Predicting Forest Structure from Airborne Videography for Wildlife Management. *International Journal of Remote Sensing*, **18** (12), 2677-2682.

Coops, N.C., and Catling, P.C. (1997b). Utilising Airborne Multispectral Videography to Predict Forest Structure in Eucalypt Forests for Wildlife management. *Wildlife Research*, **24**,691-703.

Coops, N.C. and Culvenor, D. (2000). Utilizing local variance of simulated high spatial resolution imagery to predict spatial pattern of forest stands. *Remote Sensing of Environment*, **71**, 248-260.

Coops, N.C., Culvenor, D. and Catling, P.C. (1998). Utilising airborne multispectral videography to predict habitat and structure attributes in eucalypt forests. *Australian Forestry*, **61**, 244-252.

Davenport *et al.,* (2000). Improving bird population models using airborne remote sensing. *Int. J. Remote Sensing*, **21**, 2705-2717.

Dubayah, R., Blair, J.B., Bufton, J.L. *et al.* (1997). The Vegetation Canopy Lidar mission. In *Land Satellite Information in the new Decade II: Sources and Applications*, ASPRS, Washington, DC, 11-112.

Dubayah, R.O. and Drake, J.B. (2000). Lidar remote sensing for forestry. *Journal of Forestry*, June 2000.

Enquist, B.J., Brown, J.H. and West, G.B. (1998). Allometric scaling of plant energetics and population density. *Nature*, **395**, 163-165.

Fournier, R.A., Rich, P.M. and Landry, R. (1997). Hierarchical characterisation of canopy architecture. *Journal of Geophysical Research*, **102**, 29,445-29,454.

Fraser, C.S., Jonas, D.A., and Turton, D.A. (1999). Report on 1998 Airborne Laser Scanner Trials. *Internal Report for AAM Surveys Pty Ltd.*, August 1999.

Garcia, O. (1998). Estimating top height with variable plot sizes. *Canadian Journal of Forest Research*, **28**, 1509-1517.

Gates, D.J. and Wescott, M. (1984). A direct derivation of Miller's formula for average foliage density. *Australian Journal of Botany*, **32**, 117-119.

Gholz, H.L., Fitz, F.K. and Waring, R.H. (1976). Leaf area differences associated with old-growth forest communities in the western Oregan Cascades. *Canadian Journal of Forest Research*, **6**, 49-57.

Goel, N.S. and Strebel, D.E. (1984). Simple beta distribution of leaf orientation in vegetation canopies. *Agronomy Journal*, **76**, 800-802.

Grosenbaugh, L.R. (1952). Plotless timber estimates – new, fast, easy. *Journal of Forestry*, **50**, 32-37.

Halldorsson, T. and Langerholc, J. (1978). Geometrical form factors for the lidar function. *Applied Optics*, **17**(2), 240-244.

Harding, D.J., Blair, J.B., Garvin, J.G. and Lawrence, W.T. (1994). Laser altimeter waveform measurement of vegetation canopy structure. In *Proceedings of IGARSS'94*, Pasadena, Ca, Vol II, pp 1250-1253.

Harding, D.J. (2000). Airborne Laser Altimeter Characterization of Canopy Structure and Sub-canopy Topography at BOREAS Tower Flux Sites. In collected data of The Boreal Ecosystem-Atmosphere Study. Eds J. Newcomer, D. Landis. S. Conrad, S. Curd, K. Huemmrich, D. Knapp, A. Morrell, J. Nickerson, A. Papagno, D. Rinker, R. Strub, T. Twine, F. Hall and P. Sellers. CD-ROM, NASA.

Harding, D.J., Blair, J.B., Rabine, D.L. and Still, K.L. (2000). SLICER Airborne Laser Altimeter Characterization of Canopy Structure and Sub-canopy Topography for the BOREAS Northern and Southern Study Regions: Instrument and Data Product Description, NASA Technical Memorandum NASA/TM-2000-209891.
[Also available at: http://www-eosdis.ornl.gov/BOREAS/guides/SLICER.html]

IPCC/OECD (1995). Greenhouse Gas Inventory Workbook. *IPCC Guidelines for National Greenhouse Gas Inventories.* Volume 2., Bracknell, UK.

Holgate, P. (1967). The angle-count method. *Biometrika*, **54**, 615-623.

Jupp, D.L.B., Anderson, M.C., Adomeit, E.M.. and Witts, S.J. (1980) Pisces - a computer program for analysing hemispherical canopy photographs. *Technical Memorandum 80/23*. CSIRO Institute of Earth Resources, Division of Land Use Research, Canberra..

Jupp, D.L.B., Walker, J., and Penridge, L.K. (1986). Interpretation of vegetation structure in Landsat MSS imagery: a case study in disturbed semi-arid eucalypt woodland. Part 2. Model based analysis. *Journal of Environmental Management*, **23**, 35-57.

Jupp, D.L.B., Strahler, A.H., and Woodcock, C.E. (1988). Autocorrelation and regularization in digital images. I. Basic Theory. *IEEE Trans. on Geoscience & Remote Sensing*, **26**, 463-473.

Jupp, D.L.B., Strahler, A.H., and Woodcock, C.E. (1989). Autocorrelation and regularization in digital images. II. Simple image models. *IEEE Trans. on Geoscience & Remote Sensing*, **27**, 247-258.

Jupp, D.L.B. and Strahler, A.H. (1991). A Hotspot Model for leaf canopies. *Remote Sensing of Environment*, **38**, 193-210.

Jupp, D.L.B. and Walker, J. (1996). Detecting structural and growth changes in woodlands and forests: the challenge for remote sensing and the role of geometric optical modelling. In: Gholz, H.L., Nakane, K. and Shimoda, H. (eds*). The Use of Remote Sensing in the Modeling of Forest Productivity at Scales from the Stand to the Globe*. Kluwer Academic Publishers, Dordrecht.

Kendall, D.G. (1974). An introduction to stochastic geometry. In *Stochastic Geometry* (E.F. Harding and D.G. Kendall, Eds) pp 1-9, London, Wiley.

Kitchen, M. and Barson, M. (1998). *Monitoring land cover change: Specifications for the remote sensing of agricultural land cover change 1990-1995 project*. Bureau of Rural Sciences, Canberra ACT, 65p.

Koike, F. (1985). Reconstruction of two-dimensional tree and forest canopy profiles using photographs. *Journal of Applied Ecology*, **22**, 921-929.

Kuusela, K. (1965). A method for estimating the volume and taper curve of tree stem for preparing volume functions and tables. *Communicationes Instituti Forestalis Fenniae*, **60**, 1-18.

Landsberg, J.J. and Waring, R.H. (1997). A generalised model of forest productivity using simplified concepts of radiation-use efficiency, carbon balance and partitioning. *Forest Ecology and Management*, **95**, 209-228.

Lang, A.R.G. (1986). Leaf area and average leaf angle from transmission of direct sunlight. *Australian Journal of Botany*, **34**, 349-355.

Lang, A.R.G. (1997). Simplified estimate of leaf area index from transmittance of the sun's beam. *Agricultural & Forest Meteorology*, **54**,

Leech, J.W. and Correll, R.L. (1993). Sampling precision of plantation inventory in South Australia. *Forest Ecology and Management*, **57**, 191-200.

Lefsky, M.A. (1997). *Application of lidar remote sensing to the estimation of forest canopy and stand structure*. PhD thesis, Dept of Environmental Science, University of Virginia.

Lefsky, M.A., Harding, D., Cohen, W.B., Parker, G. and Shugart, H.H. (1999a). Surface Lidar remote sensing of basal area and biomass in deciduous forests of eastern Maryland, USA. *Remote Sensing of Environment*, **67**, 83-98.

Lefsky, M.A., Cohen, W.B., Acker, S.A., Spies, T.A., Parker, G.G. and Harding, D. (1998). Lidar remote sensing of forest canopy structure and related biophysical parameters at H.J. Andrews experimental forest, Oregon, USA. *Proceedings IGARSS98*, Seattle, WA, USA vol **3**, 1252-1254

Lefsky, M.A., Cohen, W.B., Acker, A., Parker, G.G., Spies, T.A. and Harding, D. (1999b). Lidar remote sensing of the canopy structure and biophysical properties of Douglas-Fir Western Hemlock forests. *Remote Sensing of Environment*, **70**, 339-361.

Lewis, (1971). *Site assessment in South Australian pine plantations*. Paper to 15th IUFRO congress, Florida, 1971, section 21.

Li, X., and Strahler, A.H. (1985). Geometric-optical modeling of a conifer forest canopy. *IEEE Transactions on Geoscience & Remote Sensing*, GE**23**(5), 705-721.

Li, X., and Strahler, A.H. (1986). Geometric-optical bidirectional reflectance modeling of a coniferous forest canopy. *IEEE Transactions on Geoscience and Remote Sensing*, GE**24**(6), 906-919.

Li, X., and Strahler, A.H. (1988). Modeling the gap probability of a discontinuous vegetation canopy. *IEEE Transactions on Geoscience and Remote Sensing*, GE**26**, 161-170.

Li, X. and Strahler, A.H. (1992). Geometrical-Optical bidirectional reflectance modelling of the discrete-crown vegetation canopy: effect of crown shape and mutual shadowing. *IEEE Transactions on Geoscience and Remote Sensing*, **30**, 276-292.

Li, X., Strahler, A.H. and Woodcock, C.E. (1995). A hybrid geometric optical-radiative transfer approach for modeling albedo and directional reflectance of discontinuous canopies. *IEEE Transactions on Geoscience and Remote Sensing*, **33**, 466-480.

Loetsch, F., Zohrer, F. and Haller, K.E. (1973). *Forest inventory. Vol. 2*, BLV, Munich.

MacArthur, Robert H. and MacArthur, John W. (1961). On bird species diversity. *Ecology*, **42**(3), 594-598.

MacArthur, R.H. and Horn, H.S. (1969). Foliage Profile by vertical measurements. *Ecology*, **50**, 802-804.

Maclean, G.A. and Krabill, W.B. (1986). Gross-merchantable timber volume estimation using an airborne Lidar system. *Canadian Journal of Remote Sensing*, **12**, 7-18.

McCormick, M.P. (1995). Spaceborne Lidars. *The Review of Laser Engineering*, **23**(2), 89-93.

McDonald, E.R. (1993). *Estimating vegetation structure from remotely sensed images*. Honours Thesis, University of Canberra.

McVicar, T.R., Walker, J., Jupp, D.L.B., Pierce, L.L., Byrne, G.T. and Dallwitz, R. (1996). Relating AVHRR vegetation indices to *in situ* measurements of Leaf Area Index. *CSIRO Division of Water Resources Technical Memorandum*, 96.5, 54pp.

Magnussen, S. and Boudewyn, P. (1998). Derivations of stand heights from airborne laser scanner data with canopy-based quantile estimators. *Canadian Journal of Forest Research*, **28**, 1016-1031.

Magnussen, S., Eggermont, P. and LaRiccia, V. (1999). Recovering tree heights from airborne laser scanner data. *Forest Science*, **45**, 407-422.

Masuyama, M. (1953). A rapid method of estimating basal area in timber survey – an application of integral geometry to areal sampling problems. *Sankhya*, **12**, 291-302.

Matern, B. (1960). Spatial variation. *Meddelanden fran statens Skogsforskningsinstitut*, **49**(5), 1-144.

Matern, B. (1971). Doubly stochastic Poisson processes in the plane. In Patil, G.P., Pielou, E.C. & Waters, W.E. (Eds) *Statistical Ecology 1*., University Park, Pennsylvania State University Press. 195-213.

Matern, B. (1976). Om skattning av ovre hojden. *Sver. Skogsvaardsfoerb. Tidskr.*, **74**, 51-53.

Means, J.E., Acker, S.A., Harding, D.J., Blair, J.B., Lefsky, M.A., ohen, W.B., Harmon, m.E. and McKee, W.A. (1999). Use of large footprint scanning airborne Lidar to estimate forest stand characteristics in the Western Cascades of Oregon. *Remote Sensing of Environment*, **67**, 298-305.

Measures, R.M. (1992). *Laser remote sensing: fundamentals and applications*. Krieger Publishing Company, Malabar, Florida, 510p.

Miller, J.B. (1964). An integral equation from phytology. *Journal of the Australian Mathematical Society*, **4**, 397-402.

Miller, J.B. (1967). A formula for average foliage density. *Australian Journal of Botany*, **15**, 141-144.

Naesset, E. (1997a). Estimating timber volume of forest stands using airborne laser scanner data. *Remote Sensing of Environment*, **61**, 246-253.

Naesset, E. (1997b). Determination of mean tree height of forest stands using airborne laser scanner data. *ISPRS J. Photogrammetry and Remote Sens*ing, **52**, 49-56.

Nakajima, T.Y., Uchino, O., Nagai, T. and Moriyama, T. (1996). Possibility of cloud and aerosol observations by spaceborne mie lidar. *IRS'96, Current Problems in Atmospheric Radiation*. Smith and Stamnes (Eds).

National Land & Water Resources Audit (2000a). *Australian vegetation attributes version 5.0*. Audit, Canberra.

Nelson, R.L., Krabil, W.B. and MacLean, G.A. (1984). Determining forest canopy characteristics using airborne laser data. *Remote Sensing of Environment*, **15**, 210.

Ni, W., N., Woodcock, C.E. and Jupp, D.L.B. (1999) Variance in bidirectional reflectance over discontinuous plant canopies. *Remote Sensing of Environment*, **69**(1), 1-15.

Ni, W., Jupp, D.L.B. and Dubayah, R. (2001). Modelling Lidar waveforms in heterogeneous and discrete canopies. *IEEE Transactions on Geoscience and Remote Sensing*, **39**(9), 1943-1958.

Nilson, T. (1971). A theoretical analysis of the frequency of gaps in plant stands. *Agricultural Meteorology*, **8**, 25-38.

Nilson, T. (1999). Inversion of gap frequency data in forest stands. *Agricultural & Forest Meteorology*, **98-99**, 437-448.

Norman, J.M., Miller, E.E. and Tanner, C.B. (1971). Light intensity and sunfleck-size distribution in plant canopies. *Agronomy Journal*, **63**, 743-748.

Ondok, J.P. (1984). Simulation of stand geometry in photosynthetic models based on hemispherical photographs. *Photosynthetica*, **18**, 231-239.

Opie, J.E. (1976). Volume functions for trees of all sizes. Victorian Forests Commission, *Forestry Technical Papers*, **25**, 27-30.

Penridge, L.K. (1984). FOLIG: A computer program to generate foliage profiles. *CSIRO Division of Water and Land Resources, Technical Memorandum*, TM 84/29.

Penridge, L.K. (1987). FOL-PROF: A fortran-77 package for the generation of foliage profiles. Part 2 Programmer manual. *CSIRO Division of Water Resources, Canberra, Technical Memorandum*, TM 87/10.

Penridge, L.S. and Walker, J. (1988). The crown-gap ratio (C) and cover percent: II Derivation and simulation study. *Aust. J. Ecol*., **13**, 109-120.

Peterson, S.R. (1982). A preliminary survey of forest bird communities in Northern Idaho. *Northwest Science*, **56**, 287-298.

Philip, J.R. (1965). The distribution of foliage density with foliage angle estimated from inclined point quadrat observations. *Australian Journal of Botany*, **13**, 357-366.

Rich, P.M. (1990). Characterising plant canopies with hemispherical photographs. In: N.S. Goel and J.M. Norman (Eds). Instrumentation for studying vegetation

canopies for remote sensing in optical and thermal infrared regions. *Remote Sensing Reviews*.

Ritman, K.T. (1995). *Structural Vegetation Data: A specifications manual for the Murray Darling Basin Project M305*. NSW Department of Land and Water Conservation, Land Information Centre.

Ross, J. (1981). *The radiation regime and architecture of plant stands*. W. Junk, The Hague, 391p.

Sasano, Y., Shimizu, H., Takeuchi, N. and Okuda, M. (1979). Geometrical form factor in the laser radar equation: an experimental determination. *Applied Optics*, **18**(23), 3908-3910.

Serra, J. (1974). Theoretical bases of the LEITZ-Texture Analysing System. (LEITZ-T.A.S.), *Scientific and Technical Information Supplement*, 1(4), 125-136.

Serra, J. (1980). The Boolean model and random sets. *Computer Graphics and Image Processing*, **12**, 99-126.

Serra, J. (1982). *Image Analysis and Mathematical Morphology*. Academic Press, London, New York.

Shapiro, J.H. (1982). Target-reflectivity theory for coherent laser radars. *Applied Optics*, **21**, 3398-3407.

Shugart, H.H. (1984). *A theory of forest dynamics: the ecological implications of forest succession models*. Springer-Verlag.

Smith, J.A., Oliver, R.E. and Berry, J.K. (1977). A comparison of two photographic techniques for estimating foliage angle distribution. *Aust. J. Bot*. **25**, 545-553.

Specht, R.L. (1970). Vegetation. In *The Australian Environment 4th Edition*. Leeper, G.W. (Ed) CSIRO-Melbourne, University Press, Melbourne. Pp 44-67.

Specht, R.L., Roe, E.M. and Boughton, V.H. (1974). Conservation of major plant communities in Australia and Papua New Guinea. *Aust. J. Bot.*, Supplement No 7.

Specht, R.L., Hegarty, E.E., Whelan, M.B. and Specht, A. (1995). *Conservation atlas of plant communities in Australia*. Southern Cross University. Centre for Coastal Management, Lismore.

Strahler, A.H., and Jupp, D.L.B. (1991). Modeling bidirectional reflectance of forests and woodlands using Boolean models and geometric optics. *Remote Sensing of Environment*, **34**, 153-166.

Strahler, A.H. and Li, X. (1981). An invertible coniferous forest canopy reflectance model. In *Proc. 15th Int. Symp. Remote Sensing Environ.* Ann Arbor, MI, 1237-1244.

Suits, G.H. (1972a). The calculation of the directional reflectance of a vegetative canopy. *Remote Sensing of Environment*, **2**, 117-125.

Suits, G.H. (1972b). The cause of azimuthal variations in directional reflectance. *Remote Sensing of Environment*, **2**, 175-182.

Sumida, A. (1993). Growth of tree species in a broadleaved secondary forest as related to the light environment of crowns. *J. Jpn. For. Sci.*, **75**, 278-286.

Tickle,P., Witte, C., Danaher, T., Jones, K. (1998). The Application of large-Scale Video and Laser Altimetry to Forest Inventory. *Proceedings, 9th Australiasian Remote Sensing and Photogrammetry Conference*.

Ulaby, F.T., Sarabandi, K., McDonald, K., Whitt, M. and Dobson, M.C. (1990). Michigan microwave canopy scattering model. *International Journal of Remote Sensing*, **11**, 1223-1253.

Verhoef, W. (1984). Light scattering by leaf layers with application to canopy reflectance modelling: the SAIL model. *Remote Sensing of Environment*, **16**, 125-141.

Vertessy, R.A., Benyon, R.G., O'Sullivan, .S.K. and Gribben, P.R. (1994). *Leaf area and tree water use in a 15 year old mountain ash forest, Central Highlands, Victoria*. Cooperative Research Centre for Catchment Hydrology, Report 94/3, May 1994.

Vertessy, R.A., Benyon, R.G., O'Sullivan, .S.K. and Gribben, P.R. (1995). Relationships between stem diameter, sapwood area, leaf area and transpiration in a young mountain ash forest. *Tree Physiology*, **15**, 559-567.

Vertessy, R.A., Hatton, T.J., Benyon, R.J. and Dawes, W.R. (1996): Long term growth and water balance predictions for a mountain ash (E. regnans) forest subject to clearfelling and regeneration. *Tree Physiology*, **16**:221-232.

Walker, J. and Gillison, A.N. (1982). "Australian Savannas". Chapter 2 in B.J. Huntley and B.H. Walker (Eds) *Ecology of Tropical Savannas*, Springer-Verlag, Berlin Heidelberg New Yoprk, p. 5-24.

Walker, J. and Penridge, L.K. (1987). The crown-gap ratio methodology: crown cover estimation and foliage profile construction. *CSIRO Division of Water Resources Research Technical Memorandum*, TM87/.

Walker, J. and Hopkins, M.S. (1990). Vegetation. In: *Australian Soil and Land Survey: Field Handbook*. McDonald, R.C., Isbell, R.F., Speight, J.G., Walker, J. and Hopkins, M.S. (Eds). Second Edition, Inkata Press, Melbourne.

Walker, J., Crapper, P. and Penridge, L.S. (1988). The crown-gap ratio (C) and cover percent: I. The field study. *Aust. J. Ecol.*, **13**, 101-108.

Wang, Y.P. and Jarvis, P.G. (1990). Description and validation of an array model – MAESTRO. *Agricultural and Forest Meteorology*, **51**, 257-280.

Warren Wilson, J. (1959a). Analysis of the spatial distribution of foliage by means of two-dimensional point quadrats. *New Phytologist*, **58**, 92-101.

Warren Wilson, J. (1959b). Analysis of the distribution of foliage area in grassland. In: J.D. Ivins (Ed). *The measurement of grassland productivity*, Academic Press, London UK, 51-61.

Warren Wilson, J. (1960). Inclined point quadrats. *New Phytologist*, **59**, 1-8.

Warren Wilson, J. (1963). Estimation of foliage denseness and foliage angle by inclined point quadrats. *Australian Journal of Botany*, **11**, 95-105.

Warren Wilson, J. (1965a). Point quadrat analysis of foliage distribution for plants growing singly or in rows. *Australian Journal of Botany*, **13**, 405-409.

Warren Wilson, J. (1965b). Stand structure and light penetration. I. Analysis by point quadrats. *J. Appl. Ecol.*, **2**, 383-390.

Warren Wilson, J. (1967). Stand structure and light penetration. III. Sunlit foliage area. *J. Appl. Ecol.*, **4**, 159-165.

Welles, J.M. and Norman, J.M. (1991). Instrument for indirect measurement of canopy architecture. *Agronomy Journal*, **83**, 818-825.

Whitmore, T.C. (1989). Canopy gaps and the two major groups of forest trees. *Ecology*, **70**(3), 536-538.

Williams, R.J. (1950). Vegetation Regions. In *Atlas of Australia, 1st Series*. Canberra: Department of National Development.

Witte, C., Norman, P., Denham, R., Turton, D., Jonas, D. and Tickle, P. (2000). *Airborne laser scanning – A tool for monitoring and assessing the forests and woodlands of Australia*. Forest Ecosystem Research and assessment Technical Papers, 00-10, Queensland Department of Natural Resources.

Wood, G., Turner, B.J. and Brack, C.L. (Eds) (1999). *Code of forest mensuration practice*. Canberra ACT, ANU Department of Forestry.

Wood, J.G. (1930). Ecological concepts and nomenclature. *Trans. R. Soc. Aust.*, **63**, 215-233.

Yang, X., Witcosky, J.J. and Miller, D.R. (1999). Vertical overstory canopy architecture of temperate deciduous hardwood forests in the eastern United States. *Forest Science*, **45**, 349-358.

10 APPENDIX 1: CARNAHAN VEGETATION CODES

10.1 Explanation

The first three (occasionally four) characters of the code refer to the tallest stratum. The first, a lower-case letter, indicates the predominant floristic type (eg. e=*Eucalyptus*). Occasionally, where two types are of near-equal abundance, two lower-case code letters are shown, the first indicating the slightly more abundant type. The next character, an upper-case letter, indicates the growth form (eg. T=*tall trees*). The following character, a number, indicates the projective foliage cover of this stratum. The numbers assigned according to percent cover are: 1 (<10%); 2 (10-30%); 3 (30-70%) and 4 (>70%).

The next one or two characters refer to the lower stratum if it has a foliage cover of more than 10%. Where the foliage cover of the upper stratum is greater than 10% only the growth form of the lower stratum is indicated (by an upper-case letter). Where the foliage cover of the upper stratum is less than 10%, the predominant floristic type of the lower stratum is indicated by a lower-case letter followed by an upper-case letter indicating the growth form. In a few cases two lower-case floristic code letters are given for the lower stratum, indicating near-equal abundance.

10.2 Floristic types

Code	Genus, Family or Group
b	Banksia
c	Casuarina including Allocasuarina
e	Eucalyptus
h	Hakea
k	Chenopodiaceae (eg. Saltbush and Bluebush)
m	Melaleuca
n	Nothofagus
o	Owenia (Desert Walnut)
p	Conifers
q	Myoporum (Sugarwood)
r	Heterodendrum (Rosewood)
w	Acacia (Wattle) including Racosperma
t	Triodia and/or Plectrachne
a	Astrebla (Mitchell Grass)
d	Dichanthium
f	Fabaceae (includs clovers and medics)
g	Graminoids
v	Saccharum (Sugar Cane)
y	Other Grasses
z	Asteraceae (Dasies)
x	Mixed or other
u	Cereals

10.3 Growth Forms

Code	Description
T	Tall trees >30m
M	Medium trees 10-30m
L	Low trees <10m
S	Tall shrubs >2m
Z	Low shrubs <2m
H	Hummock grasses
G	Tussocky or tufted grasses
F	Other herbaceous plants

10.4 Cover

Number	Crown Cover Range	Description
1	<10%	Sparse
2	10% to 30%	Woodland
3	30% to 70%	Open
4	>70%	Closed

For example, ewL1yG has an upper storey of low trees with 0-10% cover and species Eucalyptus and Acacia. The understorey is tussocky grass of non-specific species.

10.5 Cover/Height (Structure Diagram)

		Canopy cover (percentage)			
		Closed forest	Open forest	Woodland	Non-forest
Height (metres)		>70%	30-70%	10-30%	<10%
Tall trees	>30m	T4	T3	T2	T1
Medium trees	10-30m	M4	M3	M2	M1
Low trees	6-10m	L4	L3	L2	L1
Tall shrubs	2-6 m	S4	S3	S2	S1

At the most aggregated level the structural codes define a set of areas on the structure diagram and are generally only based on the dominant stratum. The above Table of 16 codes represents the broadest level of structural classification and is often used for vegetation mapping at continental scale.

However, it is not always clear on what base plot area these terms are defined. As we have seen, cover variation changes with plot size and normally used measures of height, such as top height, can vary with plot size. The most common unit has been the 0.04 ha or 20 m by 20 m plot. However, this leads to high variation between plots and leaves the issue of how plot and regional information relate to one another unresolved. Hopefully, the development of the NVIS will address this issue.

11 APPENDIX 2 – SOLUTION FOR UN-CALIBRATED DATA

Assume that the calibration in the region where there are data has the form (out of the close range area where k(r) is operating):

$$C(r) = \frac{\tilde{C}}{r^2}$$

In this equation the constant $\tilde{C}$ may be unknown. It follows that we can define:

$$\tilde{S}(r) = \tilde{C}\rho_{app}(r) = r^2 \frac{E(r)}{E_0} = -\tilde{C}\rho_v \frac{dP_{gap}(r)}{dr}$$

Again, we can integrate this quantity over the profile to obtain:

$$\begin{aligned}\tilde{H}(r) &= \int_0^r \tilde{S}(r')dr' \\ &= \tilde{C}\rho_v(1 - P_{gap}(r))\end{aligned}$$

and at the ground the relationship holds that:

$$\begin{aligned}\tilde{S}(h) &= \tilde{C}\rho_g P_{gap}(h) \\ &= \tilde{C}\rho_g \left(1 - \frac{\tilde{H}(h)}{\tilde{C}\rho_v}\right) \\ &= \tilde{C}\rho_g - \frac{\rho_g}{\rho_v}\tilde{H}(h)\end{aligned}$$

Hence, if the ratio of the ground and vegetation reflectance is known this relationship gives us $\tilde{C}\rho_g$ and hence $\tilde{C}\rho_v$ giving us the integrated gap profile $P_{gap}(r)$ and including $P_{gap}(r)$. If some shots do not have ground returns due to dense canopies the local estimate of the $\tilde{C}\rho_v$ can then be used to provide a gap profile.

$$\begin{aligned}\tilde{C}\rho_g &= \tilde{S}(h) + \frac{\rho_g}{\rho_v}\tilde{H}(h) \\ \tilde{C}\rho_v &= \frac{\rho_v}{\rho_g}\tilde{C}\rho_g \\ &= \frac{\rho_v}{\rho_g}\left[\tilde{S}(h) + \frac{\rho_g}{\rho_v}\tilde{H}(h)\right]\end{aligned}$$

That is, in general:

$$P_{gap}(r) = 1 - \text{cover}(r)$$
$$= 1 - \frac{\tilde{H}(r)}{\tilde{H}(h) + \frac{\rho_v}{\rho_g}\tilde{S}(h)}$$

To achieve this result operationally requires separating the ground signal from the above ground signal, identifying start of data and the background noise threshold. Automated processing provides some challenges and the value of deconvolution needs to be investigated to make this operational.

12 APPENDIX 3 –CROWN FACTOR AND LEAF AREA DENSITY

If the foliage density is uniform through the interior of the crown then it may be approximately estimated from the crown factor, or crown openness (CF).

If the foliage elements are relatively small and randomly distributed through the crown volume with a uniform leaf area volume density F then the probability that a ray of length s in direction μ within the canopy will not hit a foliage element is:

$$P_{gap,W}(s,\mu) = e^{-G(\mu)Fs}$$

G is the Ross G-function, or the ratio of the projected area of foliage elements in the direction μ to the one-sided area as used for the FAI and F in this ATBD. For randomly distributed leaves, G=0.5 for all directions.

The CF can be modelled by a simple method to get a starting value for a more complex method to define an equivalent F for the crown. In the simple method, the mean length of intercepts (s) vertically through the crown are used with the gap model to estimate CF and in the second the mean P_{gap} over the area covered by the crown using the same intercepts is used. The second is the "accurate" estimate.

12.1 Foliage Density for Ellipsoidal Crowns

For an ellipsoidal crown it may be shown that the mean vertical path through the crown is 2/3T where T is the crown thickness. In this case an initial rough estimate for the mean gap fraction for the crown looking vertically up would be:

$$\begin{aligned}\overline{P}_{gap} &= 1 - CF/100 \\ &\approx e^{-\frac{2}{3}GFT}\end{aligned}$$

where G here is the vertical Ross G-function.

A more accurate estimate is to average $P_{gap,W}$ over the crown area which results in:

$$\begin{aligned}\overline{P}_{gap,W} &= \frac{2}{r^2}\int_0^r \rho e^{-X\left(1-\frac{\rho^2}{r^2}\right)^{1/2}} d\rho \\ &= \frac{2}{X^2}\left(1-(1+X)e^{-X}\right) \\ X &= GFT\end{aligned}$$

If the simple estimate is used to get a first approximation to X then a refined estimate of X can be rapidly obtained by iteration allowing GF to be obtained for each Type from the CF data.

The missing data in the normal Walker/Hopkins field data set is G. We can use G as 0.5 (random case) to make a start but ideally some idea of the foliage angle distribution should be provided for each crown type and/or species. Even indications of foliage angle such as "erectophile" (vertical foliage), "planophile" (horizontal foliage) and "random" would be helpful.

However, such data can also be inferred if the species of the foliage type has been recorded in the field data and/or photographs are taken at the sites. The photographic method uses hemispherical photography in areas of measured structure to invert G and F.

12.2 Foliage Density for Conical Crowns

For cones the simple estimate is:

$$\begin{aligned}\overline{P}_{gap,W} &= 1 - CF/100 \\ &\approx e^{-\frac{1}{3}GFT}\end{aligned}$$

and the more accurate method leads to:

$$\begin{aligned}\overline{P}_{gap,W} &= \frac{2}{r^2}\int_0^r \rho e^{-X\frac{(r-\rho)}{r}} d\rho \\ &= \frac{2}{X}\left(1 - \frac{1}{X}(1-e^{-X})\right) \\ X &= G\,F\,T\end{aligned}$$

Hence, again the field data leads to an estimate for GF and some assumption about G is needed to obtain F by itself. However, note that GF is what is needed to model vertical Lidar returns so not all is lost!

12.3 Foliage Density for Grass

For grass, the data usually available are height and cover. If we denote the grass height by T then we get:

$$\begin{aligned}\overline{P}_{gap,G} &= (1 - \frac{\text{cover}}{100}) \\ &= e^{-GFT}\end{aligned}$$

so that again GF is available from the field data for the grass canopy Type. But, again, some knowledge of G will be needed to obtain the complete actual Foliage Profile.

13 APPENDIX 4: SPATIAL MODELS FOR VEGETATION

13.1 Introduction

Many of the models underlying measurements of vegetation for environmental, ecological, forestry and for remote sensing applications have a statistical basis. It has led to a broad and diverse terminology as well as some confusion of the underlying principles being used in any specific instance.

In our Lidar investigations there is a common, underlying set of spatial models that will be outlined below. The terminology we have chosen may be different from other publications but will be defined and in some cases compared with alternatives that can be found in the mainstream literature.

Terms like “random”, “clumped”, “homogeneous” and “isotropic” need to be defined and used carefully.

13.2 Discrete vs Continuous

A continuous canopy model is one where the parameters (such as foliage density) vary continuously in the region of the canopy. Continuous models are more common in radiative transfer and remote sensing than in forestry and ecology. A canopy is treated much like a water mass or a layer of the atmosphere.

To some extent such models also fit easily with the “continuous field” models of hydrology and topographic variation of environmental resources. They link easily to the notion of a spatial random function $Z(x)$ as used in such continuous field methods and their statistical analyses.

However, in the fields of forestry and ecology it is more natural to treat canopies as discrete. That is, they are modelled as being composed of elementary objects, or “phyto-elements”. In this, the models are naturally those of the random sets models described by Kendall (1974) and Serra (1982).

In the development of these models, there is an interaction between the choice of phyto-elements and the scale of the application. From the leaf structure used in studies of leaf reflectance and transmittance through leaves, stems, shoots, modules, crowns, trees, sites and stands to forests there is a natural aggregation that matches the level of measurement scale.

This is matched in the common models of canopies as leaves and stems that are distributed in some random way or in models where tree crowns are distributed in some random way but are also filled with leaf material that is either treated as continuous or as a discrete collection of individual leaves.

At a broad landscape scale, tree cover and density may well be able to be treated as a continuous spatial random function on a continuous topographic surface. However, at

the scales we will work at with canopy Lidar and in forest measurement the delineation of individual trees as discrete objects is a minimal model and for crops, the delineation of leaves and stems as base phyto-elements or objects seem to be mandatory.

13.3 Density and Dispersion

A collection of objects will have properties that belong to the objects, such as size, shape and orientation as well as dispersion or the way they are distributed in the space they occupy.

This obviously needs a coordinate system to describe the dispersion and an embedded coordinate system to describe size and shape of an object. The relationships between these can be used to describe orientation. Objects usually have a "centre" corresponding to the origin of the embedded coordinate system. The spatial dispersion of these centres is the normal measure of the dispersion of the phyto-elements.

Studies of the dispersion of individuals have been common and extensive in ecology and many of the basic models have wide use in forestry and environmental studies. Often, the basic individuals are small and their extent is ignored so that the point pattern of the dispersion of the centres is referred to as the dispersion of the individuals. However, the finite extent of the discrete objects is often highly significant so we will carefully use these tools as descriptions of the way the centres are dispersed.

Because a point pattern has no area or volume, the definition of a random point set is accomplished through a counting function on the subsets of the plane or volume in which the model is being defined. That is, the measure:

$$\mu(B) = \{\# \mid x \in B\}$$

where B is a (Borel) subset of the region in which the points are dispersed. For a probability function defined on this measure (P) there is an intensity measure of the process defined as:

$$\Lambda(B) = \int \mu(B)\, P(d\mu) \quad B \in R^n$$

and an intensity function which is the Radon-Nikodym derivative of the intensity defined implicitly by:

$$\Lambda(B) = E(\mu(B)) = \int_B \lambda(x)\, d|x|$$

That is, the limiting expectation of the density of individuals is λ.

For such a general set of definitions, the point process it will generate is called stationary if its distribution is independent of arbitrary translations of the origin and

isotropic if its distribution is invariant under an arbitrary rotation about the origin. Stationarity is often called "homogeneity".

Clearly, processes can be stationary (homogeneous) in given directions in planes and not in other directions and isotropic in planes without being isotropic in the whole space. Note, however, that a process can be stationary and isotropic and therefore certainly homogeneous and still have spatial dependence and correlation that may lead to clustering and clumping of the points in the space. These are separate ideas that are often defined against the base of a simple model.

13.4 The "Random" or homogeneous Poisson point process

In ecology and other environmental areas, descriptions of the point patterns of the dispersion of individuals have generally been based on comparison with a "random" distribution. This is somewhat confusing because all of the models we are discussing are "random" but what is meant there is the homogeneous Poisson point process.

The Poisson probability distribution with density λ is defined as:

$$P(x) = Poisson\{\lambda\} = \frac{e^{-\lambda}\lambda^{x}}{x!}$$

The homogeneous Poisson point process is then defined by the two properties:

1. The number of points in any (Borel) subset A is Poisson distributed with density $\lambda|A|$;
2. The numbers of points in disjoint sets are independent.

Such Poisson point processes have many useful and important properties and computable measures such as distances to nearest neighbours, summation of densities of Poisson processes and divisibility. For example, if the sizes of the objects are independent of the dispersion then by selecting objects with a size range the resulting centres are again a Poisson point process with lower density.

Ecologists have often assumed that the presence of a Poisson point process for the dispersion of individuals indicates a lack of control by environmental or ecological processes on the dispersion. It is therefore in a sense a "null" hypothesis.

Two measures that may be derived for a wide range of stationary and homogeneous distributions and computed for realisations of point patterns are the following:

$$G_k(t) = \Pr\{KNN_i \le t\}$$
$$F_k(t) = \Pr\{KNN_x \le t\}$$

where KNN is the k'th nearest point (or k'th nearest neighbour) to (respectively) an arbitrary individual (i) or an arbitrary point (x). For a Poisson point process (and *only*

for a Poisson point process) they are the same. Also, if the process is anisotropic the definitions can still hold if "t" is a vector in a specific direction.

Our interests are therefore (like the ecologists) what the departures from the Poisson point process will mean about the natural processes operating in the area of interest. The above and other measures have been used to measure these departures. Specifically, the interest is in measuring the degree of "clumping" that is occurring in the dispersion of the points.

13.5 Clustered/attractive and regular/repulsive point processes

Departures from the test model of the homogeneous Poisson point process can be measured variously by:

- Comparison between the observed variances of the numbers of points in subsets of the plane compared with the actual;
- Computing the ratio of the variance to the mean;
- Assessing the differences between k'th nearest neighbours from individuals and from arbitrary points; and/or
- Computing the actual distribution of numbers of points in specific subsets of the space of interest and comparing it with the homogeneous Poisson model.

If the point pattern is more clustered than the Poisson case then variance is higher than the mean, the distribution of the numbers of individuals in subsets is broader and the distances from individuals to near neighbours are lower than from arbitrary points to the near neighbours. The opposite cases indicate that individuals are dispersed more regularly than "random" (i.e. than they are for the homogeneous Poisson point process).

Among ecologists, the idea has been that clustering and regularity as departures from the homogeneous Poisson indicate the influence of environmental and/or competitive effects. They are therefore significant when the issue is the dispersion of plants in a landscape but possibly need more insightful assessment when the apparent clustering of leaves is simply due to leaves being in crowns in a forest.

Table 8. Types of spatial model

Point Pattern	Alternatives	Ecological Process
Regular	Dispersed Repulsive Uniform	Competitive
"Random"	Homogeneous Poisson	Independent
Clustered	Aggregated Attractive Clumped	Contagious

There are many terms used in the literature to describe dispersion of points and (by inference) objects in spatial models. Table 8 collects some of them and also indicates the ecological "process" descriptions that are often applied to their occurrence:

The terms “regular, random and clustered” seem to have general acceptance or at least be understood by most people in the field. They will be used in our work.

13.6 Generalisations of the “Random” model

The departures from the random case described above are generally seen to arise (and are generally modelled) from changes to the conditions of the homogeneous Poisson process. One obvious departure is to allow the Poisson density to vary spatially. This may, for example, indicate changes to the resource availability over a landscape. In this case, the inhomogeneous or non-stationary Poisson process is defined by the two conditions:

1. The number of points ($\mu(A)$) in any (Borel) subset A is Poisson distributed with density $\int_A \lambda(x)\, d|x|$
2. The numbers of points in disjoint sets are independent.

The independence is a key attribute of this model for computing expected measurements.

Such dispersions can clearly be apparently clustered or uniform and vary in clustering or uniformity over the space of interest. To give some structure to the model, it is often assumed that the density is itself a two-dimensional stochastic process. If it is itself Poisson the model is the “double Poisson” as described together with other variants by Matern (1971).

Another means of generalising the Poisson is to develop Poisson cluster models. An important specific example is the Neyman-Scott process that can be described as follows:

1. A Poisson process generates “parents” with density ρ;
2. Each parent produces M “daughters” according to a specific distribution;
3. The daughters are located independently according to a density function h(x).

The result is obviously a clustered point process. It may well be a model for the effects of seed dispersion or for the foliage in crowns of trees. In many cases, a wide range of statistics and measures can be derived for such models as described by Matern (1960 & 1971).

13.7 Large object discrete models

Focussing on the point patterns may often hide the degree to which structure can be represented in the models by the objects that are dispersed through the process. The combination of a random dispersion of object centres and a random sets model for the size, shape and orientation of the objects can provide a rich structure of description

and allow the properties of the simpler random models to be used to advantage. Such models include the very useful "Boolean Models" described by Serra (1982).

For example, trees may be modelled as randomly varying (e.g. in size and height) spheroids on stems that are dispersed in a homogeneous Poisson model on the plane or on a background of varying topography. If the modules within the crowns (which may be shoots or leaves and stems) are assumed randomly dispersed with a given density and size the Neyman-Scott describes the overall process but in most cases the problem may be treated hierarchically as in the within and between crown gap probability functions used to interpret Lidar data. The associated "Boolean" Model (Serra, 1981) is described elsewhere and allows a wide range of spatial statistics of forest canopies and stands to be computed.

By using a hierarchical model the focus of issues such as "clumping" resolves to the dispersion of individuals within and between the elements of the hierarchy. That is, leaves within trees may be clustered into modules or the dispersion of the trees may vary with resource availability or inter-species competition.

13.8 Terminology for the models used in the Lidar work

In the Lidar work, as was also the case in the analysis of hemispherical photographs or point quadrats, the base underlying models were often quite close to the "turbid medium" models used by radiative transfer modellers in plant canopy description.

Basically, by assuming plant elements are very small with centres distributed as a Poisson process it is possible to derive very convenient solutions to the expected data from these kinds of measurements.

It is generally assumed that the (centres of the) phyto-elements are distributed with a Poisson point process that is homogeneous in the horizontal direction. Vertical homogeneity is not necessary or desirable since leaf density varies significantly with height in crops and grasslands – not to mention forests. The independence properties of the Poisson are retained between layers that are thick enough for phyto-elements to be essentially only in one layer. This creates the need to assume small phyto-elements if differential equation models are to be used.

For example, the normal methods used to interpret hemispherical photographs assume horizontal homogeneity and inhomogeneous Poisson dispersion of small phyto-elements in the vertical direction. Most of the common radiative transfer models for crops and dense canopies assume the same.

It is not always necessary to assume horizontal isotropy. A row crop or plantation may well be anisotropic. However, in native forests the starting assumption is often one of horizontal homogeneity (i.e. stationarity) and isotropy. Any breakdown of the model will generally therefore involve some clustering of the phyto-elements (either vertically or horizontally) or significant spatial dependence either vertically or horizontally. This dependence can, of course, arise through the influence of the size of the dispersed phyto-elements as well as centres of clustering in individual plants.

When the size of the phyto-elements cannot be neglected (such as when then leaves are quite large) the correlation between layers must be taken into account when a discrete model is used. That is, in the random models it is assumed that adjacent layers are independent even if the layers are thin. In terms of the centres of the phyto-elements this is fine if the dispersion is Poisson. However, the phyto-elements themselves will overlap between layers. This creates correlations between layers so that gap probability attributed to a layer is not a function only of the phyto-element centres that fall within it. The thickness of layers or distances between non-adjacent layers such that they are independent is an important canopy measure and in Hotspot models is sometimes called the "decorrelation depth". When the phyto-element size is significant and these effects cannot be ignored, a discrete object model should be used.

In fully discrete models, such as those that cluster small leaves and stems into crowns and trees and disperse the (randomly varying) trees by a point process, terms like "clumping" to describe departures from the model should be used with care. The model has already introduced a clumping of the base phyto-elements (i.e. leaves or stems) relative to a homogeneous Poisson process distributing the leaves, but it is well controlled and modelled – often by hierarchical Poisson models. "Clumping" in this case could well be reserved to refer to additional effects between crowns due to clustering or dependence of the trees or within crowns due to the clustering of leaves into shoots or modules or spatial dependence in the leaf and stem dispersion. Hence, each time the model is extended, the issue of "clumping" may need to be revised to describe the presence of non-Poisson components or interactions.

13.9 Conclusions

The models developed to interpret Lidar data rely on separating a vegetation canopy into objects and modelling their dispersion. The model must describe the (varying) size, shape and orientation of the objects and their dispersion in the space of interest. Terms such as "clumped", "random", "clustered" and "regular" generally arise from the study of point patterns and therefore mainly reside with the dispersion of the centres of the objects.

The base model used in the past to analyse data ranging from hemispherical photographs to point quadrats and Lidar data is one in which basic phyto-elements are distributed in a thick layer (the canopy) according to a Poisson process. The process is assumed to be horizontally homogeneous but not vertically homogeneous. In order for the collection of phyto-elements to approximately have the independence properties of the point process in thin vertical layers it is necessary that they be small.

This model, which is also the basic model for Suits (1972a, 1972b) and SAIL (Verhoef, 1984) radiative transfer models, has many useful properties and associated methods for analysis. However, there are departures found in the field that are often assumed to be due to "clumping". Such departures can be due to either the non-random behaviours of the vertical or horizontal components of the point process or to spatial dependence of the elements such as is created by large objects, clustering into plant aggregates or correlated dispersion.

A wide range of discrete models can be used to describe such situations. These include the Li-Strahler and GORT models. They can also be hierarchical with objects being composed of smaller objects which themselves have size, shape, orientation and dispersion. It is important, however, to distinguish between the non-random effects introduced by the models and any variations from the model assumptions that are implied in the use of "clumping".

For example, a Neyman model can be developed by fixing centres of areas using a homogeneous Poisson process and then distributing individuals within the areas by a second homogeneous Poisson process. The distribution of the individuals will be clumped just as leaves in crowns are clumped relative to total dispersion in space. However, questions about the within-crown clustering or the clustering of crowns become much more significant as modelling issues and extra "clumping" in these aspects represents a departure from the model rather than clustering *per se*.

Most (if not all) of the models we use are horizontally homogeneous. This is true of the tree centres in Li-Strahler models as much as for all of the phyto-elements in turbid-medium radiative transfer models. It is the independence properties of the Poisson process that are most significant for the development of the simple interpretations of Lidar and other data (such as hemispherical photography). Nilson (1971) and Ross (1981) have made use of mathematical models incorporating spatial dependence, but it is usually better to model the causes of the dependence (such as leaf size and shape or the existence of intermediate modules) than to use general mathematical descriptions such as Markov models.

Contact Us
Phone: 1300 363 400
+61 3 9545 2176
Email: enquiries@csiro.au
Web: www.csiro.au

Your CSIRO

Australia is founding its future on science and innovation. Its national science agency, CSIRO, is a powerhouse of ideas, technologies and skills for building prosperity, growth, health and sustainability. It serves governments, industries, business and communities across the nation.